Anja Amlacher, BSc

Nonlinear Transport in dissipative Tight-Binding Chains

Master Thesis

For obtaining the academic degree
Diplom-Ingenieurin

Master Programme of
Technical Physics

Graz University of Technology

Supervisor:
Univ.-Prof. Dipl-Ing. Dr.techn. Wolfgang von der Linden
Institute of Theoretical and Computational Physics

Graz, June 2014

EIDESSTATTLICHE ERKLÄRUNG

AFFIDAVIT

Ich erkläre an Eides statt, dass ich die vorliegende Arbeit selbstständig verfasst, andere als die angegebenen Quellen/Hilfsmittel nicht benutzt, und die den benutzten Quellen wörtlich und inhaltlich entnommenen Stellen als solche kenntlich gemacht habe. Das in TUGRAZonline hochgeladene Textdokument ist mit der vorliegenden Masterarbeit identisch.

I declare that I have authored this thesis independently, that I have not used other than the declared sources/resources, and that I have explicitly indicated all material which has been quoted either literally or by content from the sources used. The text document uploaded to TUGRAZonline is identical to the present master's thesis.

Datum / Date

Unterschrift / Signature

Abstract

In this work we study transport properties of systems, consisting of a central region, a N-site tight-binding chain where each site is coupled to semi-infinite chains acting like an energy reservoir, and two coupled leads on the right and left edge of the chain. Furthermore we apply an electric field to the system and thus it gets tilted, as if there was a bias voltage between the leads and a current starts to flow. For the investigation of the transport problem in this system we apply the cluster perturbation theory (CPT) with the Greens function method and Dyson's equation to calculate the current. We show that charge carriers act differently for low and for high fields. Where the scattering picture (displaced Fermi seas) can be used in the low-field regime (linear current to field relation), the current can be understood via Bloch Oscillations in the high field regime.

Afterwards we investigate the behaviour of the current if there was a potential on every second place of the central chain applied. This simulates a semiconductor where the current is carried through resonant tunneling. The transmission coefficient is calculated via a transfer matrix method and a Greens function approach and is compared to the current. We see steps in the current characteristics, that come from resonant tunneling of the charge carriers at the resonance energies.

Kurzfassung

In dieser Arbeit werden Transportphänomene in einem System behandelt, das aus einer zentralen Region (tight-binding Kette, in der jeder Platz mit einer unendlichen Kette verbunden ist, die als Energie Reservoir dient) und zwei gekoppelten Leitern (Source und Drain) besteht. Des Weiteren wird ein elektrisches Feld angelegt, so dass es geneigt wird und so das Anlegen einer Bias-Spannung zwischen den Leitern simuliert wird, damit ein Strom fließen kann. Für die Behandlung dieses Transportproblems wurde die cluster perturbation theory (CPT) mit der Methode der Greens Funktionen und der Dyson Gleichung verwendet. Wie sich herausstellt, verhält sich der Strom unterschiedlich für hohe und niedrige Felder. Im Bereich der niederen Felder genügt der Strom dem Ohm'schen Gesetz und kann mit der Streutheorie der Elektronen beschrieben werden. Für hohe Felder entsteht aber ein oszillierender Strom, der mit zunehmendem elektrischen Feld langsam abnimmt und dessen Mechanismus im Bild der Bloch Oszillationen zu verstehen ist.

Weiters wurde ein alternierendes Potential in diesem System eingebaut und damit ein Halbleiter simuliert. Der Strom resultiert hier aus resonantem Tunneln. Der Transmissionskoeffizient wird mit der Transfermatrix Methode und der Methode der Greens Funktionen berechnet und wird mit dem Strom verglichen. Hier erkennt man sprunghaftes Zunehmen des Stromes, was aus dem resonantem Tunneln bei den Resonanz Energien resultiert.

Acknowledgement

First I want to thank my supervisor Univ.-Prof. Dipl-Ing. Dr.techn. Wolfgang von der Linden for the support in writing this Master's Thesis. He always had a sympathetic ear for my questions and took time for discussions. A special thanks goes to Univ.-Prof. Dr.rer.nat. Enrico Arrigoni for the animated talks with him and his supportive documents.

A Thank-you goes to my fellow students for the great time we spent here in Graz and the mutually support in studies.

I also want to thank my parents who made it possible for me to study and for the financial support, of prime importance my mother for the mental backing she gave me and my remaining family who always believed in me.

Another thanks go to my partner Jörg. His love, loyalty and the discussions with him helped me doing this work.

All these thanks couldn't be done, if there weren't people all over the last century, that advocated women suffrage, equal ranking of women and the possibility for them to study. Finally I'm very glad that I grew up in Middle Europe where prosperity and the access to education reign.

. . . to Jörg

Contents

List of Figures

1 Basis

In this section the tight-binding model, the Greens function technique and the cluster perturbation theory (CPT) are discussed. Then they are applied to the calculation of the Greens function of an infinite tight-binding chain under an uniform electric field.

1.1 Model

For the calculations in the following chapters the tight-binding model in second quantization was used:

$$\hat{\mathrm{H}} = \sum_{\mathrm{ij}} \mathrm{t_{ij}} \left(\hat{\mathrm{a}}_\mathrm{i}^\dagger \hat{\mathrm{a}}_\mathrm{j} + \hat{\mathrm{a}}_\mathrm{j}^\dagger \hat{\mathrm{a}}_\mathrm{i} \right) - \mu \sum_{\mathrm{i}} \hat{\mathrm{a}}_\mathrm{i}^\dagger \hat{\mathrm{a}}_\mathrm{i} + \sum_{\mathrm{i}} \epsilon_\mathrm{i} \hat{\mathrm{a}}_\mathrm{i}^\dagger \hat{\mathrm{a}}_\mathrm{i} \tag{1.1}$$

This model is used for different geometries and on-site energies. The indices i and j can also contain spin σ. The first sum describes the hopping between neighbouring sites with strength t, μ is the chemical potential and ϵ_i is the on-site energy. In our case μ equals zero which means that the bands are half filled if $\epsilon_\mathrm{i} = 0$. $\hat{\mathrm{a}}^\dagger$ and $\hat{\mathrm{a}}$ are the creation an annihilation operators. There is a defined commutation relation for them:

$$\begin{aligned} \left[\hat{\mathrm{a}}_\mathrm{i}, \hat{\mathrm{a}}_\mathrm{j}^\dagger \right]_{-\eta} &= \delta_\mathrm{ij} \\ \left[\hat{\mathrm{a}}_\mathrm{i}, \hat{\mathrm{a}}_\mathrm{j} \right]_{-\eta} &= \left[\hat{\mathrm{a}}_\mathrm{i}^\dagger, \hat{\mathrm{a}}_\mathrm{j}^\dagger \right]_{-\eta} = 0 \end{aligned} \tag{1.2}$$

$\eta = 1$ defines the commutator algebra for bosons and η=-1 stands for the anticommutator algebra for fermions ([1]).
The tight-binding model describes the motion of tightly bound electrons in a periodic crystal structure. Tightly bound means that the electrons should rarely interact with surrouding atoms or potentials. Hence the wave functions can be approximated by the atomic orbital functions ([11]). For a detailed derivation see [12], [3] and [11].
In the tight-binding model we assume that the crystal potential is strong. An electron in the crystal structure is therefore tightly bound to one atom. We now want to have a look at the effects of the presence of other atoms on the atomic orbital $\Phi_\nu(\mathrm{x})$. Hence we

choose a Bloch function,

$$\Psi_{\mathrm{k}}(\mathrm{x}) = \frac{1}{\mathrm{N}^{1/2}} \sum_{\mathrm{j}=1}^{\mathrm{N}} \exp(i\mathrm{kX_j}) \Phi_\nu(\mathrm{x} - \mathrm{X_j})$$

and sum over all atoms. $\mathrm{X_j} = \mathrm{ja}$ is the position of the $\mathrm{j^{th}}$ atom and a is the lattice constant. $\Phi_\nu(\mathrm{x} - \mathrm{X_j})$ is the function of the orbital centered around j, which is sharply peaked.

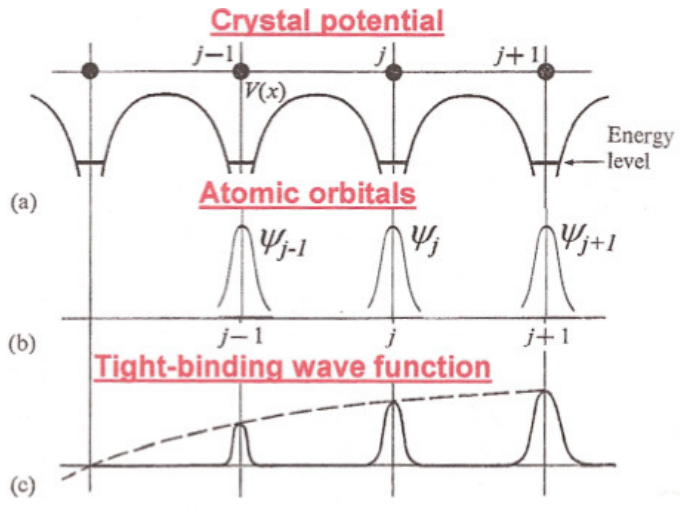

Figure 1.1: This figure stems from [3]. It shows (a) the crystal potential, (b) the localised atomic functions and (c) the corresponding Bloch function.

This means that there is only little overlap between orbitals ([3]). The function Ψ can be rewritten into a periodic form, which describes the motion of the propagating electron waves and is proportional to the atomic orbital.

$$\Psi_{\mathrm{k}}(\mathrm{x}) \propto \exp(i\mathrm{kX_j}) \Phi_\nu(\mathrm{x} - \mathrm{X_j}) \tag{1.3}$$

In the neighbourhood of the $\mathrm{j^{th}}$ site the crystal orbital behaves like an atomic one. This agrees with the basic assumption of the tight-binding model.

With it the energy of the electron can be calculated:

$$\begin{aligned} \mathrm{E(k)} &= \langle \Psi_\mathrm{k} | \, \hat{\mathrm{H}} \, | \Psi_\mathrm{k} \rangle \\ \mathrm{E(k)} &= \langle \Phi_\nu(\mathrm{x}) | \, \hat{\mathrm{H}} \, | \Phi_\nu(\mathrm{x}) \rangle + \sum_{\mathrm{j}=1}^{\mathrm{N}} \exp(i\mathrm{kX_j}) \, \langle \Phi_\nu(\mathrm{x}) | \, \hat{\mathrm{H}} \, | \Phi_\nu(\mathrm{x} - \mathrm{X_j}) \rangle \end{aligned} \tag{1.4}$$

The first term is the localization energy and the second term includes effects of tunneling. The sum (responsible for band structure) stands for nearest neighbours because from this point on the overlap between the functions get negligible.
If we have a look at the Hamiltonian, we see that it consists of the kinetic and the potential energy, while the potential can be written as a sum of atomic potentials:

$$\hat{\mathrm{H}} = \hat{\mathrm{T}} + \underbrace{\sum_{\mathrm{j}} \mathrm{v(x - X_j)}}_{\hat{\mathrm{V}}(\mathrm{x})} \tag{1.5}$$

The potential is split into two terms $\hat{\mathrm{V}}(\mathrm{x}) = \mathrm{v(x)} + \tilde{\mathrm{V}}(\mathrm{x})$ where v(x) is the amotic potential at the origin and $\tilde{\mathrm{V}}(\mathrm{x})$ is that of all other atoms.

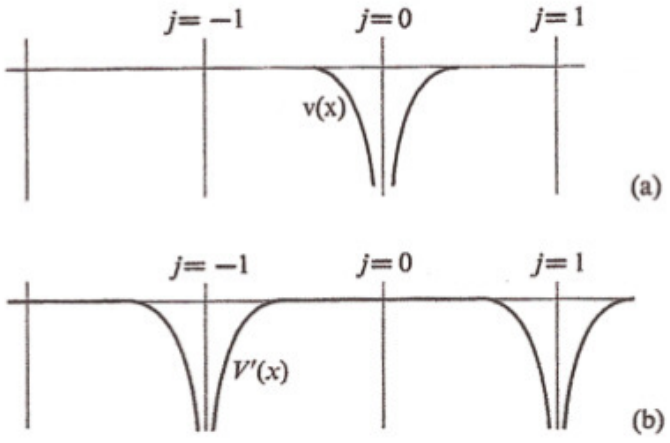

Figure 1.2: This figure stems from [3]. Shows the splitting of the potential in the (a) atomic potential v(x) and (b) the remainder V'(x).

Plugging this into the upper equation gives us:

$$\begin{aligned}\langle\Phi_\nu(\mathrm{x})|\,\hat{\mathrm{H}}\,|\Phi_\nu(\mathrm{x})\rangle &= \langle\Psi_\nu|\left[\hat{\mathrm{T}}+\mathrm{v(x)}\right]|\Psi_\nu\rangle + \underbrace{\langle\Phi_\nu(\mathrm{x})|\,\mathrm{V'(x)}\,|\Phi_\nu(\mathrm{x})\rangle}_{-\alpha} \\ &= \mathrm{E}_\nu - \alpha\end{aligned} \tag{1.6}$$

The interaction term turns to:

$$\langle\Phi_\nu(\mathrm{x})|\,\hat{\mathrm{H}}\,|\Phi_\nu(\mathrm{x}-\mathrm{a})\rangle = \langle\Phi_\nu(\mathrm{x})|\left[\hat{\mathrm{T}}+\mathrm{v(x\text{-}a)}\right]|\Phi_\nu(\mathrm{x\text{-}a})\rangle + \underbrace{\langle\Phi_\nu(\mathrm{x})|\,\mathrm{V'(x\text{-}a)}\,|\Phi_\nu(\mathrm{x\text{-}a})\rangle}_{-\gamma} \tag{1.7}$$

γ is the overlap integral and depends on the overlap of orbitals centered at neighbouring atoms. Now we can write for the energy:

$$\begin{aligned}\mathrm{E(k)} &= \mathrm{E}_\nu - \alpha - \gamma\sum_{\mathrm{j}=\pm1}\exp(i\mathrm{kX_j}) \\ &= \mathrm{E}_\nu - \alpha - 2\gamma\cos(\mathrm{ka})\end{aligned} \tag{1.8}$$

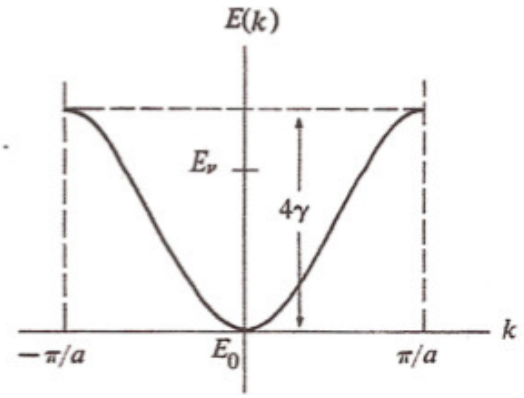

Figure 1.3: This figure stems from [3]. It shows the dispersion curve in this model.

k = 0 corresponds to the bottom of the band (E_0) and the width equals 4γ, which is proportional to the overlap intergral (As the overlap rises, the interaction gets stronger and the band gets wider). The bottom is lower than the atomic energy E_ν because the

presence of atoms suppresses the potential through the system. The second term in eq.(1.8) is the kinetic energy because the electron can now move through the crystal. At the bottom of the band, the electron has an effective mass:

$$\mathrm{m}^* = \frac{\hbar^2}{\mathrm{a}} \frac{1}{\gamma} \tag{1.9}$$

which means, that the mass is indirect proportional to the overlap. As the overlap rises, the mass decreases and it gets easier for the electron to tunnel to another atomic site. At the maximum point the electron has a negative effective mass.

Each atomic level leads to a band and in the tight-binding model it broadens into a band because of the interaction.

1.2 Greens function

For the following introduction to the Greens function method [5] and [4] were used as a support.

The Greens function is a possibility to solve an inhomogenous linear differential equation with specific initial conditions. In many-body theory, the Greens function is used to refer to correlation functions.

If we want to know the response of a system to a perturbation we can use the linear response theory to calculate the resulting physical quantities of the system. This response can be expressed by the Greens function:

$$\mathrm{G_{AB}}(\mathrm{t},\mathrm{t}') = \begin{cases} -i\Theta\left(\mathrm{t}-\mathrm{t}'\right)\left\langle\left[\hat{\mathrm{A}}_{(\mathrm{t})},\hat{\mathrm{B}}_{(\mathrm{t}')}\right]_{-\eta}\right\rangle & \text{retarded} \\ +i\Theta\left(\mathrm{t}-\mathrm{t}'\right)\left\langle\left[\hat{\mathrm{A}}_{(\mathrm{t})},\hat{\mathrm{B}}_{(\mathrm{t}')}\right]_{-\eta}\right\rangle & \text{advanced} \end{cases} \tag{1.10}$$

$\eta = -1$ forces the anticommutator relation for fermions and $\eta = 1$ forces the commutator algebra for bosons. $\hat{\mathrm{A}}$ and $\hat{\mathrm{B}}$ are time dependent operators and $\Theta(\mathrm{t}-\mathrm{t}')$ ensures the causality.

- **Retarded Greens function:** Describes the reaction of the system to a perturbation if $\mathrm{t} > \mathrm{t}'$. This means, that the perturbation has to be set in before the system reacts.

- **Advanced Green function:** Is the reverse of the retarded Greens function. The system reacts before the perturbation has set in. This means, that the function is not zero for $\mathrm{t}' > \mathrm{t}$.

The Greens function consists of two expectation values. It can be shown that it is only dependent on the time difference with the property that the trace is invariant against

cyclic permutations, if the hamiltonian isn't time dependend ($\frac{\partial}{\partial t}\hat{H}(t) = 0$):

$$\begin{aligned}\langle \hat{A}_{(t)}\hat{B}_{(t')}\rangle &= \langle \exp(i\hat{H}t)\hat{A}\exp(-i\hat{H}t)\exp(i\hat{H}t')\hat{B}\exp(-i\hat{H}t')\rangle \\ &= \langle \hat{A}\exp(-i\hat{H}(t-t'))\hat{B}\exp(-i\hat{H}(t-t'))\rangle \\ &= \langle \hat{A}\hat{B}_{(t-t')}\rangle = \langle \hat{A}_{(t-t')}\hat{B}\rangle\end{aligned}$$

This means, that the Greens function only depends on the time difference:

$$G_{AB}(t,t') = G_{AB}(t-t') \tag{1.11}$$

We also want to know the Greens function in frequency space. Therefore we execute a Fourier transform:

$$G_{AB}(t,t') = \frac{1}{2\pi}\int d\omega G_{AB}(\omega)\exp(-i\omega(t-t')) \tag{1.12}$$

The equation of motion for the calculation of the Green function in time space and after a Fourier transform in frequency space read:

$$\begin{aligned} i\frac{\partial}{\partial t}G_{AB}(t,t') &= \delta(t-t')\,\langle\left[\hat{A},\hat{B}\right]_{-\eta}\rangle + G_{\langle[\hat{A},\hat{H}],\hat{B}\rangle}(t,t') \\ \omega G_{AB}(\omega) &= \langle[\hat{A},\hat{B}]_{-\eta}\rangle + G_{\langle[\hat{A},\hat{H}],\hat{B}\rangle}(\omega)\end{aligned} \tag{1.13}$$

Where $G_{\langle[\hat{A},\hat{H}],\hat{B}\rangle}(t,t')$ and $G_{\langle[\hat{A},\hat{H}],\hat{B}\rangle}(\omega)$ are Greens functions of higher order. To calculate it, the series has to interrupt somewhere. We now try to calculate the Greens function of a tight-binding chain with following Hamiltonian in frequency space:

$$\hat{H} = t\sum_{\langle ij\rangle} a_i^\dagger a_j \tag{1.14}$$

The operators A and B are now a_i and $a_j^\dagger$. The equation of motion reads:

$$\omega\,\langle\langle a_i, a_j^\dagger\rangle\rangle = \langle\left[a_i, a_j^\dagger\right]_{-\eta}\rangle + \langle\langle[a_i,\hat{H}], a_j^\dagger\rangle\rangle$$

For the tight-binding model, we get:

$$\begin{aligned} \left[a_i, a_j^\dagger\right]_{-\eta} &= \delta_{ij} \\ \left[a_i, \hat{H}\right] &= t \sum_l a_l \\ \langle\langle [a_i, \hat{H}], a_j^\dagger \rangle\rangle &= t \sum_l \langle\langle a_l, a_j^\dagger \rangle\rangle \end{aligned} \tag{1.15}$$

Plugging this into the equation of motion gives us:

$$\omega \bar{G} = \mathbb{1} + \bar{T}\bar{G}$$

$\bar{T}$ is the hopping matrix and $\bar{G}$ the Greens function matrix.

If there was an interaction in the system, there would be another factor called the self-energy Σ, that describes the full interaction.

$$\bar{G} = \frac{\mathbb{1}}{\omega - \bar{T} - \Sigma}$$

For the tight-binding model we can write the Greens function easily:

$$G_k = \frac{1}{\omega - \epsilon_k} \tag{1.16}$$

G_k is now a function and no matrix anymore and ω can be rewritten with a complex factor. The Greens function exhibits poles at the excitation energies ϵ_k. The position of these poles get shifted by the self-energy, that consists of a real and an imaginary part. Normally the peaks are delta-shaped, but with the imaginary part of Σ they get Lorentzian style (the peaks get broadened). The real part of Σ shifts the position of the poles.

In time-space the factor Θ ensures causality. In frequency space one has to add a complex factor to the Greens function, which ensures poles in the lower/upper complex plane.

$$G_k = \frac{1}{\omega - \epsilon_k \pm \mathbf{i}o^+} \tag{1.17}$$

For the retarded Greens function we choose $-i\mathrm{o}^+$. This means, that their poles lay in the negativ complex plane. For the advanced Greens function one chooses $+i\mathrm{o}^+$ and their poles lay in the upper complex plane.
To compute the Greens function in time space we have to execute a Fourier transform:

$$\mathrm{G(t)} = \frac{1}{2\pi}\int_{-\infty}^{\infty}\frac{\exp(-i\omega\mathrm{t})}{\omega - \epsilon_\mathrm{k} \pm i\mathrm{o}^+}\mathrm{d}\omega$$

For the evaluation one has to use the Residue theorem and we get following characteristics for the Greens function:

$$\begin{aligned} &\mathrm{G(t)} \propto \frac{1}{2\pi}\exp(-i\epsilon_\mathrm{k}\mathrm{t}) \\ &\mathrm{G^r(t)} = 0 \qquad \mathrm{t} < 0 \\ &\mathrm{G^a(t)} = 0 \qquad \mathrm{t} > 0 \end{aligned} \tag{1.18}$$

This means, while $\mathrm{G}(\omega)$ has poles at the excitation energies, $\mathrm{G(t)}$ oscillates with ϵ_k.

If we treat a system in non-equilibrium, we have to change over to Keldysh space, where the full Greens function can be notated as a matrix containing the retarded, advanced and a Keldysh part:

$$\bar{\mathrm{G}} = \begin{pmatrix} \bar{\mathrm{G}}^\mathrm{r} & \bar{\mathrm{G}}^\mathrm{K} \\ 0 & \bar{\mathrm{G}}^\mathrm{a} \end{pmatrix} \tag{1.19}$$

With following relation between retarded and advanced part:

$$\mathrm{G^r}(\omega) = (\mathrm{G^a}(\omega))^*$$

For more and detailed information in the Keldysh nonequilibrium Green function technique [6] serves as a supportive literature.

1.3 Cluster Perturbation Theory (CPT)

For the considerations in this Chapter [7] and [8] were used as supportive literature. The Cluster Perturbation Theory is a very good way to calculate properties of the following considered systems very easily.

The CPT proceeds by tiling the lattice into clusters. These clusters can be solved exactly and the hopping between them is treated in first order perturbation theory, as for as the self energy is concerned. With it, the single-particle Greens function of a strongly correlated system can be calculated. This approach takes short-range correlations into account but those beyond the cluster size are neglected. After coupling the Greens functions of the clusters within perturbation theory, the full function in the thermodynamic limit can be recovered.

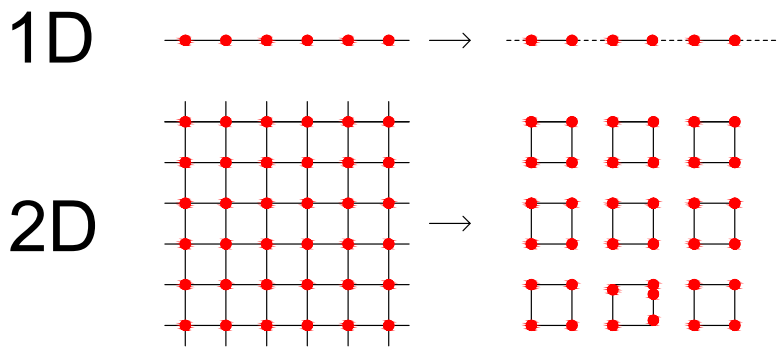

Figure 1.4: Shows the possible tiling of the lattice for one and two dimensions.

The upper Figure shows a possibility of cluster tiling. In 1D the tiling is straight forward, but in 2D the number of sites and the shape of the cluster can be chosen arbitrarily. Many tilings are possible. The Hamiltonian of the system after the division reads:

$$\hat{\mathrm{H}} = \sum_{\mathrm{R}} \left[\hat{\mathrm{H}}_0^{(\mathrm{c})}(\mathrm{R}) + \hat{\mathrm{H}}_1(\mathrm{R}) \right] + \sum_{\mathrm{R},\mathrm{R}'} \hat{\mathrm{H}}_0^{(\mathrm{i})}(\mathrm{R},\mathrm{R}') \tag{1.20}$$

$\hat{H}_0^{(c)}(R)$ is the single particle term, that only acts inside a single cluster, and $\hat{H}_1(R)$ the corresponding interaction term. R denotes the individual clusters. $\hat{H}_0^{(i)}(R, R')$ stands for the inter-cluster hopping and is given by:

$$\hat{H}_0^{(i)}(R, R') = \sum_{a,b} T_{a,b}^{R,R'} c_{R,a}^{\dagger} c_{R',b} \tag{1.21}$$

$T_{a,b}^{R,R'}$ is the hopping matrix, which is non-zero for hopping across the cluster boundaries. The indices a and b stand for quantum numbers within the cluster.
The quantity we are interested in, is the single-particle Greens function. Therefore we calculate the cluster Greens function $G'_{R',a,b}(\omega)$ first and treat the hopping between the clusters perturbatively (using the Dyson equation). Then we get the Greens function $G_{R,a,R',b}$ of the full system.

$$\mathbf{G}^{-1}(\omega) = \mathbf{G'}^{-1}(\omega) - \mathbf{T} \tag{1.22}$$

These matrices, written bold, have indices (R,a) and (R',b). The cluster Greens function **G**' is block-diagonal in R. **T** is the inter-cluster hopping and is off-diagonal.
CPT breaks translational invariance on the original lattice, but it is conserved on the superlattice (originates from the tiling of the lattice into clusters). We label the states by a wavevector $\tilde{\mathbf{k}}$ in the Brillouin zone of the superlattice. Therefore we start to write the second term in eq.(1.20) in a different way:

$$\begin{aligned} \hat{O} &= \sum_{R,R'} \hat{H}_0^{(i)}(R, R') = \sum_{R,\Delta} \hat{H}_0^{(i)}(R, \Delta) \\ &= \sum_{R,\Delta} \sum_{a,b} T_{a,b}(\Delta) c_{R+\Delta,a}^{\dagger} c_{R,b} \end{aligned} \tag{1.23}$$

With the Fourier transformation:

$$\begin{aligned} c_{R+\Delta,a}^{\dagger} &= \frac{1}{\sqrt{L}} \sum_{\tilde{\mathbf{k}}} \exp(-i\tilde{\mathbf{k}}(R+\Delta)) c_{\tilde{\mathbf{k}},a} \\ c_{R,b} &= \frac{1}{\sqrt{L}} \sum_{\tilde{\mathbf{k}}} \exp(i\tilde{\mathbf{k}}R) c_{\tilde{\mathbf{k}},b} \end{aligned}$$

we get:

$$\hat{O} = \sum_{\tilde{\mathbf{k}}} \sum_{\mathrm{a,b}} \underbrace{\left[\sum_{\Delta} \mathrm{T_{a,b}}(\Delta) \exp(-i\tilde{\mathbf{k}}\Delta) \right]}_{\mathrm{T_{a,b}}(\tilde{\mathbf{k}})} \mathrm{c}^{\dagger}_{\tilde{\mathbf{k}},\mathrm{a}} \mathrm{c}_{\tilde{\mathbf{k}},\mathrm{b}} \tag{1.24}$$

$\mathrm{T_{a,b}}(\tilde{\mathbf{k}})$ is the superlattice Fourier-transformed hopping. Δ has to be given in units of the lattice spacing ($\Delta = \pm \mathrm{L}$). The CPT Greens function is then also diagonal in $\tilde{\mathbf{k}}$ and the Dyson equation for the evaluation of the full Greens function reads:

$$\mathbf{G}^{-1}(\tilde{\mathbf{k}}, \omega) = \mathbf{G'}^{-1}(\omega) - \mathbf{T}(\tilde{\mathbf{k}}) \tag{1.25}$$

We can also write the CPT expression in terms of the self-energy:

$$\mathbf{G}^{-1}(\tilde{\mathbf{k}}, \omega) = \mathbf{G}_0^{-1}(\tilde{\mathbf{k}}, \omega) - \mathbf{\Sigma}(\omega) \tag{1.26}$$

where $\mathbf{G}_0^{-1}(\tilde{\mathbf{k}}, \omega)$ is the non-interacting Greens function.

$$\mathbf{G}_0^{-1} = \omega - \mathbf{t'} - \mathbf{T} \tag{1.27}$$

t' is the intra-cluster hopping. This gives us:

$$\mathbf{G'}^{-1}(\omega) = \mathbf{G}_0^{-1}(\omega) + \mathbf{T} - \mathbf{\Sigma'}(\omega) \tag{1.28}$$

$\mathbf{\Sigma'}(\omega)$ is the cluster self-energy. With these expressions we can can calculate the full Greens function:

$$\mathbf{G}^{-1}(\tilde{\mathbf{k}}, \omega) = \mathbf{G'}^{-1}(\omega) - \mathbf{T}(\tilde{\mathbf{k}}) - (\mathbf{\Sigma}(\omega) - \mathbf{\Sigma'}(\omega)) \tag{1.29}$$

Since the form of the inter-cluster hopping $\mathbf{T}(\tilde{\mathbf{k}})$ is known, the Green function is computed once the cluster function is known. The calculated CPT Green function has the same properties as the exact function. It has poles on the real axis, which show the quasiparticle excitations.

Following holds for CPT for the equilibrium Greens function:

- It is exact in the non-interacting limit U=0, because the self-energy dissapears.
- It's also exact in t→0 (strong coupling).
- CPT is obviously exact in the limit $N_c \to \infty$ (for large clusters).
- From the Greens function the spectral function can be evaluated, which is useful to compare numerical calculations to ARPES-data.
- CPT can't describe broken symmetry states. They can be described by VCA (Variational Cluster Approach, [9]).
- We have to treat open boundary conditions in CPT. Calculations with periodic boundary conditions are unsatisfactory.

1.4 Greens function for electrons in an electric field

In this section we first want to calculate the Greens function of a semi-infinite chain under an uniform electric field, where each site is coupled to a bath, which modeled by another semi-infinite tight-binding chain. In the next step (Section 1.4.1) we can combine two semi-infinite systems to an infinite chain.
We have a look at a model consisting of an infinite one-dimensional tight-binding chain where each site is coupled to a bath. The Hamiltonian for this system reads:

$$\begin{aligned} \hat{\mathrm{H}} &= \hat{\mathrm{H}}_{\mathrm{c}} + \sum_{\mathrm{n}} \left(\hat{\mathrm{H}}_{\mathrm{bn}} + \hat{\mathrm{H}}_{\mathrm{cbn}} \right) \\ \hat{\mathrm{H}}_{\mathrm{c}} &= \sum_{\mathrm{n}} \left(\epsilon_{\mathrm{n}} \mathrm{c}_{\mathrm{n}}^{\dagger} \mathrm{c}_{\mathrm{n}} - \mathrm{t} \left(\mathrm{c}_{\mathrm{n}}^{\dagger} \mathrm{c}_{\mathrm{n+1}} + \mathrm{h.c} \right) \right) \end{aligned} \tag{1.30}$$

where $\hat{\mathrm{H}}_{\mathrm{c}}$ describes a chain with nearest neighbour hopping and applied electric field $\epsilon_{\mathrm{n}} = \mathrm{n} \cdot \mathrm{E}$. $\hat{\mathrm{H}}_{\mathrm{bn}}$ is the Hamiltonian of non-interacting bath fermions and $\hat{\mathrm{H}}_{\mathrm{cbn}}$ is the coupling between the chain and the baths.

Approach:

- couple system site to the baths
- couple the sites to each other to achieve a half-infinite chain
- calculate the infinite chain

As for as the bath sites are concerned, onne only has to know the bath Greens function $\mathrm{g}_{\mathrm{bn0}}(\omega)$ at site l=0. It is given by the function of a semi-infinite chain in the wide-band limit, which means, that the hopping in the baths is very high:

$$\begin{aligned} \textbf{retarded}: \quad & \mathrm{g}_{\mathrm{b0}}^{\mathrm{r}}(\omega) = \frac{1}{\omega + i\Gamma} \\ \textbf{Keldysh}: \quad & \mathrm{g}_{\mathrm{b0}}^{\mathrm{K}}(\omega) = 2i \Im \mathrm{g}_{\mathrm{bn0}}^{\mathrm{r}}(\omega) \left(1 - 2\mathrm{f}_{\mathrm{F}}(\omega - \mu_{\mathrm{n}})\right) \end{aligned} \tag{1.31}$$

($\mu_n = \mu_0 + n \cdot E$). This definition of the retarded component only holds in the wide band limit, where the hopping of the bands t_{bb} is so high, that the bands are getting plane in the middle and therefore the imaginary part $i\Gamma$ is added to achieve this behaviour. Normally the retarded Greens function of a semi-infinite tight-binding chain reads:

$$\begin{aligned}\kappa &= \frac{\omega - \epsilon}{2t_{bb}} \\ g_b^r &= \frac{1}{t_{bb}} \left[\kappa - \sqrt{\kappa^2 - 1}\,(\Theta(\kappa - 1) - \Theta(-\kappa - 1)) - i\sqrt{1 - \kappa^2}\Theta(1 - |\kappa|)\right]\end{aligned}$$

For the translational invariance the baths have to be shifted towards the same electrical fields as the corresponding chain site:

$$g_{bn0}^r(\omega) = g_b^r(\omega - nE) \tag{1.32}$$

For the calculation of the Greens function of the system one can make an iterative approach. This means, that the Greens function in Keldysh space for site n is connected to that other site n+1,via:

$$\bar{G}_n^{-1} = g_n^{-1} - t^2 \bar{G}_{n+1} - v^2 g_{bn0} \tag{1.33}$$

t is the hopping between the sites on the chain and v is the hopping from the chain to the baths. g_n is the Green function of an isolated site. It reads:

$$\begin{aligned} g_n^r &= \frac{1}{\omega - nE} \\ (g_n^K)^{-1} &= 0 \end{aligned} \tag{1.34}$$

(The factor io^+ is included in ω and doesn't written explicitely). These calculations have to be considered in Keldysh space (all Green functions are matrices containing the retarded, Keldysh and avanced part). Dysons equation holds in Keldysh space. Besides the relation (1.33) there is a second one between the function for site n and n+1:

$$\bar{G}_n(\omega) = \bar{G}_{n+1}(\omega + E) \tag{1.35}$$

With eq.(1.33) and (1.35) one can calculate the retarded and the Keldysh component.

Retarded part:

$$\begin{aligned}
\bar{\mathrm{G}}_{\mathrm{n}}^{-1} &= (\omega - \mathrm{nE}) - \mathrm{t}^2 \bar{\mathrm{G}}_{\mathrm{n}}(\omega - \mathrm{E}) - \mathrm{v}^2 \frac{1}{\omega - \mathrm{nE} + i\Gamma} && / : \mathrm{t} \\
\frac{1}{\mathrm{t}} \bar{\mathrm{G}}_{\mathrm{n}}^{-1} &= \frac{1}{\mathrm{t}} \left[(\omega - \mathrm{nE}) - \frac{\mathrm{v}^2}{\omega - \mathrm{nE} + i\Gamma} \right] - \mathrm{t} \bar{\mathrm{G}}_{\mathrm{n}}(\omega - \mathrm{E}) && / \mathrm{F}(\omega) = \frac{1}{\mathrm{t}} \left(\omega - \frac{\mathrm{v}^2}{\omega + i\Gamma} \right) \\
\frac{1}{\mathrm{t}} \bar{\mathrm{G}}_{\mathrm{n}}^{-1} &= \mathrm{F}(\omega - \mathrm{nE}) - \mathrm{t} \bar{\mathrm{G}}_{\mathrm{n}}(\omega - \mathrm{E}) && / \mathrm{F}_{\mathrm{n}}(\omega) = \mathrm{F}(\omega - \mathrm{nE}) \\
\frac{1}{\mathrm{t}} \bar{\mathrm{G}}_{\mathrm{n}}^{-1} &= \mathrm{F}_{\mathrm{n}}(\omega) - \mathrm{t} \bar{\mathrm{G}}_{\mathrm{n}}(\omega - \mathrm{E}) && / \bar{\mathrm{G}}_{\mathrm{n}}(\omega) = \mathrm{t} \bar{\mathrm{G}}_0(\omega - \mathrm{nE})
\end{aligned}$$

$$\bar{\mathrm{G}}_0(\omega) = \cfrac{1}{\mathrm{F}_0 - \cfrac{1}{\mathrm{F}_1 - \cfrac{1}{\mathrm{F}_2 - \ldots \quad - \cfrac{1}{\mathrm{F}_{\mathrm{n}} - \cfrac{\mathrm{t}}{\omega - (\mathrm{n}+1)\mathrm{E}}}}}} \tag{1.36}$$

Keldysh part:

$$\begin{aligned}
-\frac{\bar{\mathrm{G}}_{\mathrm{n}}^{\mathrm{K}}(\omega)}{|\mathrm{G}_{\mathrm{n}}^{\mathrm{r}}(\omega)|^2} &= (\mathrm{g}_{\mathrm{n}}^{K})^{-1} - \mathrm{t}^2 \bar{\mathrm{G}}_{\mathrm{n}}^{\mathrm{K}}(\omega - \mathrm{E}) - \mathrm{v}^2 \mathrm{g}_{\mathrm{bn0}}^{\mathrm{K}} \quad / (\mathrm{g}_{\mathrm{n}}^{K})^{-1} = 0 \\
\frac{\bar{\mathrm{G}}_{\mathrm{n}}^{\mathrm{K}}(\omega)}{|\mathrm{G}_{\mathrm{n}}^{\mathrm{r}}(\omega)|^2} &= \mathrm{v}^2 \mathrm{g}_{\mathrm{bn0}}^{\mathrm{K}} + \mathrm{t}^2 \bar{\mathrm{G}}_{\mathrm{n}}^{\mathrm{K}}(\omega - \mathrm{E}) && / \mathrm{F}_{\mathrm{n}}(\omega) = \mathrm{F}(\omega - \mathrm{nE}) = \mathrm{v}^2 \mathrm{g}_{\mathrm{bn0}}^{\mathrm{K}}
\end{aligned}$$

$$\bar{\mathrm{G}}_{\mathrm{n}}^{\mathrm{K}}(\omega) = |\bar{\mathrm{G}}_{\mathrm{n}}^{\mathrm{r}}(\omega)|^2 \left[\mathrm{F}_{\mathrm{n}}(\omega) + \mathrm{t}^2 \bar{\mathrm{G}}_{\mathrm{n+1}}^{\mathrm{K}}(\omega) \right] \tag{1.37}$$

In the n-th iteration step set $\bar{\mathrm{G}}_{\mathrm{n+1}}^{\mathrm{K}}(\omega) = 0$.

For the Greens function of the full system one has to calculate:

$$G_n^{-1} = \bar{G}_n^{-1} - t^2 \bar{G}_{n+1} \tag{1.38}$$

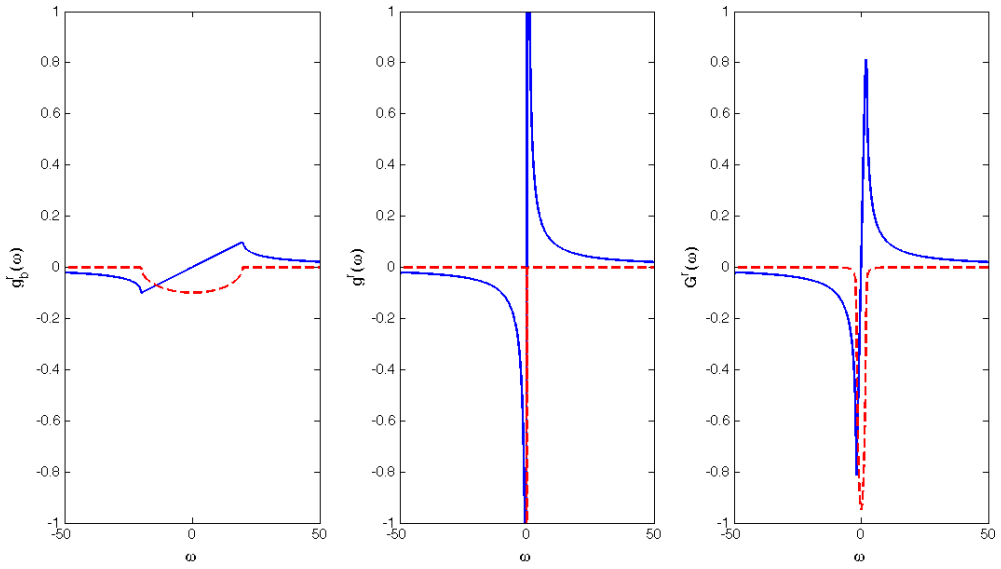

Figure 1.5: Retarded Greens function for a half infinite chain. The left plot shows the bath Greens function for the semi-infinite tight-binding chain, the middle one shows the function of an isolated site in the system and the right plot shows the Greens function of the isolated site connected to the corrresponding bath as a function of frequency. In this case no electric field is switched on. The solid (blue) line shows the real part and the dashed (red) line shows the imaginary part.

As we can see in Fig.1.5, the retarded part has it's poles in the negative complex area (this is the reason why we have to add the factor $i o^+$ in frequency space to fullfill causality) and the real part diverges at an excitation energy. In Fig.1.6 we have a look at the Greens function of a semi-infinite tight-binding chain for E=0.5.

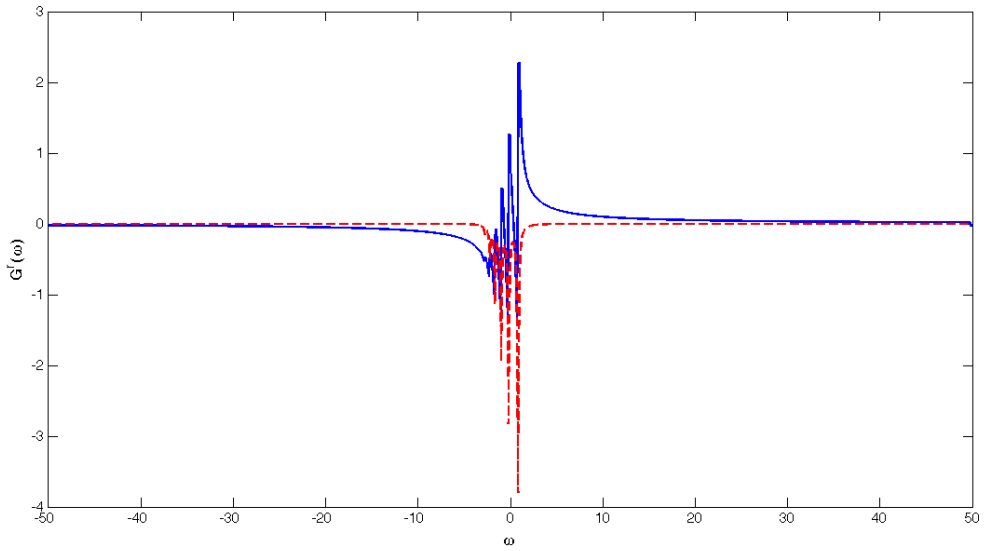

Figure 1.6: Retarded Greens function for a semi-infinite tight-binding chain under an uniform electric-field of strength E=0.5 as a function of frequency. Colors as in Fig.1.5

1.4.1 Infinite Chain

Now we want to extend the calculation for an infinite chain (coupling of two semi-infinite chains). This is very similar to the procedure in the previous chapter. First one has to calculate the Greens function for the right and left semi-infinite chain. For this one can introduce a reference system with on-site energies $\epsilon_{\mathrm{n}}^{0} = 0, \mathrm{E}, 2\mathrm{E} \ldots$. But we are really interested in $\epsilon_{\mathrm{n}} = \epsilon_{\mathrm{n}}^{0} + \frac{\mathrm{E}}{2}$ which can be reached by a spectral energy shift $\mathrm{G}^{\mathrm{r}}(\omega) = \mathrm{G}^{\mathrm{r}}(\omega - \frac{\mathrm{E}}{2})$. We only need to know the Greens function for the first isolated site of the chain and the bath Greens function. With the Dyson equation one can couple these to:

$$(\tilde{\mathrm{g}}(\omega))^{-1} = \omega - i\mathrm{o}^{+} - \mathrm{v}^{2}\mathrm{g}_{\mathrm{b}}(\omega) \tag{1.39}$$

The point is, that this function can be shifted towards other energies. This means, that the on-site energy for site 2 is shifted by +E from point 1. We have

$$\tilde{g}(\omega) = g(\omega - E) \tag{1.40}$$

And finally we get:

$$g^{-1}(\omega) = (\tilde{g}(\omega))^{-1} - t^2 g(\omega - E) \tag{1.41}$$

And for the right system one gets:

$$g^{r}(\omega) = g(\omega - \frac{E}{2}) \tag{1.42}$$

For the left semi-infinite system we introduce a reference system with $\epsilon_n^0 = 0, -E, -2E \ldots$ but we are really interested in $\epsilon_n = \epsilon_n^0 - \frac{E}{2}$. The other procedure is the same as for the right system but now it means:

$$g^{l}(\omega) = g(\omega + \frac{E}{2}) \tag{1.43}$$

There is a symmetry relation between the right and left system:

$$g^{l}(\omega) = (-g^{r}(-\omega))^{*} \tag{1.44}$$

For the computation of the full Greens function of the infinite chain, we have to combine the two functions via the Dyson equation.

$$\begin{pmatrix} G_{ll} & G_{lr} \\ G_{rl} & G_{rr} \end{pmatrix} = \begin{pmatrix} g_{ll} & g_{lr} \\ g_{rl} & g_{rr} \end{pmatrix} + \begin{pmatrix} g_{ll} & g_{lr} \\ g_{rl} & g_{rr} \end{pmatrix} \begin{pmatrix} 0 & t \\ t & 0 \end{pmatrix} \begin{pmatrix} G_{ll} & G_{lr} \\ G_{rl} & G_{rr} \end{pmatrix} \tag{1.45}$$

g_{lr} and g_{rl} are zero. So we get following system of equations:

$$\begin{pmatrix} G_{ll} & G_{lr} \\ G_{rl} & G_{rr} \end{pmatrix} = \begin{pmatrix} g_{ll} + t g_{ll} G_{rl} & t g_{ll} G_{rr} \\ trr G_{ll} & g_{rr} + t g_{rr} G_{lr} \end{pmatrix} \tag{1.46}$$

After solving this system in consideration of the Keldysh space, we get:

$$\begin{aligned} G_{lr}^{r/a} &= \left((g_{ll}^{r/a} g_{rr}^{r/a})^{-1} - t^2 \mathbb{1} \right)^{-1} \\ G_{lr}^{K} &= \frac{g_{ll}^{K} g_{rr}^{K}}{(g_{ll}^{r} g_{rr}^{r} - t^2 \mathbb{1})(g_{ll}^{a} g_{rr}^{a} - t^2 \mathbb{1})} \end{aligned} \tag{1.47}$$

The other components G_{ll} and G_{rr} are calculated to:

$$\begin{aligned} G_{ll}^{r/a} &= \left((g_{ll}^{r/a})^{-1} - t^2 g_{rr}^{r/a} \right)^{-1} \\ G_{ll}^{K} &= \frac{g_{ll}^{K}}{|1 - g_{ll}^{a} g_{rr}^{a}|^2} + |G_{ll}^{a}|^2 g_{rr}^{K} \end{aligned} \tag{1.48}$$

(G_{rr} similar)
In the linear electric field we have:

$$\begin{aligned} G_{ll}^{a}(\omega) &= -(G_{rr}^{a}(-\omega))^* \\ G_{ll}^{K}(\omega) &= (G_{rr}^{K}(-\omega))^* \\ G_{lr}(\omega) &= G_{rl}(\omega) \end{aligned}$$

Having calculated the Greens function one can compute the current, like it is described in Section 2.3 for the system depicted in Fig.2.1.
The second possibility to calculate the Greens function of an infinite tight-binding chain is to use the functions of an isolated site, couple this to the fermionic bath function and with the Dyson equation one can calculate the full function of this system by adding the sites up to N=∞. This is shown in Chapter 2.2. The problem with this method is, that because of the finiteness of the system (behaves like the chain was cut somewhere) boundary effects appear.

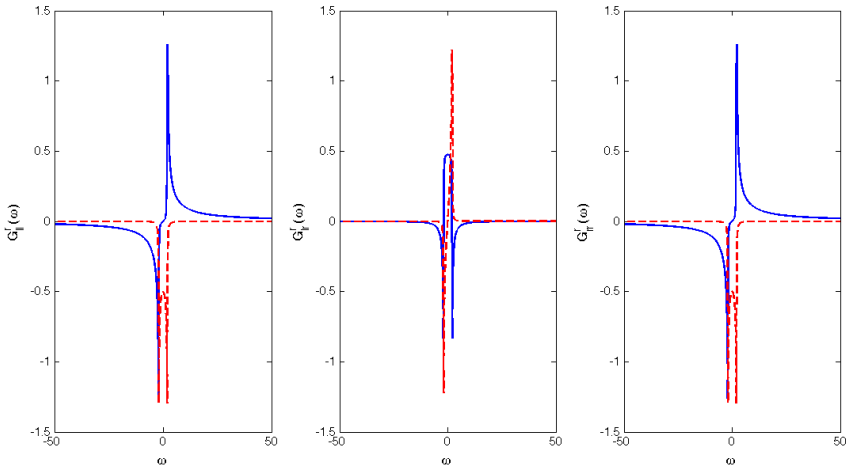

Figure 1.7: Retarded Greens function of an infinite tight-binding chain without electrical field in the middle. The left pannel shows the Greens function for the left semi-infinite chain and the right pannel the Greens function for the right chain. The solid line is the real and the dashed line the imaginary part of the function. We see the Greens function for the left, the right and the coupled system.

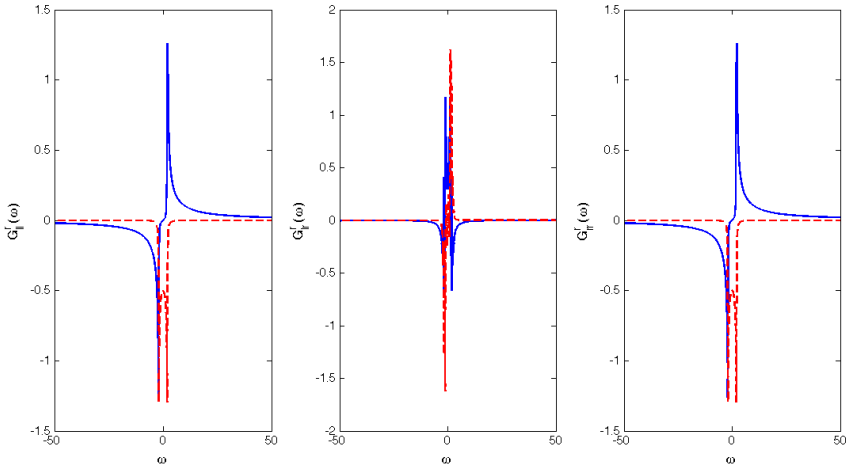

Figure 1.8: Same as before with E=0.5. We see the Greens function for the left, the right and the coupled system. Compare this to the previous figure. The field introduces new excitations.

2 Tight-binding chain coupled to fermion reservoirs with applied electric-field

2.1 Model

We have a look at a system that consists of a one-dimensional tight-binding model with N sites, where each site is connected to fermionic reservoirs, which are modeled as semi-infinite non interacting tight-binding chains. These reservoirs are responsible for the energy dissipation in the system. At the ends of the central region, consisting of the N-site chain coupled to the fermionic reservoirs, we connect leads (semi-infinite tight-binding chains). Furthermore we apply an electric-field to the system, as shown in Fig.2.1.

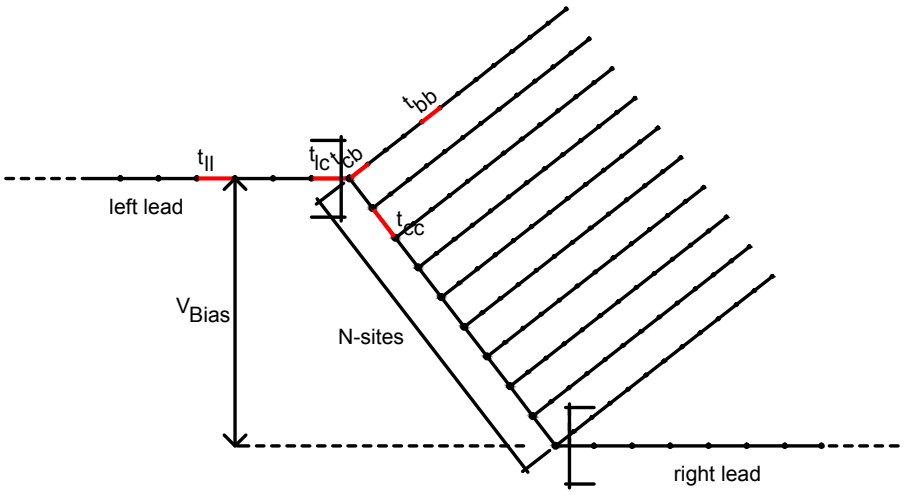

Figure 2.1: System of two leads coupled to a central region, consisting of N sites with semi-infinite fermionic baths. Hopping parameters: t_{ll} ... in lead; t_{lc} ... lead-chain; t_{cb} ... chain-bath; t_{bb} ... in bath; t_{cc} ... in chain; V_{Bias} ... bias voltage

The Hamiltonian for this system reads:

$$\begin{aligned} \hat{H} &= \hat{H}_{cc} + \sum_{\alpha=L,R} \left(\hat{H}_{\alpha}\right) + \hat{H}_{cl} + \hat{H}_{bb} + \hat{H}_{cb} \\ \hat{H}_{cc} &= -\mathrm{t}_{cc} \sum_{i=1}^{N} \left(\mathrm{c}_i^{\dagger}\mathrm{c}_{i+1} + \mathrm{c}_{i+1}^{\dagger}\mathrm{c}_i\right) + \mathrm{E} \sum_{i=1}^{N} i\mathrm{c}_i^{\dagger}\mathrm{c}_i \end{aligned} \tag{2.1}$$

$\hat{H}_{cc}$ is the Hamiltonian of the central N-site tight-binding chain. It describes the hopping of the electrons between nearest neighbour sites and the energetic tilt of the chain due to the electric-field E. $\hat{H}_{\alpha}$ describes the infinite leads to the left and the right of the central region. $\hat{H}_{cl}$ is the coupling between the first site of the central region and the last site of the left lead (and between the last site of the chain and the first site of the right lead). The two leads always have the same chemical potential as the first and the last site of the central region. $\hat{H}_{bb}$ is the Hamiltonian of the non-interacting fermionic baths with no chemical potential and $\hat{H}_{cb}$ is the coupling of the reservoir to the chain site.

If we applied an electric-field to the central region, it get's tilted. That is equal to apply a bias voltage $\mathrm{V_{Bias}}$ to the system. One can calculate the bias voltage from the electric-field:

$$\mathrm{V_{Bias}} = (\mathrm{N} - 1) \cdot \mathrm{E}$$

The left lead of the system has the same chemical potential as the first site of the chain $\mu_l = \mathrm{E_F}$. In our case, we set $\mathrm{E_F} = 0$. The right lead has then following potential $\mu_r = \mathrm{E_F} - \mathrm{V_B}$.

2.2 CPT Approach

We use the Cluster Perturbation Theory, because it is a good way to calculate the Greens function for the considered system. First we connect the isolated site to the corresponding bath. At the first and the last site of the central region we couple the infinite leads. Then we treat the hopping between the sites and couple them by using the Dyson's equation. We then use the achieved Greens function for current calculations.

For the implementation of this problem CPT (Cluster Perturbation Theory) can be used. It allows to deal efficiently with infinite systems. The Greens functions of an isolated site $\mathrm{g}_0^{r/a/K}(\omega)$ and the semi-infinite fermionic reservoirs $\mathrm{g}_b^{r/a/K}(\omega)$ are well known. First of all, these two functions get connected via the Dyson-equation:

$$\begin{aligned} \mathrm{g}_{cc}^{r/a}(\omega) &= \left(\left(\mathrm{g}_0^{r/a}(\omega) \right)^{-1} - \mathrm{t}_{cb}^2 \cdot \mathrm{g}_b^{r/a}(\omega) \right)^{-1} \\ \mathrm{g}_{cc}^{K}(\omega) &= -\mathrm{t}_{cb}^2 \cdot \frac{\mathrm{g}_b^K(\omega)}{|\mathrm{g}_0^r(\omega)|^2} \end{aligned} \tag{2.2}$$

$\mathrm{g}_{cc}^{r/a/K}(\omega)$ is now the Greens function of an isolated site connected to a reservoir-chain. The next step is to form the Greens function of the other sites. Because of the electric-field, which enters through the on-site energies, the function of the isolated site gets shifted in energy space. This means:

$$\mathrm{g}_n^{r/a/K}(\omega) = \mathrm{g}_{cc}^{r/a/K}(\omega - \mathrm{n} \cdot \mathrm{E}) \tag{2.3}$$

with n = 0,1,2,...,(N-1).
Furthermore the Greens function $\mathrm{g}_{ll}^{r/a/K}(\omega)$ of the lead gets connected to the first (n=0) and last (n=N) site of the central region:

$$\begin{aligned} \mathrm{g}_{cc}^{r/a}(\omega) &= \left(\left(\mathrm{g}_{cc}^{r/a}(\omega) \right)^{-1} - \mathrm{t}_{cl}^2 \cdot \mathrm{g}_{ll}^{r/a}(\omega) \right)^{-1} \\ \mathrm{g}_{cc}^{K}(\omega) &= \frac{\left(\frac{\mathrm{g}_{cc}^K(\omega)}{|\mathrm{g}_{cc}^r(\omega)|^2} + \mathrm{t}_{cl}^2 \mathrm{g}_{ll}^K(\omega) \right)}{\left((\mathrm{g}_{cc}^r(\omega))^{-1} - \mathrm{t}_{cl}^2 \cdot \mathrm{g}_{ll}^r(\omega) \right) \left((\mathrm{g}_{cc}^a(\omega))^{-1} - \mathrm{t}_{cl}^2 \cdot \mathrm{g}_{ll}^a(\omega) \right)} \end{aligned} \tag{2.4}$$

The last step for the calculation of the Greens function of this system is to switch on the hopping between the sites. The hopping matrix (N×N) for the system reads:

$$\mathrm{T} = -\mathrm{t}_{cc} \cdot \begin{bmatrix} 0 & 1 & 0 & 0 & \dots & 0 \\ 1 & 0 & 1 & 0 & \dots & 0 \\ 0 & 1 & 0 & 1 & \dots & 0 \\ 0 & 0 & 1 & \ddots & \ddots & \vdots \\ \vdots & 0 & 0 & \ddots & 0 & 1 \\ 0 & \dots & \dots & 0 & 1 & 0 \end{bmatrix} \tag{2.5}$$

Make use of the Dyson-equation and with $\mathrm{g}_{cc}^{r/a/K}(\omega)$ (N×N), the Greens function of the system isolated site connected to the bath, we get:

$$\begin{aligned} \mathrm{G}^{r/a}(\omega) &= \left(\left(\mathrm{g}_{cc}^{r/a}(\omega) \right)^{-1} - T \right)^{-1} \\ \mathrm{G}^{K}(\omega) &= \mathrm{G}^{r}(\omega) \cdot \frac{\mathrm{g}_{cc}^{K}(\omega)}{|\mathrm{g}_{cc}^{r}(\omega)|^2} \cdot \mathrm{G}^{a}(\omega) \end{aligned} \tag{2.6}$$

$\mathrm{G}^{r/a/K}(\omega)$ is the Greens function of the system. Because of the translational invariance of the considered system (tight-binding chain) the Greens function has several symmetries, that can be used during the calculation.

$$\mathrm{G}_{\mathrm{ij}}^{\mathrm{r/a}}(\omega) = \begin{cases} -\left(\mathrm{G}_{\mathrm{-i-j}}^{\mathrm{r/a}}(-\omega) \right)^{*} & \mathrm{i} = \pm \mathrm{j} \\ \mathrm{G}_{\mathrm{ji}}^{\mathrm{r/a}}(\omega) & \mathrm{i} \neq \mathrm{j} \\ (-1)^{|\mathrm{i}-\mathrm{j}|-1} \left(\mathrm{G}_{\mathrm{-i-j}}^{\mathrm{r/a}}(-\omega) \right)^{*} & \text{else} \end{cases} \tag{2.7}$$

For the retarded component and for the Keldysh:

$$\mathrm{G}_{\mathrm{ij}}^{\mathrm{K}}(\omega) = \begin{cases} \left(\mathrm{G}_{\mathrm{-i-j}}^{\mathrm{K}}(-\omega) \right)^{*} & \mathrm{i} = \pm \mathrm{j} \\ (-1)^{|\mathrm{i}-\mathrm{j}|} \left(\mathrm{G}_{\mathrm{-i-j}}^{\mathrm{K}}(-\omega) \right)^{*} & \mathrm{i} \neq \mathrm{j} \\ -\left(\mathrm{G}_{\mathrm{ji}}^{\mathrm{K}}(\omega) \right)^{*} & \text{else} \end{cases} \tag{2.8}$$

The indices i and j stand for the treated site on the chain. The origin of the system (site with index 0) lies in the centre of the chain. From this point on the sites are numbered consecutively: $\dots, -2, -1, 0, 1, 2, \dots$.

This Greens function can be used to calculate the currents in the system. The other possibility to calculate the Greens function of an infinite tight-binding chain is to couple two semi-infinite chains like it is shown in Section 1.4.1.

2.3 Current Calculation

This Section deals with the calculation method of the currents, we are interested in. First there is the main current in this system, which can be calculated with the current between two neighbouring sites. Secondly we are also interested in the current from the chain sites into the coupled fermionic baths. It will turn out to be zero on average, but at some points electrons flow into and at others out of the system. The next calculation is the energy current. These results will be compared to the estimated current of Jong E.Han [13].

2.3.1 Current between two neighbouring sites

For the derivation of the current in the chain we use:

$$\mathrm{j}^{(n,n+1)} = \mathrm{Re}\left(\sum \mathrm{G}^{K}_{n,n+1}(\omega)\right) \cdot \frac{\Delta\omega}{2\pi} \tag{2.9}$$

The current between two neighbouring sites should be the same everywhere along the chain. To show the behaviour of the current through the system, we calculate it at the middle of the central region. There are the smallest fluctuations because of the missing boundary effects. The detailed description follows in Section 2.4 and Fig.2.3.

2.3.2 Current from chain to bath

The current between a central site and a coupled fermion reservoir reduces to:

$$\begin{aligned} \mathrm{j}^{(n)}_{cb} &= \mathrm{t}_{cb} \cdot \mathrm{Re}\left(\sum \mathrm{G}^{K}_{cb}(\omega)\right) \cdot \frac{\Delta\omega}{2\pi} \\ \mathrm{G}^{K}_{cb}(\omega) &= (\mathrm{G}^{K}(\omega))^{(n,n)} \cdot (\mathrm{g}^{a}_{b}(\omega))^{(n,n)} + (\mathrm{G}^{r}(\omega))^{(n,n)} \cdot (\mathrm{g}^{K}_{b}(\omega))^{(n,n)} \end{aligned} \tag{2.10}$$

With $(\mathrm{G}^{K}(\omega))^{(n,n)}$ the Greens function of the system at position (n,n) and with $(\mathrm{g}^{K}_{b}(\omega))^{(n,n)}$ the bath Greens function at position (n,n). This means that g_b has to be shifted in energy space to match the site on the chain. These parameters $\mathrm{j}^{(n)}_{cb}$ are the chain-bath-currents.

We will see, that sometimes electrons flow from the chain into the bath and sometimes from the bath into chain. But the entire (averaged) chain-bath current j_{cb},

$$\mathrm{j}_{cb} = \frac{1}{\mathrm{N}} \sum_{n=1}^{\mathrm{N}} \mathrm{j}_{cb}^{(n)}$$

is always zero. (Section 2.4 and Fig.2.3)

2.3.3 Energy current

For the energy flux we can use:

$$\begin{aligned} \mathrm{j}_E^{(n,n+1)} &= \mathrm{t}_{cb}^2 \cdot \mathrm{t}_{cc} \cdot \mathrm{Re}\left(\sum (\mathrm{G}_{b,c}^K(\omega))^{(n,n+1)}\right) \frac{\Delta\omega}{2\pi} \\ (\mathrm{G}_{b,c}^K(\omega))^{(n,n+1)} &= \left((\mathrm{g}_b^K(\omega))^n + (\mathrm{g}_b^K(\omega))^{n+1}\right) (\mathrm{G}^a(\omega))^{(n,n+1)} + \\ &\quad + (\mathrm{g}_b^r(\omega))^n (\mathrm{G}^K(\omega))^{(n,n+1)} + (\mathrm{g}_b^r(\omega))^{n+1} (\mathrm{G}^K(\omega))^{(n+1,n)} \end{aligned} \tag{2.11}$$

This is now the energy current between two neighbouring sites. For the whole energy flux through the system, we calculate:

$$\mathrm{j}_E = \frac{1}{\mathrm{N}-1} \sum_{n=1}^{\mathrm{N}-1} \mathrm{j}_E^{(n,n+1)}$$

This quantity is very important. It shows characteristics of Joule heating. Further discussions are given in Section 2.4.

2.3.4 Approximative expression for the current

For the approximative derivation of the current we study an one-dimensional tight-binding model connected to fermionic reservoirs under an uniform electric-field E. This model is described by the Hamiltonian (eq.(2.1)).

J.Han approximates the DC current in [13] in the wide band limit to:

$$\mathrm{j}_{\mathrm{approx}} \approx \frac{4\mathrm{t}_{cc}\Gamma\mathrm{E}}{\pi(\mathrm{E}^2 + 4\Gamma^2)} \tag{2.12}$$

Γ is the damping and $\Gamma \ll \mathrm{t}_{cc}$. We choose Γ to be 0.1. The dependency of the damping on the fermionic reservoirs is given by $\Gamma = \pi \mathrm{t}_{cb}^2 \mathrm{N}(0)$, where $\mathrm{N}(0)$ is the density of states of the bath. As one will see, the choice of the hopping-parameters with respect to the damping is very important.

2.4 Results and Discussion of the numerical calculation

2.4.1 System with fermionic reservoirs

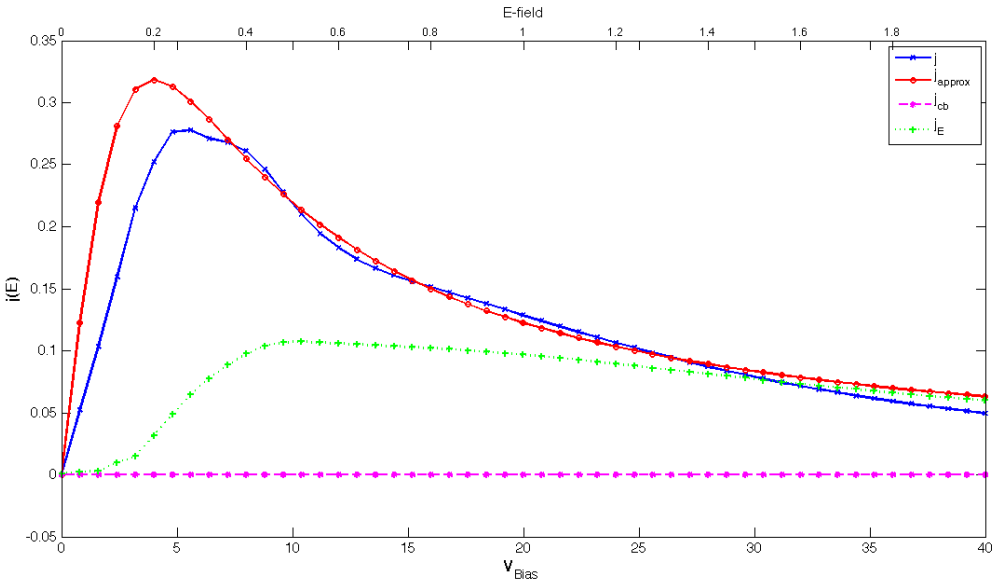

Figure 2.2: We show the behaviour of the current in a system of N=21 sites driven by an electric field, with the following parameters: $t_{cc} = 1, t_{cb} = 1, t_{bb} = 10, \Gamma = 0.1$ The blue line shows the current between neighbouring sites int the center of the centred region, calculated with equation (2.9). Furthermore equation (2.12), (2.10) and (2.11) were used to calculate the approximative current by Han (red) for an infinite chain, the chain-bath-current (purple) and the energy flux (green).

The current between chain and bath is always zero, as it was should be. For a detailed consideration we have a look at the current j between two neighbouring sites and j_{cb} for each chain-bath-site for a system consisting of 101 sites. Fig.2.3 shows the behaviour of the current j_{cb}. As one can see, it is always zero except at the beginning and the end of the chain (because of boundary effects). Particles can flow into the system at the beginning and can flow out of the system at the end of the chain through the reservoir.

This is one reason, why the current at the center of the system is used for further calculations.

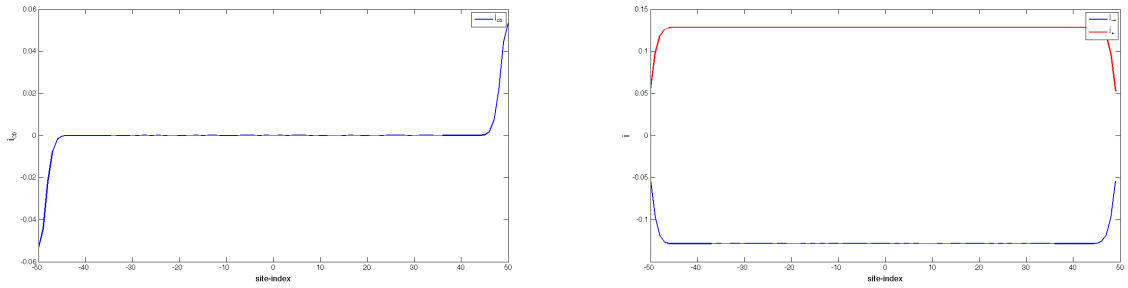

Figure 2.3: $t_{cc} = 1, t_{cb} = 1, t_{bb} = 10$, N = 101. j and j_{cb} with respect to the site-index at E = 1

The current j between neighbouring sites shows a similar behaviour. There are boundary effects at the chain-ends. Otherwise the current has always the same value. The plot shows the right- (blue) and the left-going (red) current. These currents are the same but point in different directions. The right-going current is a hole-like current (they propagate with the electric field) and the left-going current corresponds to the electron current (they propagate towards the field direction).

In Fig.2.2 one can also see the characteristics of the energy flux. It raises linearly until the current has reached its maximum and then slowly decreases. The energy current in the low-bias regime follows the rules of **Joule heating**. These are electrons which get accelerated by an electric-field, collide with the ions of the material and give off their kinetic energy in the form of thermal energy. In our considered system with the coupled baths this referes to the dissipation into the infinite baths. Which means, that energy gets transported away by these semi-infinite tight-binding chains. This refers to a two regime system in the case of coupled fermionic reservoirs. As it will be discussed later, the current has an ohmic like behaviour in the low field regime (the reservoirs have no effect on the current) and for high fields other fundamental transport mechanism take place.

The approximative formula for the current due to Jong E.Han [13] fits to the numerical

result of j very well. The right choice of the hopping-parameter t_{bb} (Han works in the wide band limit, where $t_{bb} \gg t_{cc}$) is an important factor. As we can see in Fig.2.3 j_{approx} and j coincide very well with $t_{bb} = 10$. Furthermore a smaller parameter t_{bb} leads to significant changes in the behaviour of the numerical calculated current as one can see in Fig.2.4. This means that the hopping in the baths has to be very strong to let the reservoirs act like fermionic baths to support the energy dissipation.

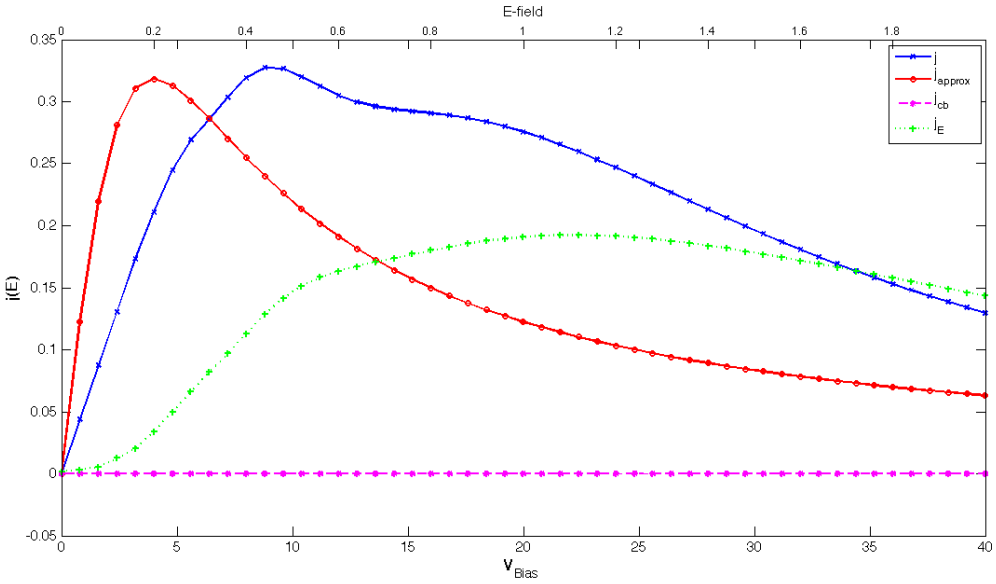

Figure 2.4: Same as Fig.2.2 but with $t_{bb} = 4$

2.4.2 Low field Regime

As predicted before, the current has different behaviour in the high- and low-field regime. To understand the low field-regime $E \ll \Gamma$ one should have a look at the scattering state formalism [14].
When the electric-field is applied to the one-dimensional tight-binding chain each site and the coupled fermion reservoir are on a potential slope. The potential drop from site to site is denoted with E. This means that the potential energy difference of the chain is given by $V_{Bias} = (N - 1) \cdot E$.

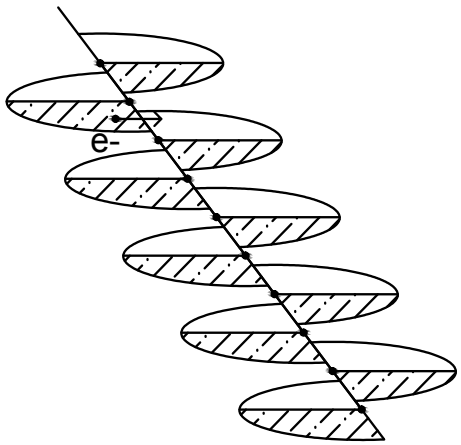

Figure 2.5: Shows the overlap of valence and conduction band in the low field regime. So that electrons can scatter in another state without absorbing energy.

In the scattering state the fermion reservoirs are open systems. If an electron scatters into a reservoir it never comes back again. The moving electron on the slope leaves electron-hole pairs in the reservoirs because of particle exchange. These pairs travel along the infinite baths. The reservoirs are responsible for inelastic processes (compareable to bosonic baths) and transport energy into the bath chains. The only flux to the reservoirs is an energy flux (Joule heating), a net current isn't present. The extent of the scattered wave is shorter than the length of the reservoir chain. This means, that the wave in the reservoir isn't being backscattered from the edge. The fermionic baths act like energy reservoirs and can be treated as bosonic baths without the resulting nonlinear effects of Bose-Einstein statistics. [14]
These fermionic reservoirs connect the model with the Boltzmann transport theory for small electric fields. In this theory the drift velocity of the electrons gets changed by the electric-field. This leads to a shift of the Fermi surface in the Brillouin zone and the electrons can scatter into the next empty state, which leads to a well-known relation. Characteristic for the low field regime is a general DC current relation and valid Ohm's law with the Drude conductivity per electron [13].

$$\mathrm{j} \propto \frac{\mathrm{E}}{\Gamma \mathrm{m}^*}$$

2.4.3 High field regime

As $E \gg \Gamma$, there is no linear regime for the shift of the Fermi surface anymore. Ohm's law isn't valid anymore.

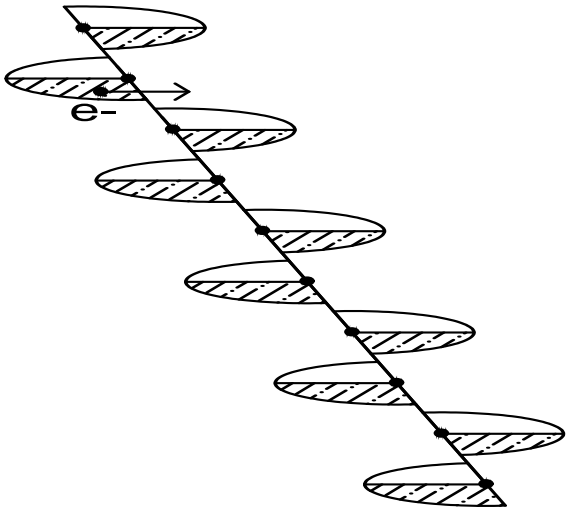

Figure 2.6: Shows the overlap of valence and conduction band in the high field regime. Electrons can't scatter and tunnel respectively.

The surfaces are shifted so far, that the electrons can't scatter into the next state. This means, that the scattering state formalism isn't valid anymore. The current now originates from a different transport mechanism. It gives raise to the so-called Bloch Oscillations, which lead to an with rising field decreasing current. (Section 3)

2.4.4 System without baths

If the fermion reservoirs aren't coupled to the central region the current behaves different to the characteristics in Fig.2.2.

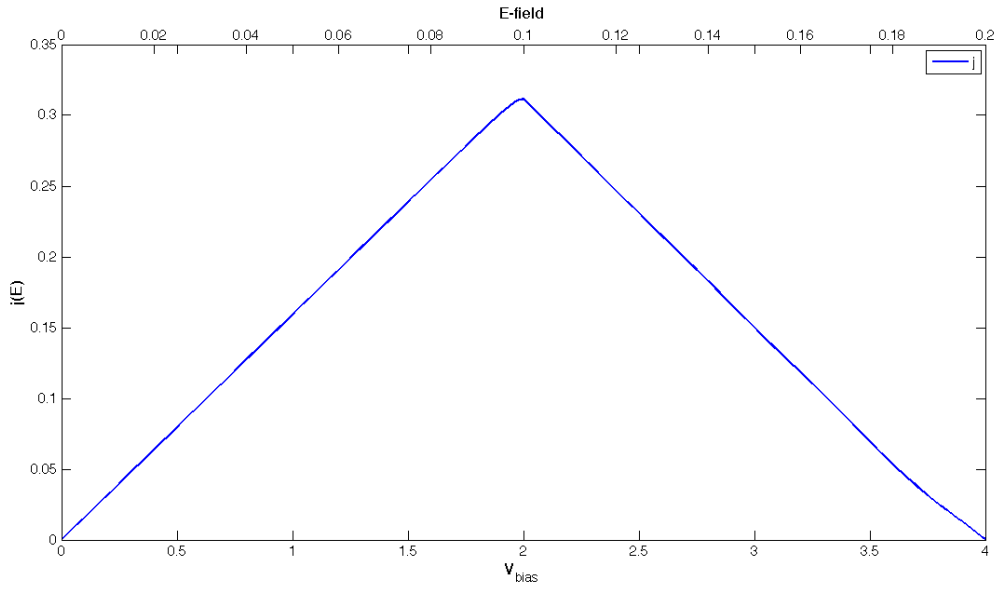

Figure 2.7: Current in the system without fermion reservoirs. With following parameters: $t_{cc} = 1, t_{cb} = 0, t_{bb} = 10, N = 21, \Gamma = 0.1$

As one can see, there is only a current flowing if the bias voltage V_{Bias} is smaller than the bandth width:

$$\Delta x = \frac{4t_{cc}}{E}$$

where Δx is the length of the chain. This implies that the coupled fermionic reservoirs are responsible for the energy dissipation in the high field regime. Due to the coupling of the baths, a current can flow for higher fields. If the bias voltage is higher than the band width bloch oscillations prevent the electrons from moving steadily through the device, which leads to the decreasing current characteristic in the high field regime.

2.4.5 Dependency on the hopping parameters

The current has a specific dependency on the hopping parameters t_{lc} and t_{cc}. In the previous sections we discussed the connection of the current with t_{bb} and t_{cb}. If we choose t_{lc} to be zero (in the case of disconnected reservoirs), there would be no current flowing in the central region. This case doesn't need to be discussed further.

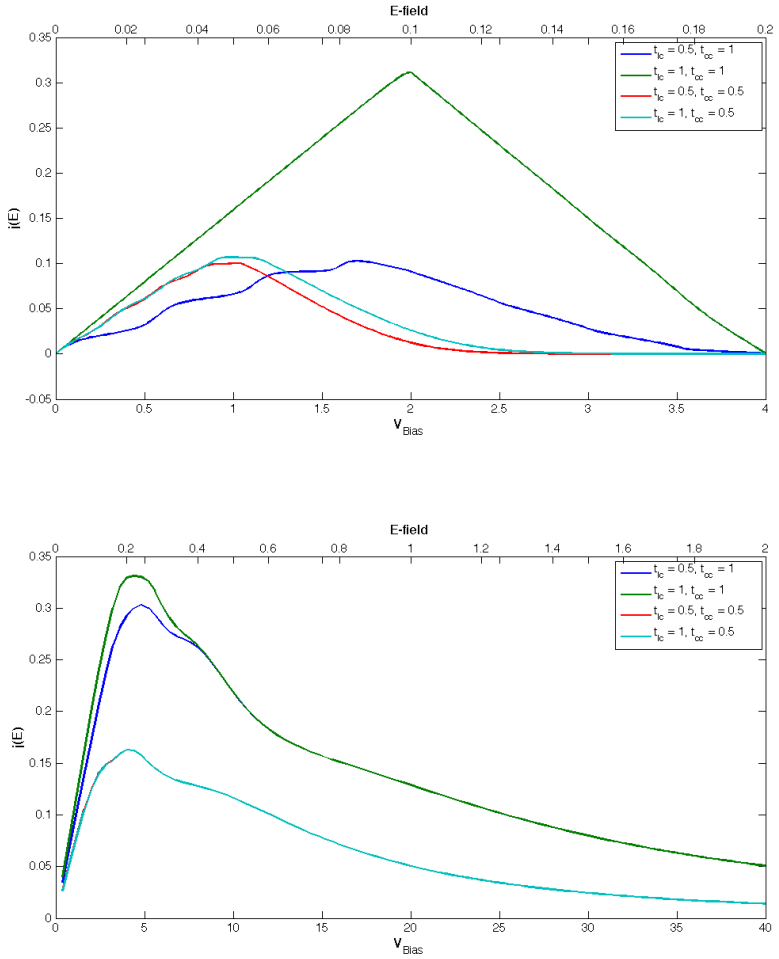

Figure 2.8: Dependency of the current on the hopping parameters t_{lc} and t_{cc} for a central region consisting of N=21 sites. The upper plot shows the characteristics without coupled fermionic reservoirs ($t_{cb} = 0$) and the lower plot the behaviour with energy dissipation ($t_{cb} = 1$).

As one can see, the modification of the hopping in the chain t_{cc} has more consequence on the current characteristic than the variation of t_{lc} when the fermionic reservoirs are switched on. In this case the hopping from the lead to the chain could also be zero, because the baths always put energy to the system so that a current can flow. If the hopping in the chain t_{cc} is decreased there isn't as much current in the system flowing as before. But the choice of these parameters have no consequence on the main behaviour of the current. The splitting in the two regimes (low electric fields with linear DC current and high fields with an oscillating current [nonlinear transport through Bloch Oscillations]) hold up. The fermionic reservoirs take effect on the current for $E \gg \Gamma$.
For the case of $t_{cb} = 0$ we find that if t_{cc} is decreased there is less current flowing (than before). If t_{lc} is decreased the maximum of the current is shifted towards lower electric fields and for $t_{lc} = 0$ there is no current flowing anymore because there are no reservoirs available for the energy supply.

2.5 Conclusion

With the inculsion of a dissipation mechanism (fermionic reservoirs) in the studied system to understand the transport properties, one can treat the flowing current in the picture of displaced Fermi surfaces at small fields. For higher fields this isn't right anymore and we recover that the current originates from Bloch oscillations.

In the low field regime $\mathrm{E} \ll \Gamma$ (inside the bandwith $\mathrm{E} < \frac{4\mathrm{t}_{cc}}{\mathrm{N}-1}$) the current can be described by the Boltzmann transport theory. The picture of the shifted Fermi seas is valid, which means that the current follows the linear response theory and the displacement of the wave number (in the scattering state formalism [13]) behaves like:

$$\delta\mathrm{k} \propto \mathrm{E}\tau$$
$$\tau \sim \Gamma^{-1}$$

The second transport mechanism in this regime is Zener tunneling. The displacement of the occupied conduction band and the empty valence band is so low that the electrons can tunnel from one to the other. Ohm's law is valid and a DC current arises:

$$\mathrm{j} = \sigma\mathrm{E}$$
$$\sigma = \frac{\mathrm{e}^2\tau\mathrm{n}}{\mathrm{m}}$$

For higher fields $\mathrm{E} \gg \Gamma$ there is an oscillating current and a nonlinear transport mechanism sets in. This can be described in terms of the Bloch oscillations. They start if:

$$\tau \gg \tau_B$$

$\tau_B \sim \frac{1}{\mathrm{E}}$ is the Bloch oscillation time. The scattering rate of the electrons has to be larger than the oscillation time. The electrons can't scatter into the next state and there is no overlap of the displaced Fermi seas (valence and conduction band) anymore so that the electrons can't tunnel respectively.

3 Bloch Oscillations

3.1 Introduction

For this chapter references [15], [16], [17] and [21] were used.
As we said in the previous chapter, there is the low field regime where tunneling and scattering cause a current and there is a high field regime where the current can only flow through a nonlinear transport mechanism, the so called Bloch Oscillations. The oscillations set in for fields higher than the bandwidth and suppress the current flow. As we will see in a later chapter, there is an expression for the amplitude of the oscillations (eq.(3.12)). One can say, that this amplitude has to be larger than N that a current can flow.

Bloch Oscillations are caused by an external electrical field. The electrons oscillate because of the relation between the effective mass and the dispersion relation in a periodic potential.

$$\mathrm{m}^* = \hbar^2 \left[\frac{\mathrm{d}^2\epsilon(\mathrm{k})}{\mathrm{dk}^2} \right]$$

It can also get negativ for high momenta. An electric-field causes an acceleration of the electrons.

$$\dot{\mathrm{x}} = \frac{\mathrm{e}}{\mathrm{m}^*} \cdot \mathrm{E}$$

If the effective mass was negative, an additional force doesn't accelerate the electrons further. Instead they get decelerated and accelerated in the other direction. Oscillations take place with an oscillation frequency:

$$\omega_\mathrm{B} = \frac{\mathrm{e}}{\hbar} \cdot \mathrm{E} \cdot \mathrm{a}$$

with a the lattice spacing. These Bloch Oscillations can be observed if the oscillation period τ_B is smaller than the scattering time of the electrons ([15]) . One cycle has to

be finished before scattering takes place The electrons move with a period:

$$\tau_{\mathrm{B}} = \hbar/\mathrm{aeE}$$

These oscillations are important because they are sources of an oscillating current. As we saw in the previous chapter Bloch Oscillations describe the transport mechanism in the high field regime. In the low field regime there is an ohmic-like current.
The Bloch Oscillations can't be seen in natural solids because of the comparatively small lattice constant. Hence the oscillation frequency ω_{B} is very small even for very high fields and the charge carriers can't finish a full oscillation within the scattering time.

3.2 Mathematical Approach

There are two possibilities for the visualization of the Bloch Oscillations. The first one is a time evolution with a diagonalization of the Hamiltonian for the system on a one-dimensional tight-binding chain (no baths and leads) and the other one is a Greens function approach.

3.2.1 Diagonalization

The Hamiltonian of this system writes:

$$\hat{\mathrm{H}} = \mathrm{t} \sum_{\langle \mathrm{ij} \rangle} \hat{\mathrm{a}}_\mathrm{i} \hat{\mathrm{a}}_\mathrm{j}^\dagger - \mathrm{E} \sum_\mathrm{i} \mathrm{i} \cdot \hat{\mathrm{n}}_\mathrm{i} \tag{3.1}$$

t is the hopping strenght of the electrons and $\hat{\mathrm{a}}, \hat{\mathrm{a}}^\dagger$ are the fermionic annihilation and generation operators. The expression $\langle \mathrm{ij} \rangle$ says that the sum extends over the nearest neighbours. E denotes the electrical field and the last sum says something about the slope of the chain. For the time evolution of a state, one can write:

$$|\psi(\mathrm{t})\rangle = \exp(i\hat{\mathrm{H}}\mathrm{t}) \, |\psi_0\rangle \tag{3.2}$$

After the diagonalization the Hamiltonian reads:

$$\hat{\mathrm{H}} = \mathrm{UDU}^{-1} \tag{3.3}$$

where D is a diagonal matrix with eigenvalues on the main diagonal and U is a matrix with the accompanying eigenvectors. The state of the system can be written as a linear combination of eigenstates of the Hamiltonian and for the evolution coefficients one can

write:

$$\begin{aligned}
\vec{c}(t) &= \exp(-i\hat{H}t)\vec{c}_0 \\
\vec{c}(t) &= U\exp(-iDt)U^{-1}\vec{c}_0 \qquad /U^{-1}\cdot \\
U^{-1}\vec{c}(t) &= \exp(-iDt)U^{-1}\vec{c}_0 \qquad /\vec{d}(t) = U^{-1}\vec{c}(t) \\
\vec{d}(t) &= \exp(-iDt)\vec{d}_0
\end{aligned} \tag{3.4}$$

With eq.(3.4) one can now calculate the time evolution of a wave packet on a tight-binding chain ([18]).

3.2.2 Greens function method

The time evolution of a state now reads ([19, pg. 9]):

$$\psi(\vec{r},t) = i\int_{-\infty}^{\infty} d\vec{r}' G^r(\vec{r},\vec{r}';t-t_0)\psi(\vec{r}',t)$$

$G^r(\vec{r},\vec{r}';t-t_0)$ denotes the retarded Greens function matrix which depends on the relativ positions of the sites on the tight-binding chain and $\psi(\vec{r}',t)$ is the starting vector for the time evolution of a wave packet.
The retarded Greens function can be evaluated by using the CPT approach. $g^r_{cc}(\vec{r},\vec{r}';\omega)$ is the Greens function of the isolated sites of the system with coupled leads and coupled fermionic reservoirs. With CPT one can calculate the full Greens function for the system with a hopping matrix T, which denotes the hopping between the nearest neighbour atoms.

$$G^r(\vec{r},\vec{r}';\omega) = \left(g^r_{cc}(\vec{r},\vec{r}';\omega)^{-1} - T\right)^{-1}$$

For the time evolution we need the Greens function in time. For the calculation one has to carry out a Fourier transformation with τ =t-t_0

$$G^r(\vec{r},\vec{r}';\tau) = \frac{1}{2\pi}\int d\omega \exp(-i\omega\tau)G^r(\vec{r},\vec{r}';\omega)$$

In the discrete space the time dependent Greens function and the time evolution of the state reads:

$$\begin{aligned} \mathrm{G^r}(\vec{\mathrm{r}},\vec{\mathrm{r}}';\tau) &= \frac{1}{2\pi}\sum_{\mathrm{n}=1}^{\mathrm{N}} \exp(-i\omega_\mathrm{n}\tau)\mathrm{G^r}(\vec{\mathrm{r}},\vec{\mathrm{r}}';\omega_\mathrm{n})\Delta\omega \\ \psi(\vec{\mathrm{r}},\mathrm{t}) &= \sum_{\vec{\mathrm{r}}'} i\mathrm{G^r}(\vec{\mathrm{r}},\vec{\mathrm{r}}';\tau)\psi(\vec{\mathrm{r}}',\mathrm{t}) \end{aligned} \tag{3.5}$$

The Greens function of an isolated site of the chain without the coupled fermionic baths ($\mathrm{t}_{cb} = 0$) reads:

$$\mathrm{g^r_{cc}}(\omega) = \frac{1}{\omega - \epsilon_\mathrm{k} + i\mathrm{o}^+}$$

ϵ_k is the on-site energy and the factor $i\mathrm{o}^+$ ensures the causality in frequency space. For an expression in time space one has to carry out a Fourier transformation:

$$\mathrm{g^r_{cc}}(\tau) = \frac{1}{2\pi}\int_{-\infty}^{\infty} \mathrm{d}\omega \exp(-i\omega\tau)\frac{1}{\omega - \epsilon_\mathrm{k} + i\mathrm{o}^+}$$

For the evaluation one has to make use of Cauchy principal value:

$$\int_{-\infty}^{\infty} \frac{\mathrm{f(k)}}{\mathrm{k} - \mathrm{k}' \pm i\mathrm{o}^+}\mathrm{dk} = P\int_{-\infty}^{\infty} \frac{\mathrm{f(k)}}{\mathrm{k} - \mathrm{k}'}\mathrm{dk} \mp \mathrm{f(k')}$$

Now there is an expression for the time dependend retarded Greens function

$$\mathrm{g^r_{cc}}(\tau) = -\frac{i}{2\pi}\Theta(\tau)\exp(-i\epsilon_\mathrm{k}\tau) \tag{3.6}$$

$\Theta(\tau)$ ensures the causality in time space, which means that there has to be a disorder of the system first and then the response follows.

$$\mathrm{g^r_{cc}}(\tau) = \begin{cases} 0 & \tau < 0 \\ \sim \exp(-i\epsilon_\mathrm{k}\tau) & \tau > 0 \end{cases} \tag{3.7}$$

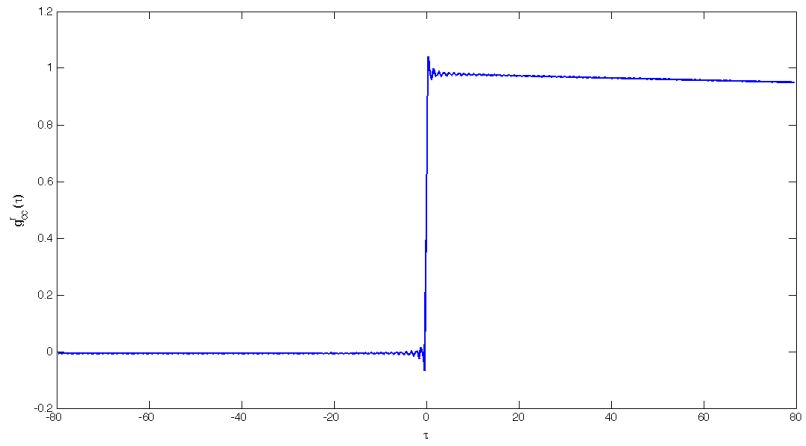

Figure 3.1: The retarded Greens function of an isolated site on a chain with $\epsilon_0 = 0$ in dependency of time. There is no electric-field and the chosen parameters are: $o^+ = 0.0004$, $N_\omega = 4000$.

This figure shows the properties of the time dependent Greens function. As one can see, the retarded function is zero for times smaller 0, which means that there is only a response after the disorder. Then it jumps to the value of 1. At this point we can see the Gibb's phenomena, which is a numerical calculation result. Normally the Greens function characteristic would oscillate there with the excitation energy of the system ϵ_k. Because of the absence of hopping t_{cc} the Greens function looks the same on every site of the chain. (For programming, the choice of the parameters o^+ and N_ω to each other is very important. If the number of frequency points was chosen too low, the step function would shift. If the complex parameter o^+ was chosen too high, the function slopes down; but it should always stay approximately at a value of 1).

Because of the symmetries of the tight-binding chain, there are symmetries for the Greens function of the full system (with hopping between the sites). The site 0 should lie in the middle of the considered system (numbered as follows: $\ldots, -2, -1, 0, 1, 2, \ldots$).

$$\begin{aligned} G^r_{i,j}(\tau) &= (-1)^{|i-j|-1} G^r_{-i,-j}(\tau) \\ G^r_{i,j}(\tau) &= G^r_{j,i}(\tau) \end{aligned} \tag{3.8}$$

3.2.3 Appraisal of the Bloch Oscillations

Following considerations are based on [20].
We have a look at the full system consisting of the central region (N-site tight-binding chain), 2 coupled leads (infinite chains). The Hamiltonian of this system reads:

$$\begin{aligned}
\hat{\mathrm{H}} &= \hat{\mathrm{H}}_{\mathrm{cc}} + \hat{\mathrm{H}}_{\mathrm{ll}} + \hat{\mathrm{H}}_{\mathrm{lc}} \\
\hat{\mathrm{H}}_{\mathrm{cc}} &= -\mathrm{t}_{cc} \sum_{\mathrm{m}=1}^{\mathrm{N}-1} \left(|\mathrm{m}\rangle \langle \mathrm{m}+1| + \mathrm{h.c} \right) + \mathrm{E} \sum_{\mathrm{m}} \mathrm{m} \, |\mathrm{m}\rangle \langle \mathrm{m}| \\
\hat{\mathrm{H}}_{\mathrm{lc}} &= -\mathrm{t}_{lc} \left(|\mathrm{M}, \mathrm{L}\rangle \langle 1| + |1, \mathrm{R}\rangle \langle \mathrm{N}| + \mathrm{h.c} \right) \\
\hat{\mathrm{H}}_{\mathrm{ll}} &= \sum_{\alpha=\mathrm{L,R}} \hat{\mathrm{H}}_{\alpha} \qquad \hat{\mathrm{H}}_{\alpha} = -\mathrm{t}_{ll} \sum_{\mathrm{m}=1}^{\mathrm{M}} |\mathrm{m}, \alpha\rangle \langle \mathrm{m}+1, \alpha|
\end{aligned}$$

$\hat{\mathrm{H}}_{\mathrm{cc}}$ is the Hamiltonian of the central region consisting of a one-dimensional tight-binding chain (N-sites) with nearest neighbour hopping and a slope caused by an uniform electric field E.
$\hat{\mathrm{H}}_{\mathrm{ll}}$ is the Hamiltonian of the left and right leads (tight-binding chains with M-sites).
$\hat{\mathrm{H}}_{\mathrm{lc}}$ is the coupling of the central region and the leads. The M-th place of the left lead has to be coupled to the first site of the central region and the first site of the right lead to the N-th place of the central region.

From the dispersion relation one can calculate the position of the relativ maximum as a function of time. For this we start out from the equation of motion for an electron in an external field and this gives us ([15]):

$$\mathrm{k(t)} = -\frac{\mathrm{eE}}{\hbar}\mathrm{t}$$

and the vector $|\mathrm{k}\rangle$ can be written as:

$$|\mathrm{k}\rangle = \frac{1}{\sqrt{\mathrm{N}}} \sum_{\mathrm{m}} \exp(-i\mathrm{kam}) \, |\mathrm{m}\rangle$$

Leads:

$$
\begin{aligned}
\epsilon(\mathrm{k}) &= -2\mathrm{t}_{ll}\cos(\mathrm{ka}) \\
\mathrm{v_L}(\mathrm{k}) &= \frac{1}{\hbar}\frac{\partial\epsilon(\mathrm{k})}{\partial\mathrm{k}} = \frac{2\mathrm{at}_{ll}}{\hbar}\sin(\mathrm{ka}) \\
\mathrm{x_L}(\mathrm{t}) &= \int \mathrm{dt}\mathrm{v_L}(\mathrm{k}(\mathrm{t})) = -\frac{2\mathrm{at_{ll}}}{\hbar}\int \mathrm{dt}\sin(\frac{\mathrm{eEa}}{\hbar}\mathrm{t}) \\
\mathrm{x_L}(\mathrm{t}) &= \frac{2\mathrm{t_{ll}}}{\mathrm{eE}}\cos(\frac{\mathrm{eEa}}{\hbar}\mathrm{t})
\end{aligned}
\tag{3.9}
$$

Coupling:

$$
\begin{aligned}
\epsilon_{\mathrm{lc}}(\mathrm{k}) &= -\mathrm{t}_{lc}\left[\frac{1}{\mathrm{N}}\sum_{\mathrm{n,m}}\exp(i\mathrm{ka(m\text{-}n)})\left(\langle\mathrm{m}|\,|\mathrm{M}\rangle\,\langle 1|\,|\mathrm{N}\rangle + \langle\mathrm{m}|\,|1\rangle\,\langle\mathrm{N}|\,|\mathrm{n}\rangle\right)\right] \\
&= -\frac{\mathrm{t}_{lc}}{\mathrm{N}}\left[(\exp(i\mathrm{ka(M\text{-}1)}) + \exp(i\mathrm{ka(N\text{-}1)})) + \mathrm{h.c}\right] \\
&= -\frac{2\mathrm{t}_{lc}}{\mathrm{N}}\left(\cos(\mathrm{ka(M\text{-}1)}) + \cos(\mathrm{ka(M\text{-}1)})\right) \\
\mathrm{v_{lc}}(\mathrm{k}) &= \frac{2\mathrm{t}_{lc}a}{\mathrm{N}\hbar}\left[(\mathrm{M}-1)\sin(\mathrm{ka(M\text{-}1)}) + (1-\mathrm{N})\sin(\mathrm{ka(1\text{-}N)})\right] \\
\mathrm{x_{cl}}(\mathrm{t}) &= \frac{2\mathrm{t}_{lc}}{\mathrm{NeE}}\left(\cos(\frac{\mathrm{eEa(M\text{-}1)}}{\hbar}\mathrm{t}) + \cos(\frac{\mathrm{eEa(1\text{-}N)}}{\hbar}\mathrm{t})\right)
\end{aligned}
\tag{3.10}
$$

Central:

$$
\begin{aligned}
\epsilon_{\mathrm{cc}}(\mathrm{k}) &= -\mathrm{t}_{cc} \sum_{\mathrm{m}} \left[\frac{1}{\sqrt{N}} \sum_{\mathrm{x,y}} \exp(i\mathrm{ka(x\text{-}y)}) \left(\langle \mathrm{x} | \, | \mathrm{m} \rangle \langle \mathrm{m}+1 | \, | \mathrm{y} \rangle + \mathrm{h.c} \right) + \frac{\mathrm{E}}{\mathrm{N}} \sum_{\mathrm{x,y}} \exp(i\mathrm{ka(x\text{-}y)}) \langle \mathrm{x} | \, | \mathrm{m} \rangle \langle \mathrm{m} | \, | \mathrm{y} \right. \\
&= -\frac{\mathrm{t}_{cc}}{\mathrm{N}} \sum_{\mathrm{m}} \left(2\cos(\mathrm{ka}) + \mathrm{E} \cdot \mathrm{m} \right) \\
&= -\mathrm{t}_{cc} \left(2\cos(\mathrm{ka}) \underbrace{\frac{1}{\mathrm{N}} \sum_{\mathrm{m}} 1}_{1} + \mathrm{E} \underbrace{\frac{1}{\mathrm{N}} \sum_{\mathrm{m}} \mathrm{m}}_{\frac{\mathrm{N}+1}{2}} \right) \\
&= -\mathrm{t}_{cc} \left(2\cos(\mathrm{ka}) + \frac{\mathrm{E}}{2}(\mathrm{N}+1) \right) \\
\mathrm{v}_{\mathrm{cc}}(\mathrm{k}) &= \frac{2\mathrm{t}_{cc}\mathrm{a}}{\hbar} \sin(\mathrm{ka}) \\
\mathrm{x}_{\mathrm{cc}}(\mathrm{t}) &= \frac{2\mathrm{t}_{cc}}{\mathrm{eE}} \cos(\frac{eEa}{\hbar}\mathrm{t})
\end{aligned}
\tag{3.11}
$$

With eq.(3.9), (3.10) and (3.11) one can write the dependency of the position on time for the full system and we have an expression for the appraisal of the Bloch Oscillations:

$$
\mathrm{x(t)} = \frac{2}{\mathrm{eE}} \cos(\frac{\mathrm{eEa}}{\hbar}\mathrm{t})(\mathrm{t}_{ll} + \mathrm{t}_{cc}) + \frac{2\mathrm{t}_{lc}\mathrm{N}}{\mathrm{eE}} \left(\cos(\frac{\mathrm{eEa(M\text{-}1)}}{\hbar}\mathrm{t}) + \cos(\frac{\mathrm{eEa(1\text{-}N)}}{\hbar}\mathrm{t}) \right) \tag{3.12}
$$

3.3 Results

For the understand of the Bloch Oscillations one has a look at the time evolution of an initial Gaussian wave packet prepared around the central site on a one-dimensional tight-binding chain. For the start wave packet following distribution was taken:

$$\psi(\vec{\mathrm{r}}, \mathrm{t}) = \frac{1}{2\pi\sigma} \exp\left(-\frac{1}{2}\left(\frac{\vec{\mathrm{r}} - \mu}{\sigma}\right)^2\right) \tag{3.13}$$

With $\rho(\mathrm{t})$ the relativ maximum of the density was denoted. We have a look at the system, where the central region consists out of N=21 sites, each site coupled to fermionic reservoirs with a strength t_{cb}, and two leads.

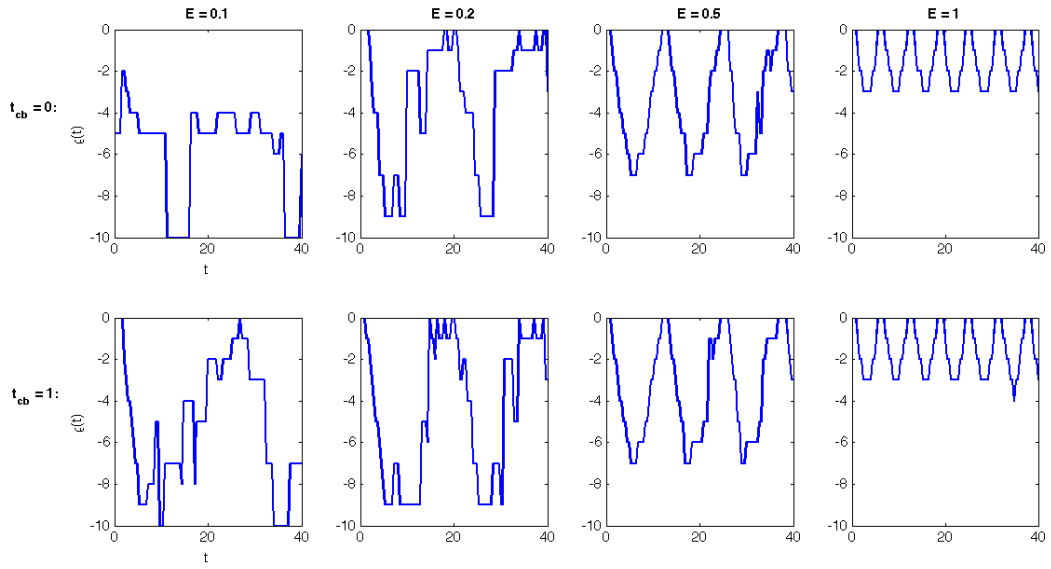

Figure 3.2: The position of the relativ maximum of the distribution in dependency of time. On the y-axis one can see the position of the maximum like the sites were numbered.

Fig.3.2 shows the position of the distribution in dependency of the time. The y-axis denotes the index of the site, where the maximum belongs to a certain time t. In the preparation every site on the chain was given a certain index were the origin lies in the middle

of the chain. This means the sites were numbered like $\ldots, -3, -2, -1, 0, 1, 2, 3, \ldots$. Hence one can see that the distribution moves to the left and back again. For small fields there are no distinct Bloch Oscillations. As the field rises the Bloch Oscillation take over and act like a nonlinear transport mechanism (compare to Fig.2.2). As the field rises the deflection gets smaller but the oscillation frequency rises. This coincides with the predictions of eq.(3.12), which says, that the amplitude is indirect proportional to the electric field E and the oscillation frequency goes with it. Fig.3.2 shows that in this case it doesn't make a difference if the fermionic reservoirs are coupled or not. First a higher deflection with coupled baths ($t_{cb} \neq 0$) was expected because they are responsible for the energy dissipation and should push the distribution further away from the central preparation site. As one can see, with coupled baths the Bloch Oscillations start a little bit earlier, but there are no other consequences because of them.

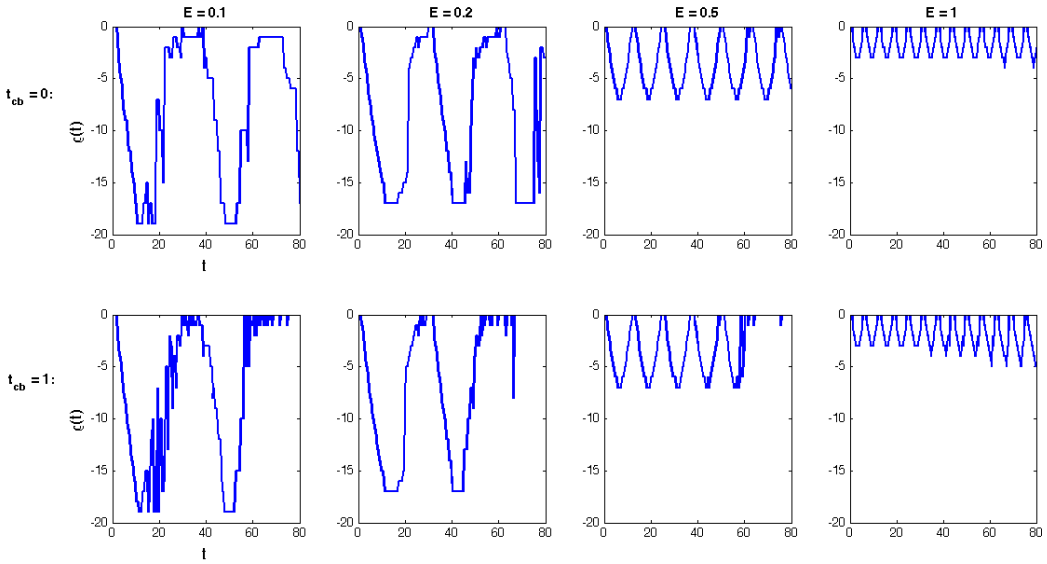

Figure 3.3: The same as Fig.3.2 but with more sites. Now we have N=41 sites.

As we compare Fig.3.2 to Fig.3.3 one can see the dependency on the system size as eq.(3.12) predicts. As the system size rises, the amplitude decreases because it is proportional to 1/N.
For a precise treatment of the dependency of the oscillation amplitude on the electric field, one can look at $\rho(\mathrm{V_{Bias}/E})$.

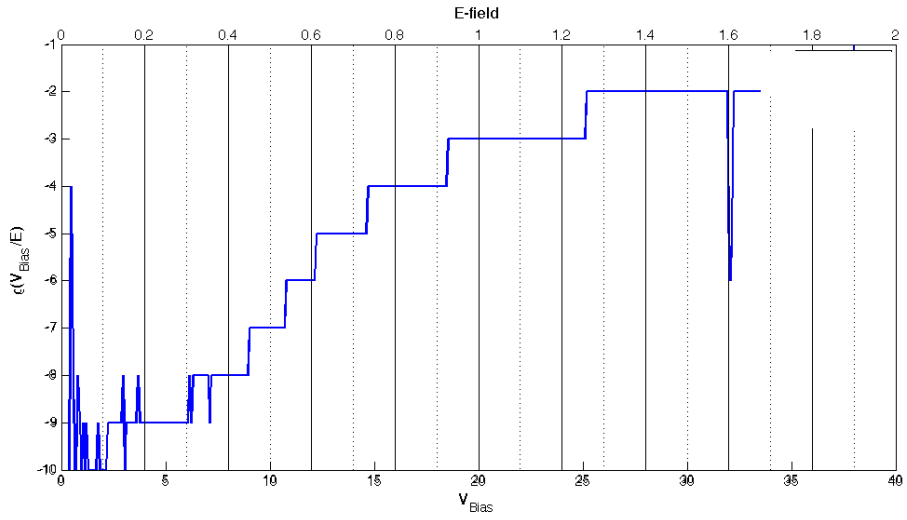

Figure 3.4: Shows the dependency of the amplitude of the Bloch Oscillations on the applied field for N=21.

As the field rises the amplitude (or the relativ position of the maximum of the distribution) decreases. Field and amplitude have a linear relation. The peaks in the low field regime come from the fact, that the Bloch Oscillations aren't distinct and those in the high field regime come from the numerical evaluation.

Fig.3.5 shows the dependency of the the amplitude on the system size. Here it is plotted versus the half system size (chain extending in one direction counted from the central site of the chain). For small fields E $\leq$ 0.2 there is a linear behaviour of the amplitude as predicted in eq.(3.12) up to high system sizes. The peak in the blue line (E=0.1) comes from the numerical evaluation. For higher fields there is a "saturation" of the extent of the oscillations. The reason is, that the fields are so high, that they can't extend any further. As the field increases (N increases), the oscillations decrease (increase).
How does the amplitude depend on the hopping parameters? The dependency on the lead-chain hopping is shown in Fig.3.6. A variation of t_{lc} doesn't have much influence on the behaviour of the Bloch amplitude.

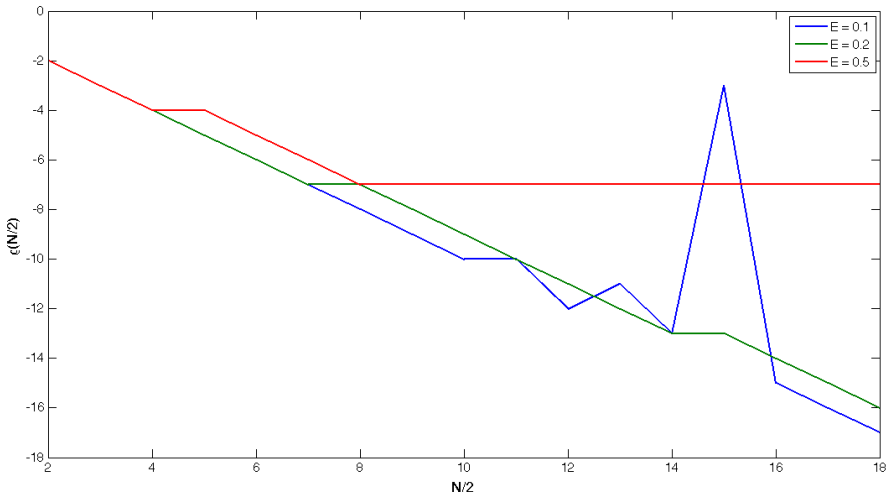

Figure 3.5: Position of the relativ maximum of the initial distribution in dependency of the half system size for various electric fields. Parameters: $t_{cb} = 0, t_{ll} = t_{cc} = t_{lc} = 1$

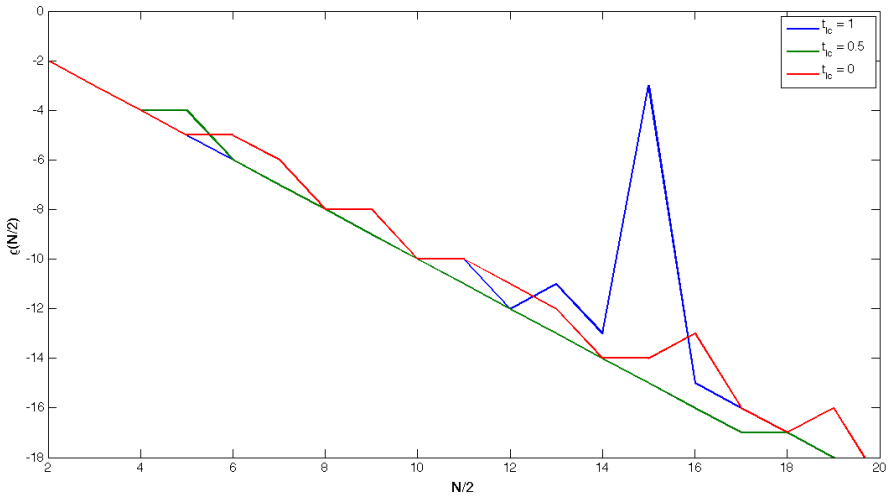

Figure 3.6: The oscillation amplitude as a function of the half system size for various choices of t_{lc} and E=0.1.
$t_{cb} = 0, t_{ll} = t_{cc} = 1$

The choice of the parameter t_{lc} isn't important for the electron transport. This can also be compared to Fig.2.4.5, which shows, that the variation of this hopping parameters doesn't have any influence on the behaviour of the current (and so the Bloch Oscillations) in the high field regime.
But as the hopping in the chain t_{cc} is reduced, the current decreases and so does the amplitude, because the transport gets supressed. Again, the variation of t_{lc} has no influence on the behaviour.

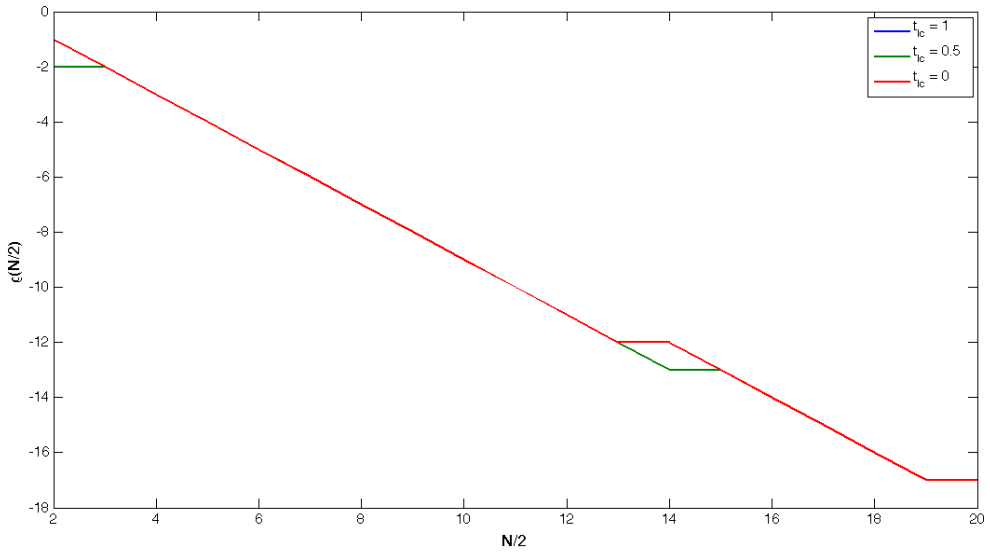

Figure 3.7: Same as Fig.3.6 but now for a lower value of t_{cc}.
E=0.1, $t_{cb} = 0, t_{ll} = 1, t_{cc} = 0.5$

This discovery coincides with the behaviour of the current as one can see in Fig.2.4.5. The reduction of t_{cc} leads to a decrease of the oscillation amplitude and the current but a reduction of t_{lc} doesn't reduce the current.

3.4 Conclusion

The Bloch Oscillations cause a non linear transport mechanism. They set in for high fields if $\tau_B \gg \tau$, which means that a circle has to be finished before the electron can scatter into the next state. As we said before, for small fields the displacement of the fermi seas is so small, that the electrons can tunnel and the current can be described by an ohmic-like behaviour. For high fields, where the displacement of the fermi seas is very high we get an oscillating current described by the Bloch Oscillations. If the amplitude of the oscillations is bigger than the half system size a current can flow. For small fields the central region has a low slope, which means that valence and conduction band overlap and the electrons can scatter into the next state and cause a current flow. For higher fields there is no overlap anymore and the Bloch Oscillations set in.
If we compare the behaviour of the current Fig.2.2 to the behaviour of the amplitude as a function of field Fig.3.4 one can see the predicted characteristics. For fields higher than the bandwidth an oscillating current takes over which slowly falls down, as the field rises. This coincides with the Bloch amplitude, that is proportional to 1/E and decreases as E increases (compare to eq.(3.12)).
This equation also shows the dependency on the system size. As N increases the oscillations increase for small fields (there is a linear dependency; Fig.3.5), but for higher fields there is a "saturation". This is because the field is so high, that the amplitude can't extent over the full system size because of the dependency on the field E.
As Fig.2.4.5, Fig.3.6 and Fig.3.7 show, the dependency on the hopping parameter t_{lc} doesn't carry weight in comparison to the dependency of t_{cc}. As t_{lc} decreases the characteristics of the current and the behaviour of the amplitude stays the same. But as t_{cc} decreases the current goes down and the Bloch amplitude decreases.

In summary one can say, that the current exhibits a linear behaviour for small fields and for higher fields it can be described by the Bloch Oscillations. For high fields the current follow a nonlinear transport mechanism.

4 Alternating Potential

4.1 Model

In this section we want to study the influence of a periodic potential on the current. We consider the following model:

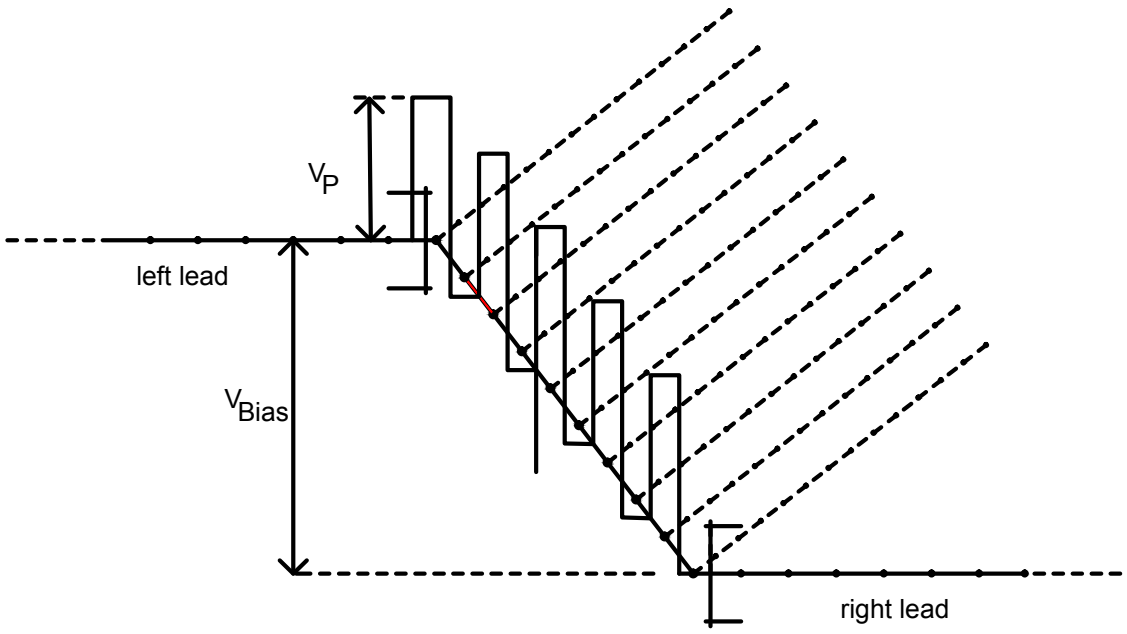

Figure 4.1: This system consists of two leads coupled to the central region with fermionic reservoirs as before. The difference is that there is a potential V_P on every odd site of the central tight-binding chain.

The bias voltage V_{Bias} is linearly distributed over all sites of the centryl system, correpsonding to an uniform electric field. $t_{ll}, t_{lc}, t_{cc}, t_{bb}, t_{cb}$ are the hopping parameters in the system. As we will see, the current characteristics exhibit modulations (oscillations) in the case of the alternating potential slope. They originate from **resonant tunneling**.

4.2 Resonant tunneling

4.2.1 Continuous calculation Double Barrier

For the following calculations references [22] and [23] were used.

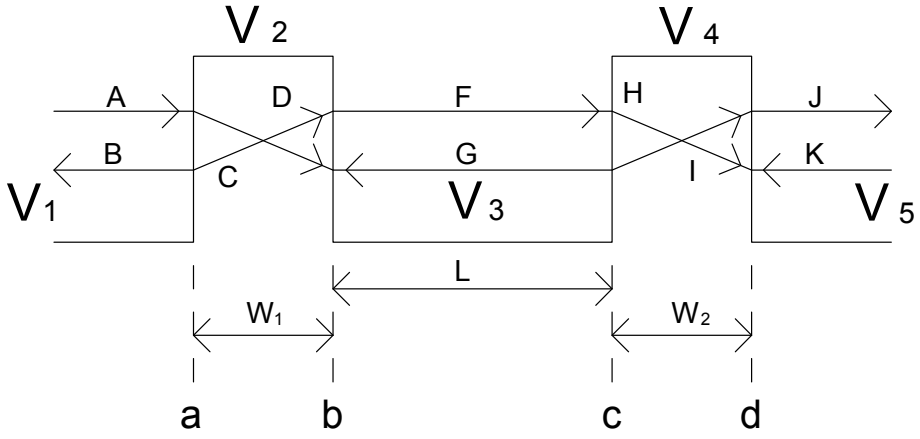

Figure 4.2: Sketch for the continous calculation of the transmission and reflection coefficient of a double barrier. One can see the amplitudes of the incoming an reflected amplitudes in every region and the parameters used for the calculation.

We want to find a possibility to calculate the transmission coefficient in continuous space. In real space the Schrödinger equation reads:

$$\left(\frac{-\hbar^2}{2\mathrm{m}}\frac{\mathrm{d}^2}{\mathrm{dx}^2} + \mathrm{V(x)}\right)\psi(\mathrm{x}) = \mathrm{E}\psi(\mathrm{x}) \tag{4.1}$$

For the wave function following ansatz is made:

$$\psi(\mathrm{x}) = \begin{cases} \mathrm{a}_1 \exp(i\mathrm{kx}) + \mathrm{a}_2 \exp(-i\mathrm{kx}) & \mathrm{k} = \frac{\sqrt{2\mathrm{m(E-V)}}}{\hbar}, \mathrm{V} < \mathrm{E} \\ \mathrm{a}_1 \exp(\mathrm{kx}) + \mathrm{a}_2 \exp(-\mathrm{kx}) & \mathrm{k} = \frac{\sqrt{2\mathrm{m(V-E)}}}{\hbar}, \mathrm{V} > \mathrm{E} \end{cases} \tag{4.2}$$

These waves have to fullfill the following conditions at the boundary of every region.

$$\begin{aligned} \psi_n(\mathrm{x_n}) &= \psi_{n+1}(\mathrm{x_n}) \\ \frac{\mathrm{d}}{\mathrm{dx}}\psi_n(\mathrm{x})|_{\mathrm{x=x_n}} &= \frac{\mathrm{d}}{\mathrm{dx}}\psi_{n+1}(\mathrm{x})|_{\mathrm{x=x_n}} \end{aligned} \tag{4.3}$$

For the case that the injection energy E is smaller than the potential barrier, we get:

$$\psi(\mathrm{x}) = \begin{cases} \mathrm{A}\exp(i\mathrm{kx}) + \mathrm{B}\exp(-i\mathrm{kx}) & \mathrm{x} <\leq \mathrm{a} \\ \mathrm{C}\exp(\mathrm{qx}) + \mathrm{D}\exp(-\mathrm{qx}) & \mathrm{a} < \mathrm{x} \leq \mathrm{b} \\ \mathrm{F}\exp(i\mathrm{k'x}) + \mathrm{G}\exp(-i\mathrm{k'x}) & \mathrm{b} < \mathrm{x} \leq \mathrm{c} \\ \mathrm{H}\exp(\mathrm{px}) + \mathrm{I}\exp(-\mathrm{px}) & \mathrm{c} < \mathrm{x} \leq \mathrm{d} \\ \mathrm{J}\exp(i\mathrm{k''x}) + \mathrm{K}\exp(-i\mathrm{k''x}) & \mathrm{d} < \mathrm{x} \end{cases} \tag{4.4}$$

$\mathrm{k} = \frac{\sqrt{2\mathrm{m(E-V_1)}}}{\hbar}$, $\mathrm{q} = \frac{\sqrt{2\mathrm{m(V_2-E)}}}{\hbar}$, $\mathrm{k'} = \frac{\sqrt{2\mathrm{m(E-V_3)}}}{\hbar}$, $\mathrm{p} = \frac{\sqrt{2\mathrm{m(V_4-E)}}}{\hbar}$, $\mathrm{k''} = \frac{\sqrt{2\mathrm{m(E-V_5)}}}{\hbar}$
To solve this problem the transfer matrix formalism is used. This means, we express eq.(4.4) in matrix form:

$$\begin{aligned} \mathrm{M_1}\begin{pmatrix} \mathrm{A} \\ \mathrm{B} \end{pmatrix} = \mathrm{M_2}\begin{pmatrix} \mathrm{C} \\ \mathrm{D} \end{pmatrix}, \mathrm{M_3}\begin{pmatrix} \mathrm{C} \\ \mathrm{D} \end{pmatrix} = \mathrm{M_4}\begin{pmatrix} \mathrm{F} \\ \mathrm{G} \end{pmatrix} \\ \mathrm{M_5}\begin{pmatrix} \mathrm{F} \\ \mathrm{G} \end{pmatrix} = \mathrm{M_6}\begin{pmatrix} \mathrm{H} \\ \mathrm{I} \end{pmatrix}, \mathrm{M_7}\begin{pmatrix} \mathrm{H} \\ \mathrm{I} \end{pmatrix} = \mathrm{M_8}\begin{pmatrix} \mathrm{J} \\ \mathrm{K} \end{pmatrix} \end{aligned} \tag{4.5}$$

$$\begin{pmatrix} \mathrm{A} \\ \mathrm{B} \end{pmatrix} = \underbrace{\mathrm{M_1^{-1}M_2M_3^{-1}M_4M_5^{-1}M_6M_7^{-1}M_8}}_{\mathrm{M_T}} \begin{pmatrix} \mathrm{J} \\ \mathrm{K} \end{pmatrix} \tag{4.6}$$

$\mathrm{M_T}$ is the transfer matrix. Another possibility to write the transfer matrix is:

$$\begin{aligned} \mathrm{M_T} &= \mathrm{M_1^{-1}M_{2,3}M_{4,5}M_{6,7}M_8} \\ \mathrm{M_m} &= \mathrm{M_{n,n+1}} = \mathrm{M_nM_{n+1}^{-1}} \end{aligned} \tag{4.7}$$

In principle one can write for a section m, that is confined by x_n and x_{n+1}:

$$M_m = \begin{cases} \begin{pmatrix} \cosh(k_m(x_{n+1}-x_n)) & -\frac{1}{k_n}\sinh(k_m(x_{n+1}-x_n)) \\ -k_n\sinh(k_m(x_{n+1}-x_n)) & \cosh(k_m(x_{n+1}-x_n)) \end{pmatrix} & E < V_n \\ \begin{pmatrix} \cos(k_m(x_{n+1}-x_n)) & -\frac{1}{k_n}\sin(k_m(x_{n+1}-x_n)) \\ k_n\sin(k_m(x_{n+1}-x_n)) & \cos(k_m(x_{n+1}-x_n)) \end{pmatrix} & E > V_n \\ \begin{pmatrix} 1 & -(x_{n+1}-x_n) \\ 0 & 1 \end{pmatrix} & E = V_n \end{cases} \tag{4.8}$$

And for the edge sections it holds:

$$M_n = \begin{cases} \begin{pmatrix} \exp(ik_nx) & \exp(-ik_nx) \\ ik_n\exp(ik_nx) & -ik_n\exp(-ik_nx) \end{pmatrix} & E > V_n \\ \begin{pmatrix} \exp(k_nx) & \exp(-k_nx) \\ k_n\exp(k_nx) & -k_n\exp(-k_nx) \end{pmatrix} & E < V_n \end{cases} \tag{4.9}$$

$$E < V_n : k_n = \frac{\sqrt{2m(V_n-E)}}{\hbar} \qquad E > V_n : k_n = \frac{\sqrt{2m(E-V_n)}}{\hbar}$$

Now to calculate the Transmission coefficient we use that the backscattered wave in the last section (denoted by K) is zero. We can define two matrices to get a relation for T:

$$\tilde{M}_1 = \begin{pmatrix} 1 & -M_{T,3} \\ 0 & -M_{T,4} \end{pmatrix} \qquad \tilde{M}_2 = \begin{pmatrix} 0 & M_{T,1} \\ -1 & -M_{T,2} \end{pmatrix} \tag{4.10}$$

With this matrices we can caluclate the scattering matrix S:

$$\begin{aligned} S = \tilde{M}_2^{-1}\tilde{M}_1 = \frac{1}{M_{T,1}} \begin{pmatrix} M_{T,2} & -M_{T,2}M_{T,3} + M_{T,1}M_{T,4} \\ 1 & -M_{T,3} \end{pmatrix} \\ \begin{pmatrix} B \\ J \end{pmatrix} = S \begin{pmatrix} A \\ K \end{pmatrix} \end{aligned} \tag{4.11}$$

We can now give an expression for the transmission and the reflection coefficient:

$$\begin{aligned} T &= |\frac{1}{M_{1,2}^T}|^2 = |S_2|^2 \\ R &= |\frac{M_{1,2}^T}{M_{1,1}^T}|^2 = |S_1|^2 \\ T + R &= 1 \end{aligned} \tag{4.12}$$

Or to use a different representation: The transmission coefficient is the ratio between the incoming in the outgoing wave and the reflection coefficient is the ratio between reflected and incoming wave:

$$\begin{aligned} T &= |\frac{J}{A}|^2 = |\frac{1}{M_{T,1}}|^2 \\ R &= |\frac{B}{A}|^2 = |\frac{M_{T,2}}{M_{T,1}}|^2 \end{aligned} \tag{4.13}$$

The transmission coefficient T exhibits it's maximum value if resonant tunneling takes place. In this case (at the resonant energies), the double barrier get's transparent for the electrons. Now we need to find a possibility to calculate the positions of these **resonant energies**. Therefore we have a look at a single potential well, because it is a good way to approximate the considered double potential well:

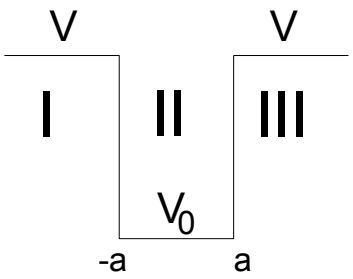

Figure 4.3: Sketch for the calculation of the resonance energies in the continous case for $V_T = 0$. There is the central region with the 2 potential barriers with height V and the well of length L=2a with potential V_0.

We restrict the calculation to the bound energies with $E < V$. The wave function in the 3 regions can be written according to:

$$\begin{aligned}
\mathbf{I} &: \psi(x) = A\exp(k'x) \\
\mathbf{II} &: \psi(x) = B\exp(ikx) + C\exp(-ikx) \\
\mathbf{III} &: \psi(x) = D\exp(-k'x)
\end{aligned}$$

$$k = \frac{\sqrt{2m(E-V_0)}}{\hbar} \qquad\qquad k' = \frac{\sqrt{2m(V-E)}}{\hbar}$$

With the boundary conditions it follows:

$$\underbrace{\begin{pmatrix} \exp(-k'a) & -\exp(-ika) & -\exp(ika) & 0 \\ -k'\exp(-k'a) & ik\exp(-ika) & -ik\exp(ika) & 0 \\ 0 & \exp(ika) & \exp(-ika) & -\exp(k'a) \\ 0 & ik\exp(ika) & -ik\exp(-ika) & k'\exp(-k'a) \end{pmatrix}}_{M} \begin{pmatrix} A \\ B \\ C \\ D \end{pmatrix} = \begin{pmatrix} 0 \\ 0 \\ 0 \\ 0 \end{pmatrix}$$

For the solution $\det(M) \stackrel{!}{=} 0$ has to be fullfilled resulting in:

$$\exp(4ika) = \frac{(k'-ik)^2}{(k'+ik)^2} \tag{4.14}$$

We have to distinguish between two cases: asymmetric and symmetric case

1.) asymmetric case:

$$\begin{aligned}
\exp(2i\mathrm{ka}) &= \frac{\mathrm{k}' - i\mathrm{k}}{\mathrm{k}' + i\mathrm{k}} \\
&= \frac{1}{\mathrm{k}'^2 + \mathrm{k}^2}\left(\mathrm{k}'^2 - \mathrm{k}^2 - 2i\mathrm{k}'\mathrm{k}\right) \\
\cos(2\mathrm{ka}) &= \frac{\mathrm{k}'^2 - \mathrm{k}^2}{\mathrm{k}'^2 + \mathrm{k}^2} \\
\sin(2\mathrm{ka}) &= -\frac{2\mathrm{k}'\mathrm{k}}{\mathrm{k}'^2 + \mathrm{k}^2}
\end{aligned}$$

With the identities $\cos(2\mathrm{x}) = 1 - 2\sin^2(\mathrm{x})$, $\sin(2\mathrm{x}) = 2\sin(\mathrm{x})\cos(\mathrm{x})$ we get:

$$-\cot(\mathrm{ka}) = \frac{\mathrm{k}'\mathrm{k}}{\mathrm{k}^2} \tag{4.15}$$

The asymmetric energies arise from the intersection point of the two sides of the transcendent equation.

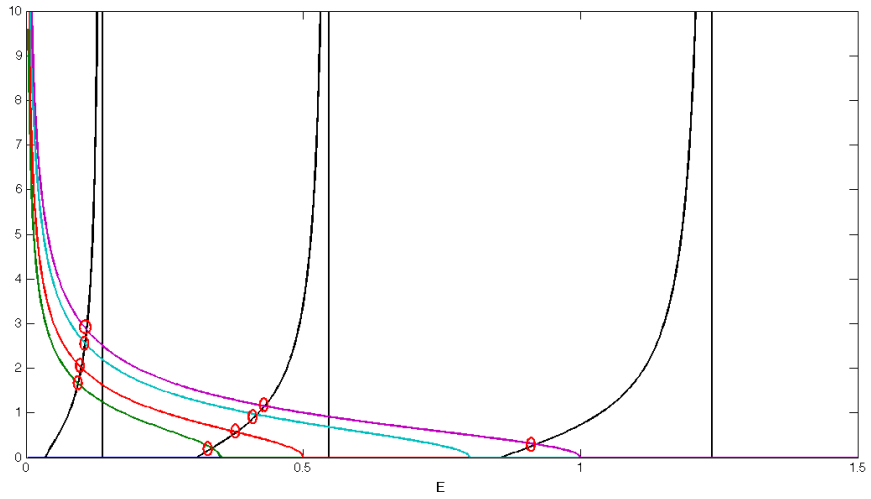

Figure 4.4: The black line shows the function $\mathrm{f}_1^{\mathrm{a}}(\mathrm{E}) = -\cot(\mathrm{ka})$ and the colored ones of $\mathrm{f}_2^{\mathrm{a}}(\mathrm{E}) = \frac{\sqrt{\zeta^2 - (\mathrm{ka})^2}}{\mathrm{ka}}$ for various choices of the potential height V. Here V_0 has been chosen to 0, a=6 and the width of the barrier is w=0.5. In this case $\zeta = \sqrt{2\mathrm{mV}}\mathrm{a}/\hbar$ and $\mathrm{k} = \sqrt{2\mathrm{mE}}/\hbar$. The red circles show the positions of the resonance energies.

The number of asymmetric solutions is given by the intersection points and depends on ζ. As V rises the number of energies increases. There is the following law for the number of asymmetric solutions n_a:

$$\frac{\pi}{2}(2n_a - 1) < \zeta < \frac{\pi}{2}(2n_a + 1)$$

There only exists asymmetric solutions if the potential height exceeds the value

$$V = \frac{\pi^2\hbar^2}{8ma^2}$$

The next figure shows the dependence on the well width L = 2a.

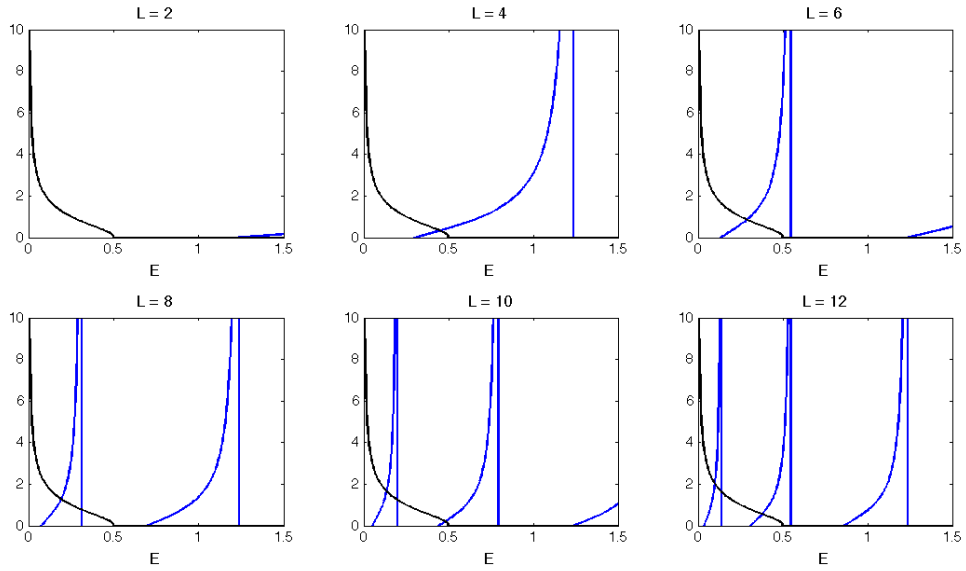

Figure 4.5: The blue line shows the characteristics of the function $f_1^a(E) = -\cot(ka)$ and the black one of $f_2^a(E) = \frac{\sqrt{\zeta^2-(ka)^2}}{ka}$ for various choices of the well width L. Here V_0 has been chosen to 0, V = 0.5 and the width of the barrier is w=0.5.

As L or rather a rises the number of intersection points increases because $f_2^a(E)$ strongly depends on the choice of a. This means the longer the well or the higher the potential barrier the more bound state energies exist.

2.) symmetric case:

$$\begin{aligned}
\exp(2i\mathrm{ka}) &= -\frac{\mathrm{k}' - i\mathrm{k}}{\mathrm{k}' + i\mathrm{k}} \\
&= -\frac{1}{\mathrm{k}'^2 + \mathrm{k}^2}\left(\mathrm{k}'^2 - \mathrm{k}^2 - 2i\mathrm{k}'\mathrm{k}\right) \\
\cos(2\mathrm{ka}) &= \frac{\mathrm{k}^2 - \mathrm{k}'^2}{\mathrm{k}'^2 + \mathrm{k}^2} \\
\sin(2\mathrm{ka}) &= \frac{2\mathrm{k}'\mathrm{k}}{\mathrm{k}'^2 + \mathrm{k}^2}
\end{aligned}$$

$$\tan(\mathrm{ka}) = \frac{\mathrm{k}'\mathrm{k}}{\mathrm{k}^2} \tag{4.16}$$

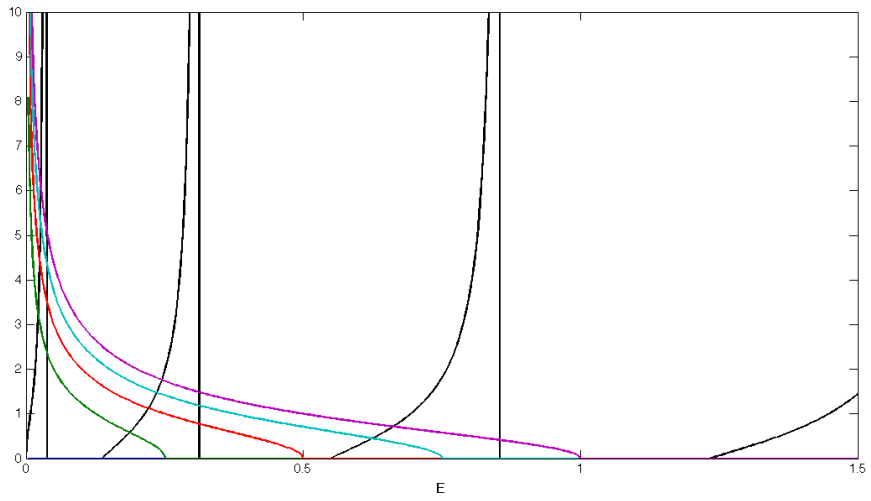

Figure 4.6: The black line shows the characteristics of the function $\mathrm{f}_1^{\mathrm{s}}(\mathrm{E}) = \tan(\mathrm{ka})$ and the colored ones of $\mathrm{f}_2^{\mathrm{s}}(\mathrm{E}) = \frac{\sqrt{\zeta^2 - (\mathrm{ka})^2}}{\mathrm{ka}}$ for various choices of the potential height V. Here V_0 has been chosen to 0, a=6 and the width of the barrier is w=0.5.

In the symmetric case it always exists a solution for V > 0. This means the number of symmetric solutions can be calculated by:

$$n_s = \lceil \frac{\zeta}{\pi} \rceil$$

For a potential with a certain potential height V there are n solutions $(n_s + n_a)$ that are given by:

$$n = \lfloor \frac{2\zeta}{\pi} \rfloor + 1 \tag{4.17}$$

The dependence of the symmetric solutions on the well length L is similar to the asymmetric case. As L rises n_s rises. But there is also a solution for very narrow barriers:

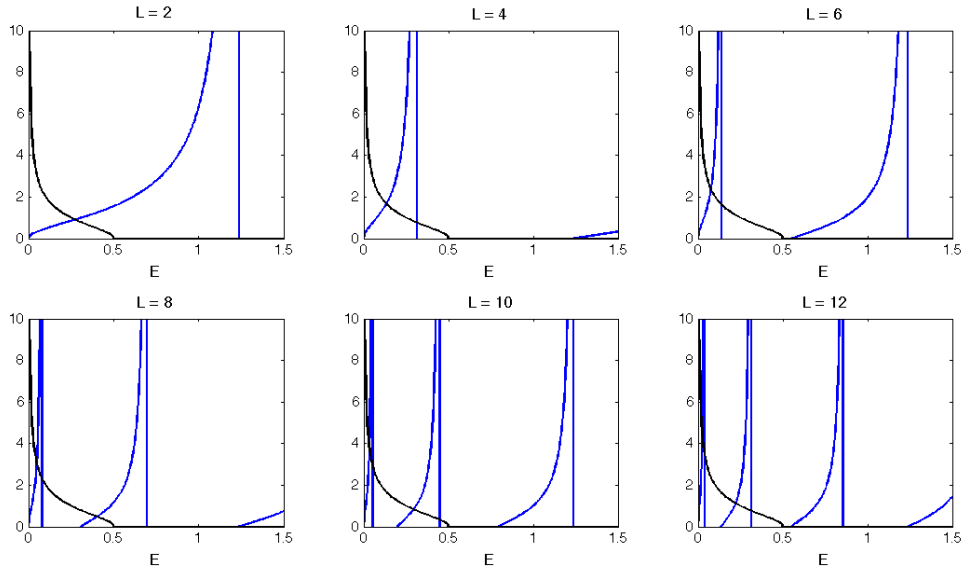

Figure 4.7: The blue line shows the characteristics of the function $f_1^s(E) = \tan(ka)$ and the black one of $f_2^s(E) = \frac{\sqrt{\zeta^2-(ka)^2}}{ka}$ for various choices of the well width L.

Before we start to show the results for the continous calculation, we have to mention that all constants m, e and $\hbar$ are set equal 1. (Same for the following discrete calculation)

4.2.2 Continuous results for a Double Barrier

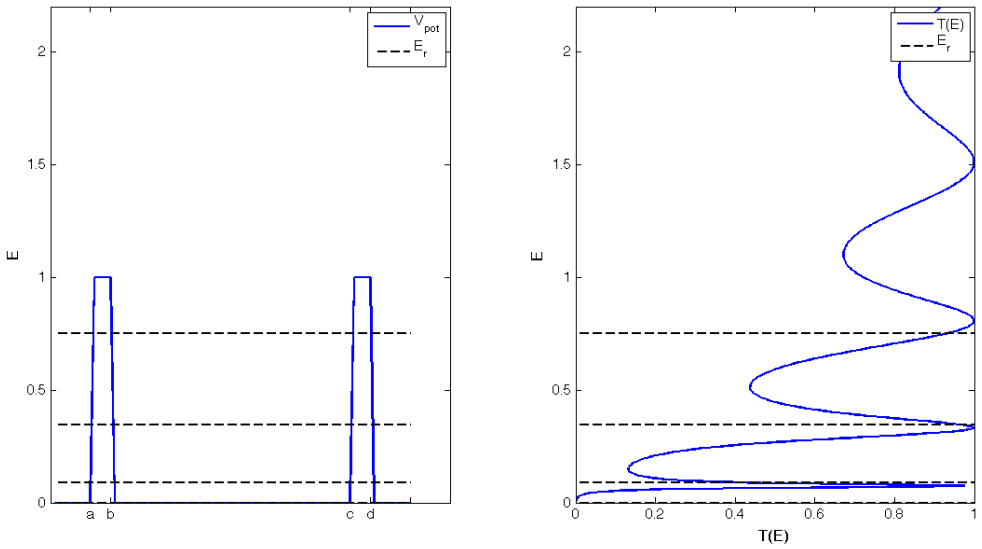

Figure 4.8: Parameters for this calculation: V = 1, w = 0.5, L = 6; On the left site one can see the potential of the double barrier and the position of the resonant energies. On the right site one can see the characteristic of the transmission coefficient T in dependence of the incoming energy E and the resonant energies E_r.

The transmission coefficient reaches its maximum value if the incoming energy is the same as a resonant energy E_r. In Figure 4.8 we can see, a small divergence between the resonant energy position and the transmission coefficient maximum. This results from the fact, that the positions were calculated using a double barrier potential. In this case the barrier gets transparent for the electrons. This means that at these certain energies a current can flow. The number of resonance energies, at which the electrons can tunnel, depends on the height of the barrier and the width of the well. Fig.4.9 shows the dependency of the transmission coefficient on the well width.

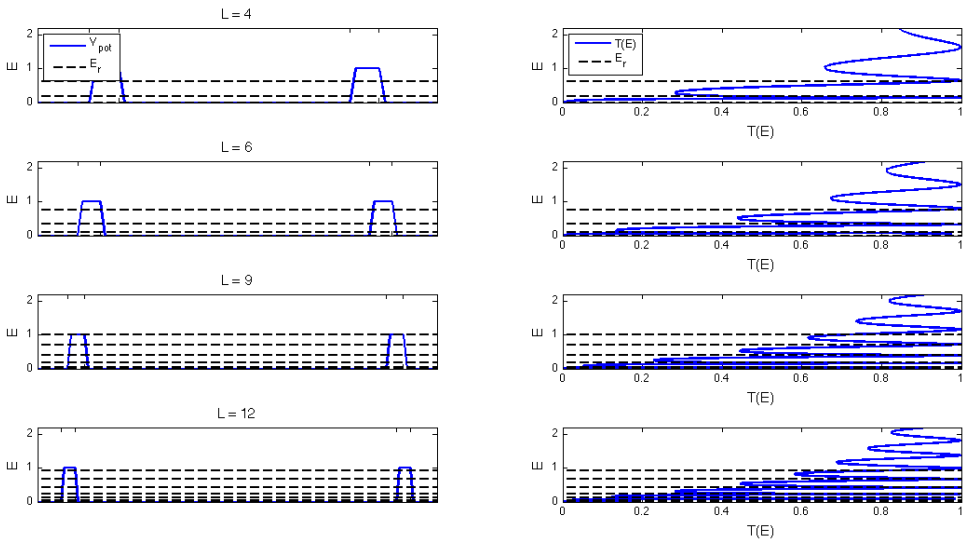

Figure 4.9: Parameters for this calculation: V = 1, w = 0.5; The transmission coefficient for various well lengths.

As we can see the transmission coefficient exhibits more peaks as L rises. There are more bound states. If the parameter L is chosen to be twice as long as before the number of resonances E_r doubles. In Chapter 4.2.1 we only discussed the bound states, but there is also resonant behaviour above the barrier edge (for energies out of the bound state regime). They come from the free states.
Conclusions for the double barrier calculations:

- The transmission coefficient exhibits its maximum value near the resonance energies. The electrons can tunnel through the barrier.

- As the length of the well goes up, the number of bound state energies rises.

- As the height of the potential barrier goes up, the number of resonance peaks in the transmission coefficient rise and they get sharper.

4.2.3 Continuous calculation for a tilted Double Barrier

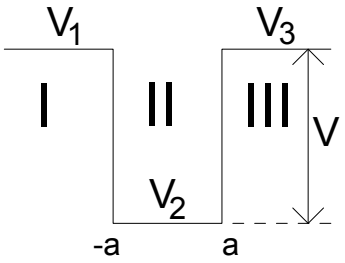

Figure 4.10: Sketch for the calculation of the resonance energies in the continous case for $V_T \neq 0$. There is the central region with the 2 potential barriers with height V_1 and V_3 and the well of length L=2a with potential V_2. The values of V_n change due to a tilting of the system.

If there is a bias voltage on the system the double barrier gets tilted. We now call the voltage to til the system V_T and one can calculate:

$$V_{Bias} = (N-1) \cdot V_T$$

With the voltage V_T the potential heights V_n get modulated. Again, we only consider the bound state energies ($E < V_3$).

$$\begin{aligned} \mathbf{I} &: \psi(x) = A \exp(qx) \\ \mathbf{II} &: \psi(x) = B \exp(ikx) + C \exp(-ikx) \\ \mathbf{III} &: \psi(x) = D \exp(-px) \end{aligned}$$

$q = \frac{\sqrt{2m(V_1-E)}}{\hbar}$ $\qquad$ $k = \frac{\sqrt{2m(E-V_2)}}{\hbar}$ $\qquad$ $p = \frac{\sqrt{2m(V_3-E)}}{\hbar}$

With the same procedure as in the case of a non tilted double barrier we get:

$$\exp(4ika) = \frac{(p-ik)(q-ik)}{(p+ik)(q+ik)} \tag{4.18}$$

1.) asymmetric case:

$$\exp(2i\mathrm{ka}) = \sqrt{\frac{(\mathrm{p}-i\mathrm{k})(\mathrm{q}-i\mathrm{k})}{(\mathrm{p}+i\mathrm{k})(\mathrm{q}+i\mathrm{k})}}$$

With the definition $\mathrm{V}_0 = \sqrt{(\mathrm{V}_1-\mathrm{V}_2)(\mathrm{V}_3-\mathrm{V}_2)}$ we get the position of the resonant energies out of the following transcendent equation (the intersection points of the two curves give the resonances):

$$-\cot(\mathrm{ka}) = \frac{\sqrt{\mathrm{E}(\mathrm{V}_0-\mathrm{E})}}{\mathrm{E}} \tag{4.19}$$

1.) symmetric case:

$$\exp(2i\mathrm{ka}) = -\sqrt{\frac{(\mathrm{p}-i\mathrm{k})(\mathrm{q}-i\mathrm{k})}{(\mathrm{p}+i\mathrm{k})(\mathrm{q}+i\mathrm{k})}}$$

$$\tan(\mathrm{ka}) = \frac{\sqrt{\mathrm{E}(\mathrm{V}_0-\mathrm{E})}}{\mathrm{E}} \tag{4.20}$$

Without $\mathrm{V_T}$ the potential heights $\mathrm{V_n}$ calculate like:

$$\mathrm{V}_1 = \mathrm{V}_2 + \mathrm{V}$$
$$\mathrm{V}_3 = \mathrm{V}_2 + V$$

If $\mathrm{V_T} \neq 0$:

$$\mathrm{V}_1 = \mathrm{V}_2 + \mathrm{V}$$
$$\mathrm{V}_2 = \mathrm{V}_2 - \mathrm{V_T}$$
$$\mathrm{V}_3 = \underbrace{\mathrm{V}_2 + \mathrm{V}}_{\mathrm{V}_3} - 2\mathrm{V_T}$$

If we plug this into the definition of V_0 we get:

$$V_0 = \sqrt{V^2 - V_T^2} \tag{4.21}$$

In the case of a tilted double barrier the resonant energies shift with rising V_T to lower energies. This means, as V_T goes up the slope of the system gets more steep.

4.2.4 Continous results for a tilted Double Barrier

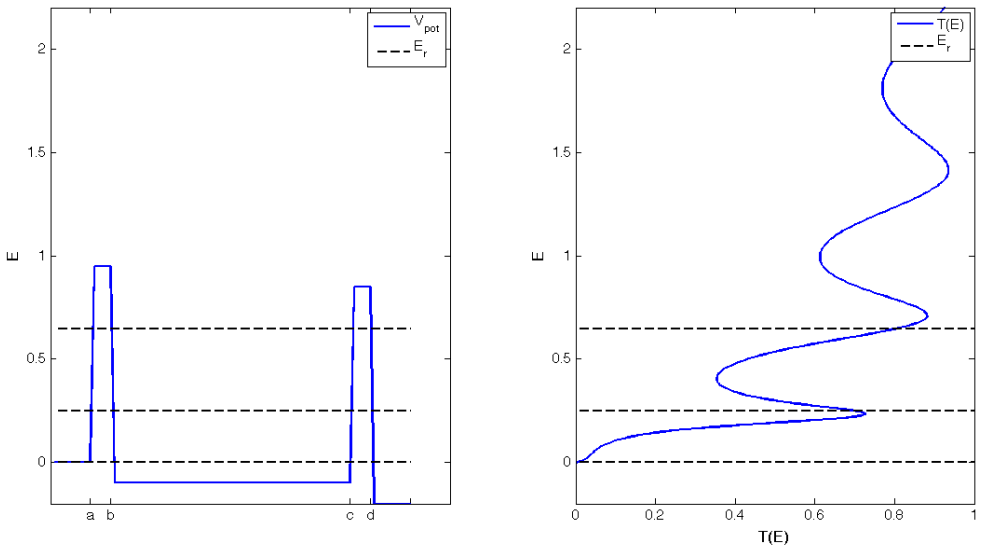

Figure 4.11: Parameters of this calculation are V = 1, w = 0.5, L = 6 and V_T = 0.05; Transmission coefficient in the case of a tilted double barrier.

Fig.4.11 in comparison to Fig.4.8 shows that in the case $V_T \neq 0$ the resonant energies are shifted down and therefore there are less resonances. At the lowest resonant energy, we can't see a transmission peak, because the incoming wave can't have energy 0. The peaks are not as sharp and the maximum of the transmission coefficient is lower as in the case of $V_T = 0$. We have a look at the transmission coefficient in dependency of the tilting V_T at a certain energy E. This energy has to be chosen to be in the range of the smallest resonant energy.

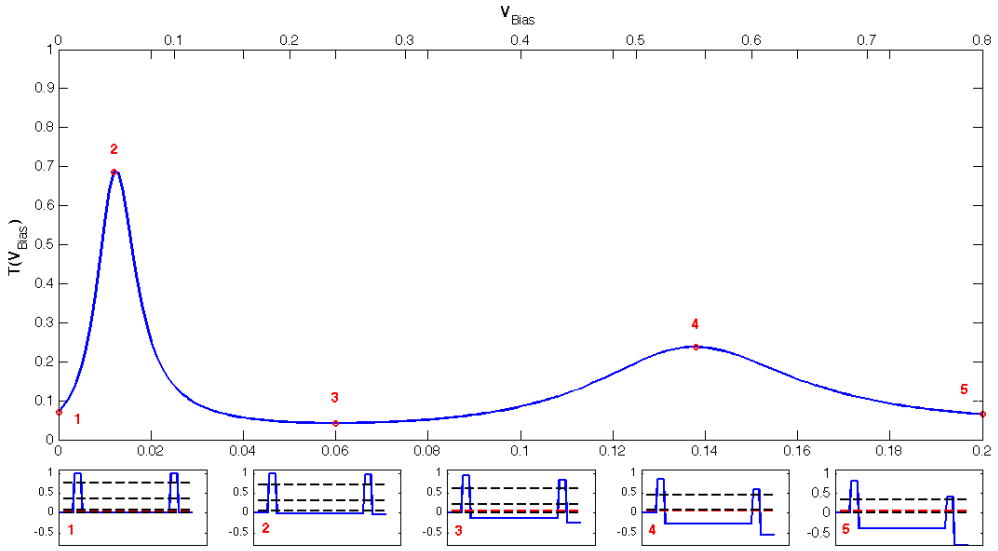

Figure 4.12: V=1, w=0.5, L=6 and the energy of the incoming wave E=0.05; Transmission coefficient in dependency of the tilting.

In the upper plot we can see T in dependency of the tilting or rather the bias voltage. The lower plots show the tilting of the double barrier for various V_T, the resonant energies (black) and the incoming energy (red). The resonances shift with rising tilt to lower energies. As one can see, the transmission coefficient exhibits resonant behaviour if E equals a resonant energy otherwise there is a minimum in T.

The most significant difference to the not tilted double potential is that T doesn't reaches it's maximum at a value of 1. Normally this comes from the fact, that the waves inside the barrier get reflected from one site to the other and somewhere there is interference. T of the whole system can get higher than the T_i's of the single barriers because of the interference. When the barrier gets tilted there are less waves that can contribute to T and therefore the transmission coefficient can't reach a value of 1 anymore.

So far we have only considered a double barrier. The characteristic of the transmission coefficient changes when there are several wells (N rises and on every second place there is a higher potential).

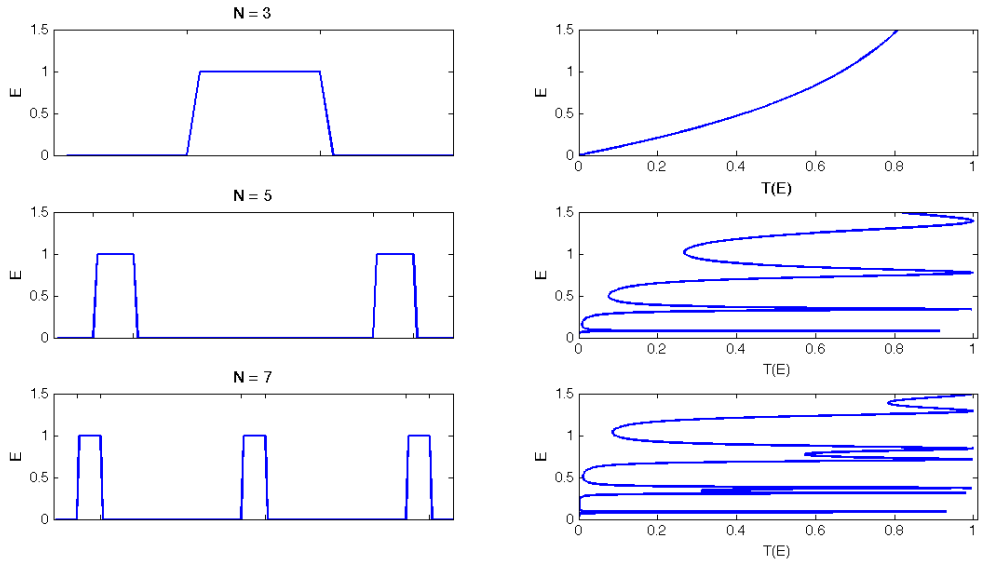

Figure 4.13: V=1, w=0.5, L=6; Transmission coefficient in dependency of N. The left plots show the potentials and the right plots the characteristics of the transmission coefficient.

Fig.4.13 shows the dependency of T on the potential. A single barrier doesn't exhibit resonances because there are no bound state energys. The double barrier shows the known behaviour of the transmission coefficient. If the number of wells increases the positions of the resonances stay the same but they get split. This means, that every resonance peak splits into the number of wells. In the case of N=7 every peak is splitted into two peaks because there are two wells in the system. If there would be 3 wells (N=9) there would be a splitting into 3 peaks.

Fig.4.14 shows the characteristics of the transmission coefficient in dependency of the tilting for N = 7 (double well). In comparison to Fig.4.12 we can see that the positions of the main resonances stay the same for more wells but they split into two peaks because of the number of wells (as seen before for the resonances without tilting).

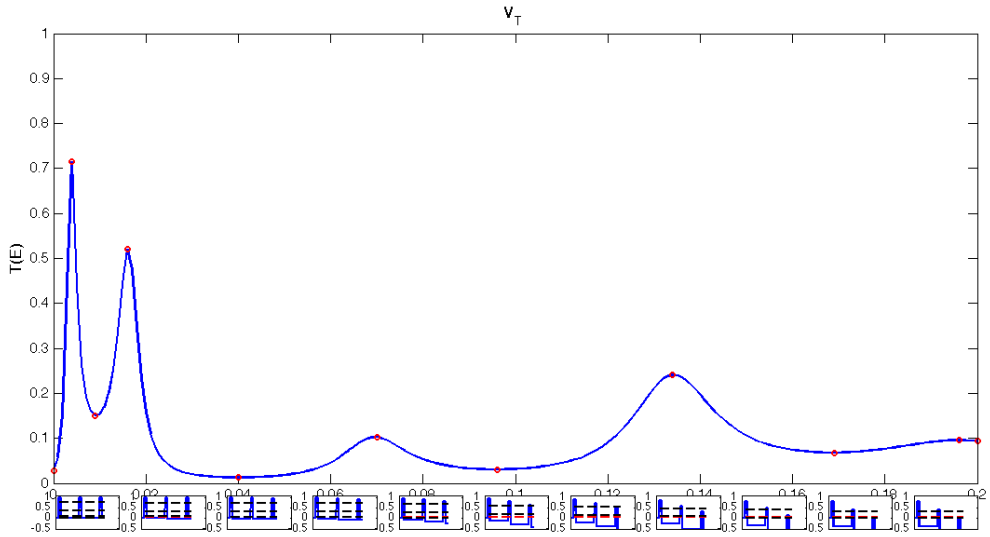

Figure 4.14: V=1, w=0.5, L=6, E=0.05; Transmission coefficient in dependency of the tilting for a double well (N=7).

4.2.5 Discrete calculation of the Double Barrier Problem on a one-dimensional tight-binding chain

Reference [24] was used as a support for the following calculations and considerations. The model used for the following considerations is extremely idealized. We only look at a strictly one-dimensional transport problem. For this we introduce a double barrier potential and use the Greens function method to calculate the transmission and reflection coefficients.

The Hamiltonian

$$\hat{\mathrm{H}} = \sum_{\mathrm{n}} \left(\epsilon_{\mathrm{n}} \left|\mathrm{n}\right\rangle \left\langle \mathrm{n}\right| + \mathrm{t} \left(\left|\mathrm{n}\right\rangle \left\langle \mathrm{n{+}1}\right| + \left|\mathrm{n}\right\rangle \left\langle \mathrm{n\text{-}1}\right| \right) \right) \tag{4.22}$$

describes a one-dimensional tight-binding chain of N sites with nearest neighbour hopping u and on-site-energies ϵ_{n}. Translational invariance $\epsilon_{\mathrm{n}} = \epsilon_0$ is assumed. The eigenfunctions of the Hamiltonian are of the Bloch-type:

$$\left|\mathrm{k}\right\rangle = \sum_{\mathrm{n}} \exp(i\mathrm{kna}) \left|\mathrm{n}\right\rangle$$

k stands for the momentum eigenstates and a for the spacing between the sites on the chain (lattice spacing). With these Bloch states one can calculate the dispersion relation:

$$\mathrm{E(k)} = \epsilon_0 + 2\mathrm{t}\cos(\mathrm{ka}) \tag{4.23}$$

The energy band of the model extends from $\epsilon_0 - 2|\mathrm{u}|$ to $\epsilon_0 + 2|\mathrm{u}|$. Therefore the first Brillouin zone spans the k interval $[-\pi/a, \pi/a]$. ϵ_0 is chosen to be $-2\mathrm{u}$, which corresponds to k=0 being the bottom of the band.
We look at following potential and want to calculate the transmission coefficient. The system consists of the central region with the potential and coupled leads at the right and the left of the central region with same on-site energies.

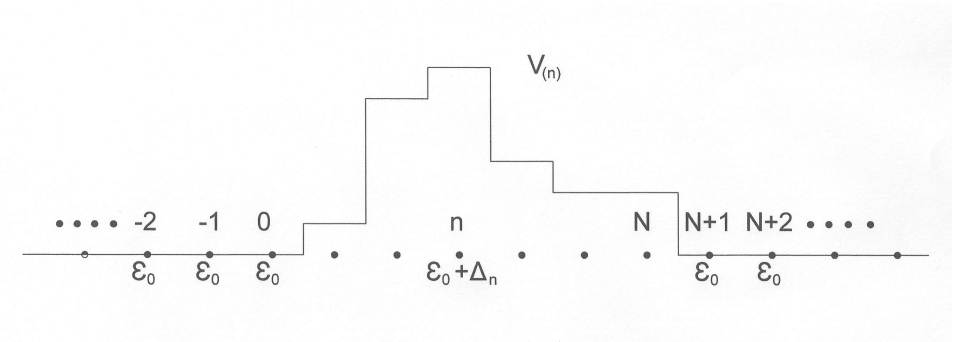

Figure 4.15: Random potential in the central region and coupled leads for the calculation of the transmission and the reflection coefficient.

A potential can be modelled by changing the on-site energies ϵ_0 by an additive term Δ. This means: $\epsilon_\mathrm{n} = \epsilon_0 + \Delta_\mathrm{n}$

The scattering problem can then be solved by finding the scattering eigenstates.

$$\underline{\mathrm{k} > 0:} \qquad \psi_\mathrm{k}(\mathrm{n}) = \begin{cases} \exp(i\mathrm{kna}) + \mathrm{r(k)}\exp(-i\mathrm{kna}) & \mathrm{n} \leq 0 \\ \mathrm{t(k)}\exp(i\mathrm{kna}) & \mathrm{n} \geq \mathrm{N}+1 \end{cases} \tag{4.24}$$

$$\underline{\mathrm{k} < 0:} \qquad \tilde{\psi}_\mathrm{k}(\mathrm{n}) = \begin{cases} \exp(i\mathrm{kna}) + \tilde{\mathrm{r}}(\mathrm{k})\exp(-i\mathrm{kna}) & \mathrm{n} \geq \mathrm{N}+1 \\ \tilde{\mathrm{t}}(\mathrm{k})\exp(i\mathrm{kna}) & \mathrm{n} \leq 0 \end{cases} \tag{4.25}$$

t(k) and r(k) are the transmission and reflection amplitudes for k>0 and $\tilde{\mathrm{t}}$(k) and $\tilde{\mathrm{r}}$(k) for k< 0. To derive an expression for the amplitudes the Greens function method was used. As before, the retarded Greens function can be calculated with a CPT approach. The sites on the chain couple with u with each other and the leads have to be included in the calculation. Hence the transmission and reflection amplitudes are given by:

$$\underline{\mathrm{k} > 0:} \qquad \begin{cases} \mathrm{t(k)} = -2it\sin(\mathrm{ka})\exp(-i(\mathrm{N}+1)\mathrm{ka})\mathrm{G}_{\mathrm{N}+1,0}(\mathrm{k}) \\ \mathrm{r(k)} = -2it\sin(\mathrm{ka})\mathrm{G}_{0,0}(\mathrm{k}) - 1 \end{cases} \tag{4.26}$$

$$\underline{\mathrm{k} < 0:} \qquad \begin{cases} \tilde{\mathrm{t}}(\mathrm{k}) = 2it\sin(\mathrm{ka})\exp(i(\mathrm{N}+1)\mathrm{ka})\mathrm{G}_{0,\mathrm{N}+1}(\mathrm{k}) \\ \tilde{\mathrm{r}}(\mathrm{k}) = (2it\sin(\mathrm{ka})\mathrm{G}_{\mathrm{N}+1,\mathrm{N}+1}(\mathrm{k}) - 1)\exp(2i(\mathrm{N}+1)\mathrm{ka}) \end{cases} \tag{4.27}$$

$G_{ij}(k)$ means that the Greens function has to be evaluated at a certain E(k). From the dispersion relation (eq.(4.23)) one can calculate the corresponding k. The transmission and reflection coefficient can then be calculated by $T(k) = |t(k)|^2$ and $R(k) = |r(k)|^2$. For a detailed calculation see [24].

If there was a voltage drop across the structure the calculation for the transmission and reflection amplitude could be made with the **transfer matrix method**. The on site-energy of the low voltage contact has to be replaced by $\epsilon_0 - V_{Bias}$ and there is no translational invariance anymore because every ϵ_n gets changed by a Δ_n. The eigenstates of the Hamiltonian are now of following type:

$$|\psi\rangle = \sum_n c_n |n\rangle$$

With this ansatz one gets an equation to determine the evolution coefficients.

$$(c_{n+1} + c_{n-1}) = \frac{E - \epsilon_n}{u} c_n \tag{4.28}$$

First a vector gets defined:

$$\vec{c}_n = \begin{pmatrix} c_n \\ c_{n-1} \end{pmatrix}$$

The matrix equation for solving the system of equations for the coefficients is now given by:

$$\begin{aligned} \vec{c}_{n+1} &= T_n \vec{c}_n \\ T_n &= \begin{pmatrix} (E - \epsilon_n)/u & -1 \\ 1 & 0 \end{pmatrix} \end{aligned} \tag{4.29}$$

where T_n is the Transfer matrix of order n. For the incoming wave $n \leq 0$ we define:

$$c_n = \exp(ikan) + r(k) \exp(-ikan)$$

and for the outgoing wave n≥(N+1):

$$c_n = t(k)\exp(ikan)$$

This gives following system of equations for the determination of t(k) and r(k):

$$\underbrace{\begin{pmatrix} t(k)\exp(ika(N+1)) \\ t(k)\exp(ikaN) \end{pmatrix}}_{\vec{c}_n} = T \underbrace{\begin{pmatrix} \exp(ika) + r(k)\exp(-ika) \\ 1 + r(k) \end{pmatrix}}_{\vec{c}_1} \tag{4.30}$$

With T the transfer matrix of the full system:

$$T = T_N \dots T_1 = \begin{pmatrix} T_{11} & T_{12} \\ T_{21} & T_{22} \end{pmatrix} \tag{4.31}$$

This gives following expression for the transmission and the reflection amplitude:

$$\begin{aligned} r(k) &= \frac{T_{11} + T_{12}\exp(-ika) - T_{21}\exp(ika) - T_{22}}{T_{22} + T_{21}\exp(-ika) - T_{12}\exp(-ika) - T_{11}\exp(-2ika)} \\ t(k) &= \exp(-ika(N+1))\left[T_{11}\exp(ika) + T_{12} + r(k)\left(T_{11}\exp(-ika) + T_{12}\right)\right] \end{aligned} \tag{4.32}$$

4.2.6 Results for a tight-binding chain

The studied systems always consist of a central region with a certain potential and two coupled leads. A calculation of the characteristics of the transmission coefficient always shows certain behaviour for a defined potential.

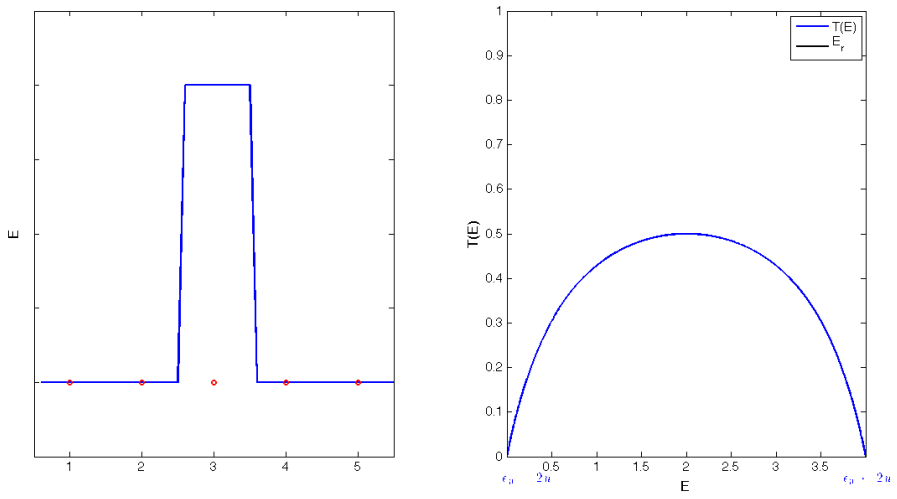

Figure 4.16: The right pannel shows the transmission coefficient for a single barrier with one atom in the barrier. The left pannel shows the transmission coefficient in dependency of the incoming energy.

The resonant behaviour normally manifests itself through a maximum value in the transmission coefficient. Resonant tunneling occurs above the barrier edge in the case of a single barrier. In this case, with a single barrier and one barrier atome only, there is no resonant behaviour.

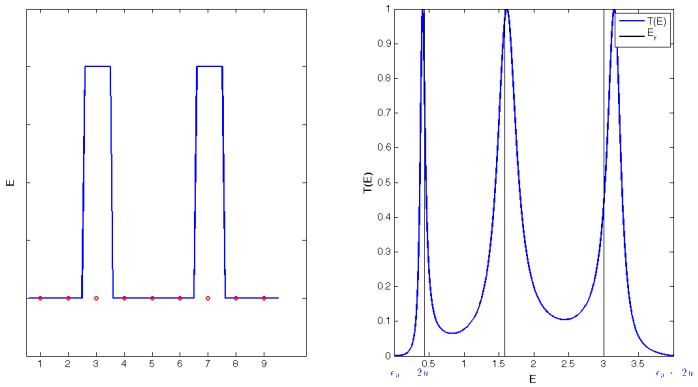

Figure 4.17: Shows the transmission of a double barrier with 3 atoms in the well and one atom in each barrier.

Next we can see, there are three resonances in the continuum band (means the considered energy window). The well with W atoms has W energy states in the energy band and they give rise to W resonances through which the electrons can tunnel. Because of the symmetric structure there is full transmission T=1 on resonance. The atoms in the barrier (in this case 3) give rise to N_b bound states above the barrier edge.

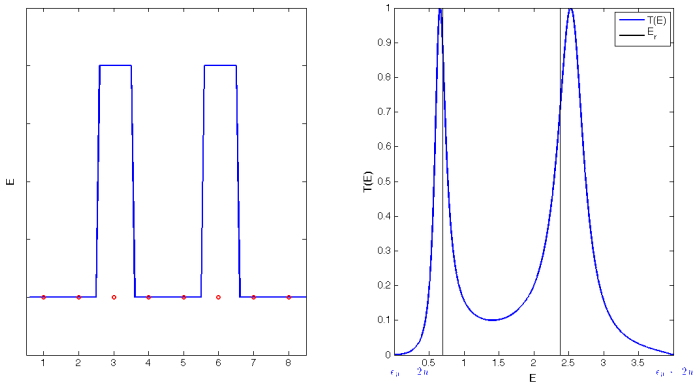

Figure 4.18: Shows the transmission of a double barrier with 2 atoms in the well and one atom in each barrier. This can be compared to Fig.4.17 (3 Atoms in the well).

In Fig.4.18 there are only two atoms in the well. The transmission coefficient only exhibits 2 resonances. This emphysizes that W well atoms give rise to W resonances in the energy band.

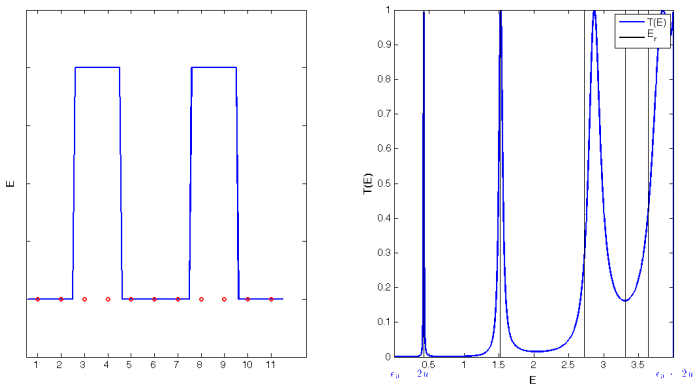

Figure 4.19: Shows the transmission coefficient of a system consisting of 3 atoms in the well and 2 in each barrier.

Fig.4.19 in comparison to Fig.4.17 shows that the well atoms give rise to 3 resonances. Now the number of barrier atoms is higher and there are more truely bound states. The position of the resonances stay the same but there appears a new resonance at the edge of the energy band. This means, that one if the barrier states must be degenerate with the continuum band $(\epsilon_0 - |2u|, \epsilon_0 + 2|u|)$ and appears as a resonance.
The following system consists of 6 atoms in the well and one atom in each barrier.

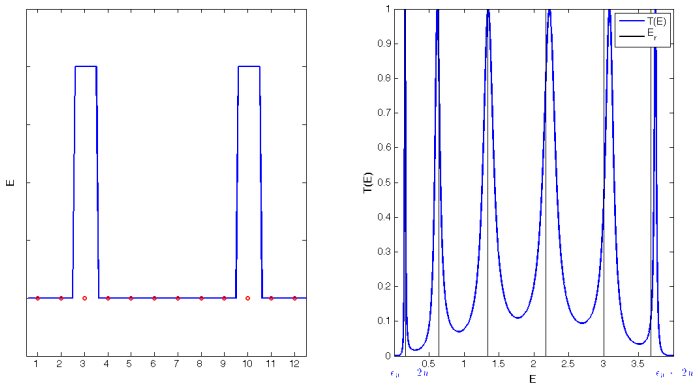

Figure 4.20: Shows the transmission of a double barrier with 6 atoms in the well and one atom in each barrier.

As one can see, the 6 atoms in the well lead to 6 resonances. If we switch on a bias voltage (or V_T) the position of the resonances shift to lower energies E.

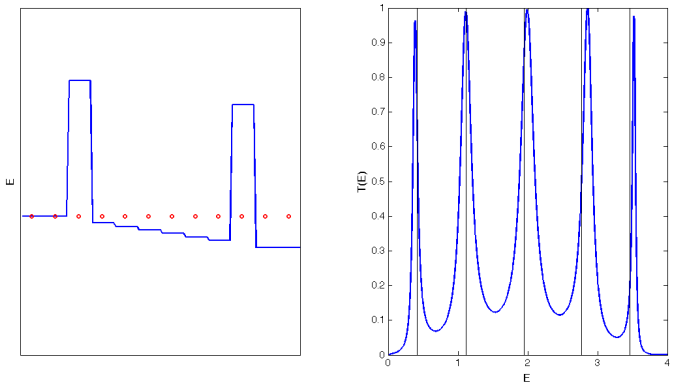

Figure 4.21: Transmission coefficient for a tilted chain ($V_T = 0.05, V_{Bias} = 0.4$) with Nw=6 and Nb=1.

The behaviour of the transmission coefficient in dependency of the tilting is similar to the continous case.

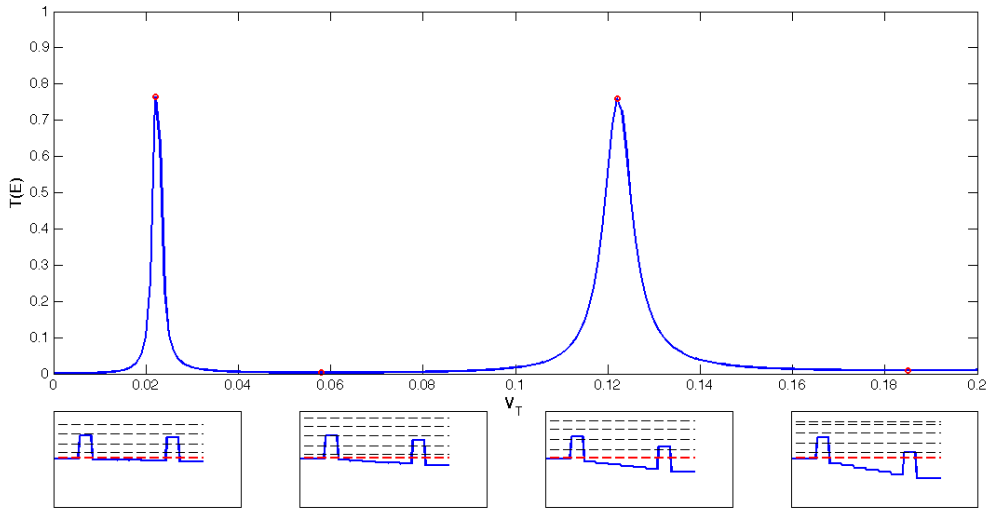

Figure 4.22: Transmission coeffcient in dependency of the tilting for an energy E=0.05.

If the energy of the incoming wave conicides with a resonance the transmission coefficient reaches a maximum value because the electrons can tunnel resonantly. With the bias voltage (or rather the tilting) the E_r get shifted towards smaller energys but the incoming energy always stays the same. In the lower plots of Fig.4.22 one can see the actual situation in case of resonant and non-resonant behaviour.

4.3 Transport in an alternating potential

Here we want to study the characteristics of the current in a system consisting of a central region and two coupled leads. It shows certain behaviour that can be compared to the transmission coefficient. The central region is a one-dimensional tight-binding chain with coupled fermion reservoirs (compare with Chapter 2) under an uniform electric field that leads to a bias voltage across the system. A difference to previous considerations is an alternating potential, which means that there is a potential barrier on every second site of the central region (Fig.4.1). With this model a semiconductor can be treated.

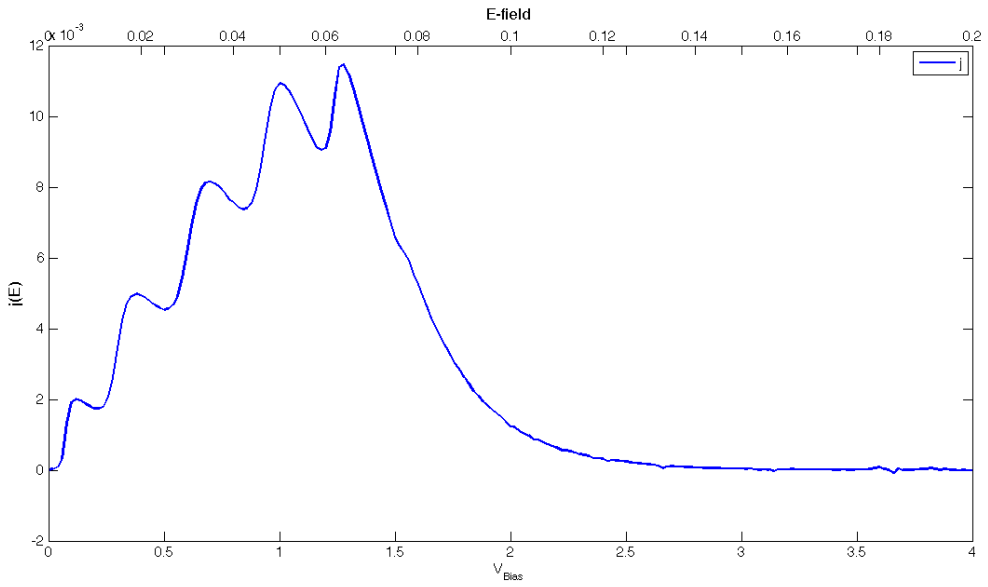

Figure 4.23: Current characteristics for a central region with N=21 sites, hopping parameters $t_{ll} = 1, t_{cc} = 1, t_{cl} = 1$, without fermion baths $t_{cb} = 0$ and applied potential barriers of height $V_P = 2$.

We start out with the current characteristics in the case with no baths. Because of the missing fermion baths there is only a current flowing in the band-width (compare to Chapter 2) but with a different behaviour because of the barriers. There is no linear behaviour of the current to the field anymore. Instead there are steps in the current characteristics. They appear because of the potential barriers. For a more detailed

interpretation we will take a look at the transmission coefficient for this system.
Fig.4.24 shows the transmission coefficient for certain values of the incoming energy. The system is not tilted, so the bias voltage equals 0. The left plot shows the system with the leads on the right and left site and the central region with an alternating potential. On the right one can see the characteristics of the transmission coefficient. There are 10 resonances because of the 10 wells. If there was only one well with a single atom inside, we would only see one resonance. Because of the number of the wells this resonance is split into more because there are more bound states (details in a previous chapter). There are also 11 exactly bound states (they come from the number of atoms in the barrier) but only appear for energies above the continuum band.

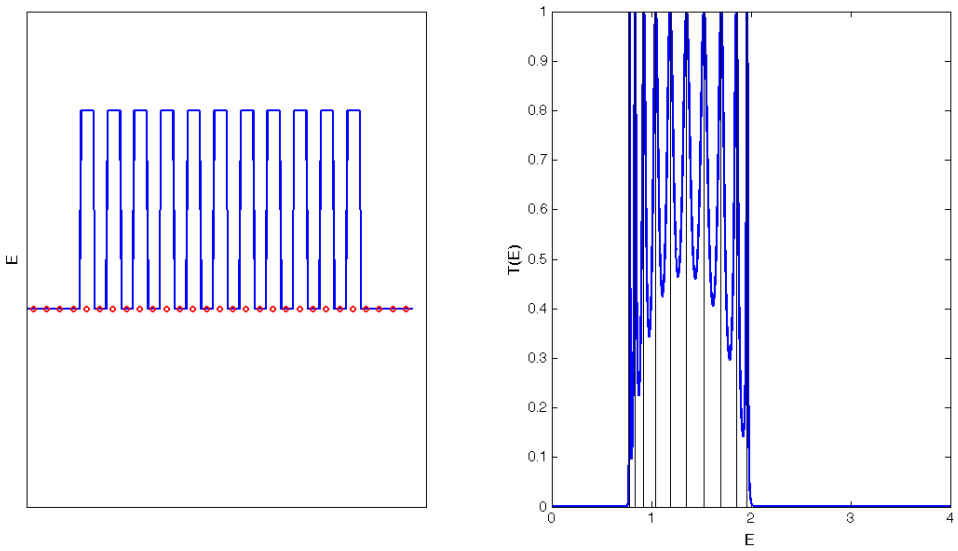

Figure 4.24: Tranmission coefficient for an alternating potential with $V_P = 2$.

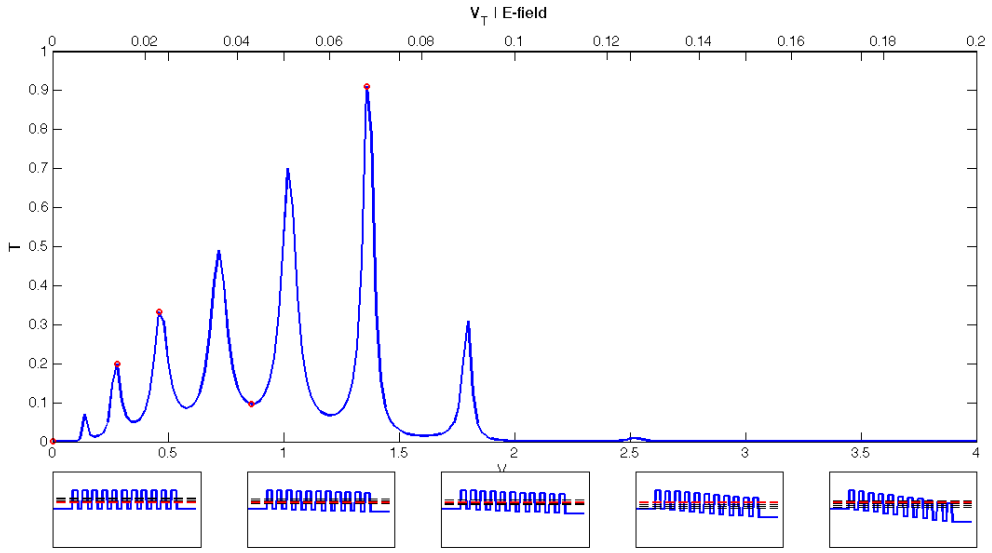

Figure 4.25: Tranmission coefficient for an alternating potential with $V_P = 2$ in dependency of the tilting. The incoming energy E = 0.7 and the system size is N = 21.

Fig.4.25 shows the transmission coefficient for an incoming energy E=0.7 versus the bias voltage (or the tilting of the system). There are also resonance peaks in T if the incoming energy strikes a resonance energy (as one can see in the lower subplots). The envelope of the transmission coefficient shows a similar behaviour as the current in this case does. For a detailed understanding one has to calculate the current from the transmission coefficient with the help of the Landauer formula ([25]):

$$\mathrm{j_T(V_{Bias})} = \frac{2\mathrm{e}}{\mathrm{h}} \int_{-\infty}^{\infty} \mathrm{dE} \quad \mathrm{T(E, V_{Bias})\,(f_s(E) - f_d(E))} \tag{4.33}$$

With the fermi function:

$$\begin{aligned} \mathrm{f_n(E)} &= \frac{1}{1 + \exp\frac{\mathrm{E}-\mu_\mathrm{n}}{\mathrm{k_B}T}} \\ \mu_\mathrm{s} = \mathrm{E_F}(=\epsilon_0) \qquad \mu_\mathrm{d} &= \mathrm{E_F} - \mathrm{eV_{Bias}} \qquad T = 0.0001K \end{aligned} \tag{4.34}$$

μ_s is the chemical potential of the leaft lead (source) and μ_d of the right lead (drain). $\mathrm{T(E,V_{Bias})}$ means that the transmission coefficient hast to be evaluated for every incoming energy E. This has to be multiplied by the difference of the fermi functions and then summed up. $\mathrm{j_T(V_{Bias})}$ denotes the current calculated by the Landauer formula out of the transmission coefficient and $\mathrm{j(V_{Bias})}$ is the current calculated by the method of greens functions from Chapter 2.

Fig.4.26 shows the coincidence of the current from the Greens function calculation and the current resulting from the calculations of the transmission coefficient. This underlines the beginning assumption that the current steps result from resonant tunneling of the electrons in an alternating potential.

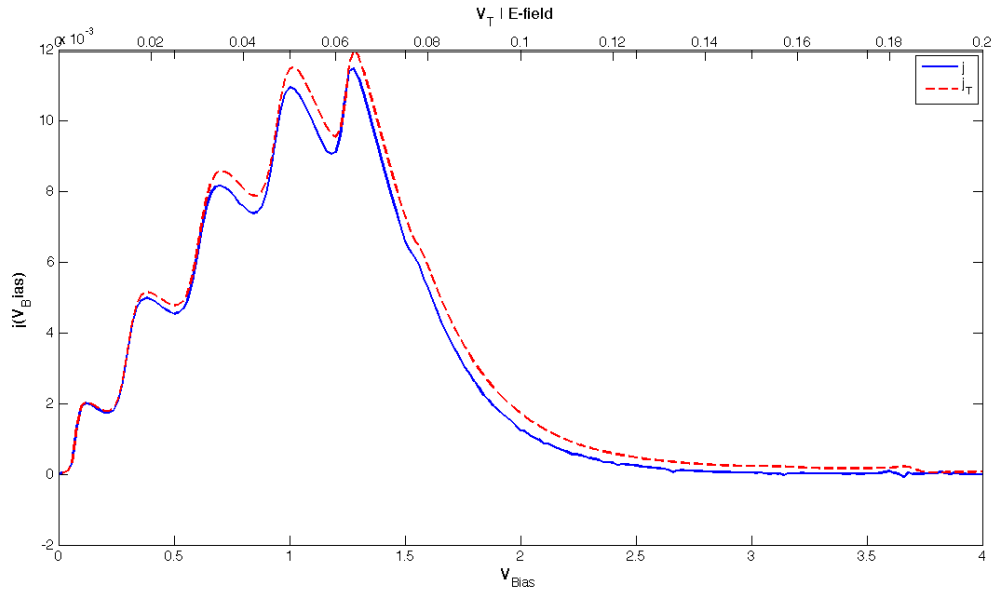

Figure 4.26: Comparison of the currents j and j_T for a central region N=21 and $V_P = 2$. For the calculations the greens function method and the Landauer formula were used.

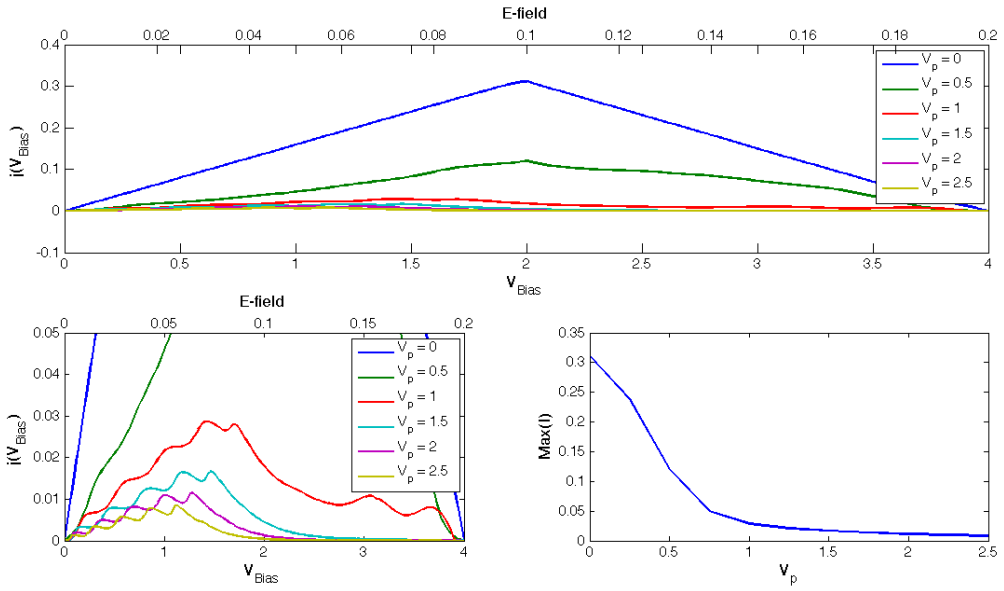

Figure 4.27: Shows the current characteristics (for $t_{cb} = 0$) for various potential heights and the behaviour of the current maximum with increasing height.

Fig.4.27 shows the current characteristics in dependency of the potential height in the central region. As the height increases, the current unfolds the behaviour of resonant tunneling (steps) and the maximum decreases. If we have a look at the maximum of the current as a function of potential height, one can see that there is a exponential decay of it with increasing V_P. At about a value of $V_P = 1$ resonant tunneling insets, for lower values the current shows no steplike behaviour. This depends on the interrelation between the resonances and the potential height. As the height increases the number of resonances increases and the transmission peaks get sharper. A reason, why there are no steps in the current for low values of the potential, could be that the resonances aren't distinct.

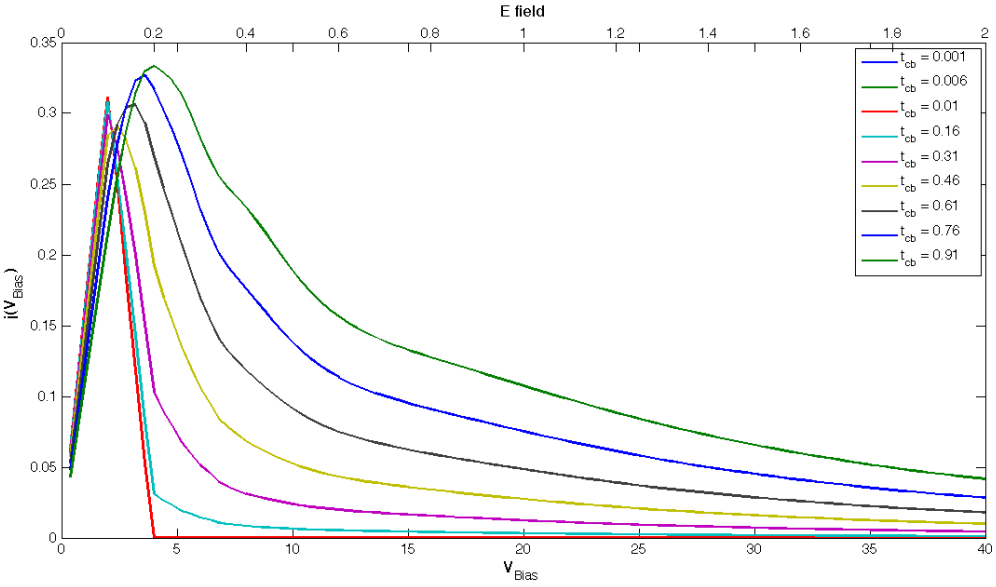

Figure 4.28: Shows the current in dependency of the chain-bath parameter t_{cb} without a potential.

In Fig.4.28 one can see the dependence of the current on the chain-bath hopping parameter. Without coupled fermion baths there is only a current flowing inside the band with. As the hopping increases, the baths get more and more important and the current develops a ohm's like behaviour in the low field regime and a exponential decaying behaviour in the high field regime because of the bloch oscillations.

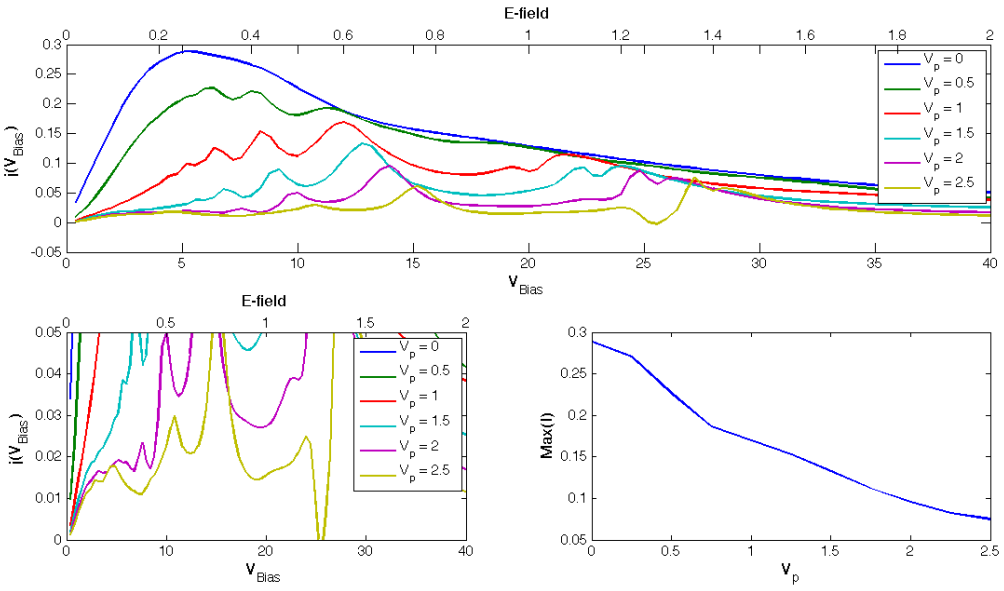

Figure 4.29: Shows the current characteristics (for $t_{cb} = 1$) for various potential heights and the behaviour of the current maximum with increasing height.

With the coupled fermion baths the current characteristics also show a decreasing current maximum with increasing potential height. But now the dependency of the current maximum on the height is not exponentially decaying but rather linearly decaying. It also exhibits steps (or rather oscillations) because of the resonant tunneling, but the steps are more seen in the high field regime. The electrons tunnel through nearly unbound resonant states (they don't depend on the atoms in the well but rather on the atoms in the barrier because their eigenenergies lay above the continuum band). As one can see the current decays for fields above 1.2. For higher fields the system is so strongly tilted that no bound states can be excited and the current goes down, because the electrons don't tunnel anymore.

4.4 Conclusion

In the case of a system with a central region consisting of an alternating potential (see Fig.4.1) the current exhibits steps. They come from so called resonant tunneling. This transport mechanism can be understand when one has a close look at the behaviour of the transmission coefficient in case of a double barrier potential. T can be calculated on a continous system (Chapter 4.2.2) or a discrete tight binding-chain (Chapter 4.2.5). In both cases it shows the same behaviour. When the energy of the incoming wave equals a resonance energy the transmission coefficient reaches its maximum value 1.
The current shows a steplike behaviour, that originates from the resonant tunneling. The current through the system can be calculated using the transmission coefficient and the Landauer formula (eq.(4.33)). In comparison the transmission current and the current calculated with the method of greens functions shows the same behaviour (Fig.4.26).
All in all, electrons tunnel resonantly through a potential barrier if the energy of the incoming wave equals the resonance energy and the main current increases.

5 Conclusion

We have considered systems like the one shown in Fig.2.1 under an uniform electric-field and analyze the transport mechanism. In the low field regime the current has an Ohmic-like behaviour because the electrons can scatter from one state to another. The fermionic reservoirs modelled as non interacting semi-infinite tight-binding chains transport the scattered electron. Because of the lenght of the reservoir it isn't scattered back and that is the reason why we can apply the Boltzmann transport picture to understand this transport regime. There is a linear relation between the field and the current.
The characteristics change as the field is increased. The current decreases with increasing field and an oscillating AC current is generated. This can be understood by the Bloch Oscillations which are responsible for the non linear transport mechanism. They appear because of the tilting of the chain caused by the high fields. The valence and conduction band don't overlap anymore and the current doesn't originate from scattering and tunneling anymore. For this transport mechanism the field has to be so high, that an electron can finish a cycle before it scatters into the next state. This means that the Bloch oscillation period has to be much smaller than the scattering rate. Relations of the oscillation amplitude and the field and the system size (eq.(3.12)) underline the found behaviour of the current. Furthermore the choice of the hopping parameter from the lead into the central region doesn't have much effect on the characteristics. Reducing the parameter t_{cc} (hopping in the chain) reduces the current and the amplitude of the Bloch Oscillations.
As an alternating potential is applied to the central region, the current characteristics change. They exhibit modulations (stepwise increase) because of another transport phenomena, resonant tunneling. The electrons in a double potential can tunnel resonantly and create a current because the potential barriers get transparent for certain energies, called the resonant energies. There is a particular relation between the potential height and well width and the number and strength of the resonances. As the height is increased the number of peaks in the transmission coefficient rises (same for increasing well width). This knowledge can be used to describe the current in such a system (Fig.4.1). The calculated current and the current resulting from the transmission coefficient calculated by the Landauer formula eq.(4.33) can be compared and it emerges that the steps in the current result from resonant tunneling.

References

[1] W.Nolting, *Grundkurs Theoretische Physik 5/1: Quantenmechanik-Grundlagen*, 7 ed. (Springer, Berlin, 2009)

[2] W.Nolting, *Grundkurs Theoretische Physik 5/2: Quantenmechanik- Methoden und Anwendungen*, 6 ed. (Springer, Berlin, 2006)

[3] M.A.Omar, *ELEMENTARY SOLID STATE PHYSICS: Principles and Applications*, [Chap. 5.8, pg. 198-205], (Addison-Wesley Pub.Co.,1993), `http://www.physics.ucdavis.edu/Classes/Physics243A/TightBinding.Basics.Omar.pdf`, (May 2014)

[4] W.Nolting, *Grundkurs Theoretische Physik 7: Viel-Teilchen-Theorie*, 7 ed. (Springer, Berlin, 2009)

[5] W.von der Linden, *Fundamentale Effekte der Vielteilchenphysik*, lecture WS 2012, `http://itp.tugraz.at/Archiv/div/Greensfunktion.pdf`

[6] A.P.Jauho, *Introduction to Keldysh nonequilibrium Green function technique*, `https://nanohub.org/resources/1878/download/jauho_negf.pdf`

[7] A.Avella, F.Mancini, *Strongly correlated system-theoretical methods*, [Chapter 8, *Cluster Perturbation Theory*, pg. 237-267], (Springer, Berlin, 2012)

[8] D. Sénéchal, *An introduction to quantum cluster methods*, arXiv:0806.2690 (May 2008)

[9] M.Knap, W. von der Linden, E.Arrigoni, *Nonequilibrium steady state for strongly-correlated many-body systems: variational cluster approach*, Phys. Rev. B **84**, 115145, (2011)

[10] M.Aichhorn, *Ordering Phenomena in Strongly-Correlated Systems: Cluster Perturbation Theory Approaches*, [Chapter 2], PhD Thesis, (2004)

[11] Wikipedia, *Tight-binding*, `http://en.wikipedia.org/wiki/Tight_binding`, (May 2014)

[12] P.Hadley, *Molecular and solid state physics*, lecture SS2014, `http://lamp.tu-graz.ac.at/~hadley/ss1/bands/tightbinding/tightbinding.php`

[13] Jong E.Han, *Solution of electric-field-driven tight-binding lattice coupled to fermion reservoirs*, Phys.Rev.B **87**, 085119 (2013)

[14] Jong E.Han and Jiajun Li, *Energy dissipation in DC-field driven electron lattice coupled to fermion baths*, Phys.Rev.B **88**, 075113 (2013)

[15] Wikipedia, *Bloch oscillations*, `http://en.wikipedia.org/wiki/Bloch_oscillations`, (May 2014)

[16] Prof. Dr. T. Brandes, *Theoretische Festkörperphysik/4.4 Die Bloch-Oszillationen*, Skriptum SS2014, `http://wwwitp.physik.tu-berlin.de/brandes/fk2010.pdf`, (May 2014)

[17] `http://www.colorado.edu/physics/phys7440/phys7440_sp03/HOMEWORK/Homework/S8.htm`, (May 2014)

[18] H.G.Evertz, *Fortgeschrittene Quantenmechanik*, lecture SS2004, `http://itp.tugraz.at/LV/evertz/QM-2/qm2.pdf`

[19] W.G.Schmidt, U.Gerstmann, *Vielteilchentheorie der Festkörper*, Skriptum WS2009, `http://homepages.uni-paderborn.de/wgs/Dlehre/VTFK-Skript.pdf`, [Chapter 1.3, pg. 7-13] (May 2014)

[20] K.H.Thomas, C.Flindt, *Waiting time distribution of non-interacting fermions on a tight-binding chain*, `http://arxiv.org/abs/1402.5033`

[21] Heinrich Kurz, Hartmut G.Roskos, Thomas Dekorsy and Klaus Köhler, *Bloch oscillations*, Phil.Trans.R.Soc.Lond.A **354**, 2295-2310 (1996)

[22] Th.G. van de Roer, *Modeling of Double Barrier Resonant Tunneling Diodes: D.C. and Noise Model*, ISBN 90-6144-285-0 (January 1995)

[23] `http://qudev.phys.ethz.ch/content/science/BuchPhysikIV/PhysikIVch9.html` (May 2014)

[24] J.A.Støvneng and E.H.Hauge, *Time-dependent resonant tunneling of wave packets in the tight binding model*, Phys.Rev.B **44**, 13582 (1991)

[25] M.Woloszyn, J.Adamowski, P.Wójcik and B.J.Spisak, *Periodicity of resonant tunneling current induced by the Stark resonances in semiconductor nanowire*, J. Appl. Phys. **114**, 164301 (2013)